Application of observability techniques to structural system identification including shear effects

Seyyedbehrad Emadi

Application of observability techniques to structural system identification including shear effects

DoctoralThesis

Doctoral thesis performed by:

Seyyedbehrad Emadi

Directors:

Prof. Dr. José Turmo Coderque

Prof. Dr. Jose Antonio Lozano Galant

Doctoral program:

Construction Engineering

Barcelona, Spain September 2020

PhD program in Construction Engineering

Application of observability techniques to structural system identification including shear effects

Doctoral thesis by:

Seyyedbehrad Emadi

Thesis advisor:

José Turmo, Jose Antonio Lozano

Department of Construction Engineering

Barcelona, 2020

The higher you build your barriers

The taller I become

The further you take my rights away

The faster I will run

No matter, 'cause there's

Something inside so strong

Labi Siffre (1945- present)

Acknowledgments

X

Abstract

According to Timoshenko's beam theory, nodal rotations in beam-like structures are produced by bending and shear effects. On the one hand, bending rotations can be easily calculated by the Euler-Bernoulli stiffness matrix method. On the other hand, shear rotations are traditionally neglected as their effects are practically negligible in most structures. In addition, calculating the shear rotation effects by the stiffness matrix method is not straight forward tasks and it presents practical limitations. Nevertheless, this assumption might lead to significant errors in the simulation of the structural response of some structures (such as deep beams and composite structures).

The shear effects are also neglected in the inverse analysis of structures (Structural System Identification) used to calibrate the mechanical properties of the structural elements from the monitoring on-site. Recently, one of the first methods for the inverse analysis of structures including the shear effects (the Observability Method, OM) was presented. This method introduced Timoshenko's beam theory into the Stiffness Matrix Method (SMM). In this way, the vertical deflections produced by shear effects were included into the simulation while the shear rotations were neglected. In this method, the mechanical properties of the structures could be obtained from the nodal deflections measured on static tests on site. One of the main controversial features of this procedure is the fact that the measurement set must include rotations. This characteristic might be especially problematic in those structures where rotations due to shear are not negligible. In fact, in this case, neglecting the shear rotations might lead to significant errors. This simplification might be especially problematic in those structures where only rotations can be measured. In addition to the OM, some other inverse analysis methods including shear deformation effects have been recently presented in the literature. Nevertheless, all these methods also fail to deal with the shear rotation effects, as they only take into account in the system of equations the vertical deflections produced by shear. Therefore, when actual rotations on site are used estimations with significant errors can be obtained.

To fill these gaps, this Ph.D. Thesis deals with the analysis of the effects of the shear deformations in beam-like structures from a direct and inverse approach. First of all, the SMM is updated to enable the calculation of the shear rotations from a direct analysis. This method is used to evaluate the effects of the shear rotations in beam-like structures with different slenderness ratios. In addition, for the first time in the literature, the slenderness ratios where the shear rotation effects can be neglected from a direct analysis are identified. Secondly, the OM is updated to enable the inverse analysis of structures with shear effects from measurement sets with only vertical deflections. This modification is based on the introduction of a numerical optimization method. With this aim, the inverse analysis of several examples of growing complexity are presented to illustrate the validity and potential of the updated method. Finally, the OM is modified to enable

the inverse analysis from shear rotations. This modification is based on the introduction of a new iterative process to estimate successively the values of the shear rotations. To illustrate the applicability and potential of the proposed method, the inverse analysis of several examples of growing complexity is presented. A set of calculation recommendations and future researches are also proposed.

Keywords: Shear, Stiffness matrix, Structural system identification. Observability method.

Resumen

De acuerdo con la teoría de vigas de Timoshenko, las rotaciones nodales en estructuras tipo viga se producen por efectos de flexión y cortante. Si bien las rotaciones por flexión pueden ser fácilmente calculadas por el método de la matriz de rigidez de Euler-Bernoulli, las rotaciones por cortante no se han tomado en cuenta tradicionalmente ya que sus efectos son prácticamente insignificantes en la mayoría de las estructuras. Así mismo, el cálculo de los efectos de la rotación por cortante mediante el método de la matriz de rigidez no es una tarea sencilla y presenta limitaciones prácticas. Sin embargo, esta omisión podría conducir a errores significativos en la simulación de la respuesta estructural de algunas estructuras (como las vigas de gran canto).

De igual forma, los efectos por cortante no han sido tomados en cuenta en el análisis inverso de las estructuras (Identificación del Sistema Estructural) que es utilizado para calibrar las propiedades mecánicas de los elementos estructurales a partir de la monitorización in situ. Recientemente, se presentó uno de los primeros métodos para el análisis inverso de las estructuras, incluidos los efectos por cortante (el método de observación, OM, por sus siglas en inglés). Este método introdujo la teoría de vigas de Timoshenko en el Método de la Matriz de Rigidez (SMM, por sus siglas en inglés). De esta manera, las flechas verticales producidas por los efectos por cortante se incluyeron en la simulación, mientras que las rotaciones por cortante se ignoraron. En este método, las propiedades mecánicas de las estructuras pudieron obtenerse a partir de las flechas nodales medidas en pruebas estáticas in situ. Una de las principales características controvertidas de este procedimiento es el hecho de que en el conjunto de mediciones se deben incluir las rotaciones. Esta característica podría ser especialmente problemática en aquellas estructuras en las que las rotaciones debidas al cortante no son despreciables. De hecho, en este caso, despreciar las rotaciones por cortante podría dar lugar a errores significativos.

Además del OM, recientemente se han presentado en la literatura otros métodos de análisis inverso que incluyen los efectos de deformación por cortante. Sin embargo, tampoco ninguno de estos métodos abordan los efectos de rotación por cortante, ya que solo tienen en cuenta en el sistema de ecuaciones las deformaciones verticales producidas por cortante. Por lo tanto, cuando se utilizan las rotaciones reales in situ se pueden obtener estimaciones con errores significativos.

Para llenar estos vacíos, esta Tesis Doctoral aborda el análisis de los efectos de las deformaciones por cortante en estructuras tipo viga desde un enfoque directo e inverso. En primer lugar, se actualiza el SMM para permitir el cálculo de las rotaciones por cortante a partir de un análisis directo. Este método se utiliza para evaluar los efectos de las rotaciones por cortante en estructuras tipo viga con diferentes ratios de esbeltez. Además, por primera vez en la literatura, se identifican los ratios de esbeltez en los que los efectos de la rotación por cortante pueden ser despreciados a partir de un análisis directo. En segundo lugar, el OM se ha actualizado para permitir el análisis inverso de estructuras con efectos de cortante a partir de un conjunto de mediciones con solo flechas verticales. Esta modificación se basa en la introducción de un método de optimización

numérica. Con este objetivo, se presenta el análisis inverso de varios ejemplos de creciente complejidad para ilustrar la validez y el potencial del método actualizado. Por último, se modifica el OM para permitir el análisis inverso a partir de las rotaciones por cortante. Esta modificación se basa en la introducción de un nuevo proceso iterativo para estimar sucesivamente los valores de las rotaciones por cortante. Para ilustrar la aplicabilidad y el potencial del método propuesto, se presenta el análisis inverso de varios ejemplos de complejidad creciente. Así mismo, se propone un conjunto de recomendaciones de cálculo e investigaciones futuras.

Palabras clave: Cortante, Matriz de rigidez, Identificación del sistema estructural. Método de observabilidad.

TABLE OF CONTENTS

LIST OF TABLES

LIST OF FIGURES

XX

Chapter 1: Objectives

1.1. Introduction

The gaps detected in the literature are as follows:

1- **Shear rotations are always neglected in the direct analysis of structures:** Most structural simulation software are based on the Stiffness Matrix Method (SMM) to calculate the nodal deflections from the applied loads with known mechanical properties (direct analysis). Although in this method shear effects can be introduced into the vertical deflections they are always neglected in rotations. In fact, the obtained rotations are the same independently if the shear effects are or are not considered. This simplification might be acceptable in some structures with reduced shear effects, might it also might lead to significant errors in other structures (such as deep beams) where shear rotations play an important role.

2- **Inverse analysis of structures with shear deformation effects requires the measurement of rotations:** The Observability Method, OM, was proposed to obtain the mechanical properties of the structures from the monitoring information on site (inverse analysis). This method was modified to deal with the shear effects in the vertical deflections by measurement sets including both vertical deflections and rotations on site. However, many infrastructure control only relies on deflection measurements (e.g. surveying through topography), being rotation measurement, and the use of clinometers much more scarce. In addition, vertical displacement measurements might be more reliable than rotations. The majority of SSI methods are based on the Euler-Bernoulli beam theory.

3- **Real rotations on site cannot be used for the inverse analysis of structures:** Real rotations on-site include both bending and shear effects. Nevertheless, all methods for the inverse analysis of structures only consider rotations due to bending. This simplification might be especially problematic in those structures where rotations due to shear are not negligible, and in those structures where only rotations can be measured. In fact, in this case, neglecting the shear rotations might lead to significant errors in the identification of the structural parameters.

To fill these gaps, new computational methods are developed and the shear effects of different structures of growing complexity are evaluated in this work. From these analyses, a set of recommendations for the analysis of the shear effects are provided.

This Ph.D. Thesis is framed into two research projects: "BIA2013-47290-R: Sistema de apoyo a la toma de decisiones durante el ciclo de vida de las infraestructuras: Smart-Infrastructures" and

"BIA2017-86811-C2-1-R: Modelos Estructurales para la gestion eficiente de infraestructuras: Smart BIM Models".

1.2. Objectives

The global objective of this work is to study the shear deformation effects in beam-like structures from both direct and inverse approaches. With this aim, the following partial objectives are defined:

1- Introducing shear rotation into the direct analysis of the traditional Stiffness Matrix Method (SSM).
2- Update the Observability Method (OM) to deal with the inverse analysis of structures from measurement sets with only vertical deflections.
3- Identify in which cases (beam slenderness ratio and loading cases) the shear effects cannot be neglected.
4- Develop a new OM for the inverse analysis of structures with significant shear deformations from the rotations measured on-site.

1.3. Thesis organization

The thesis is organized into six chapters. The main text of each chapter is intentionally kept as short as possible (introducing only the fundamental concepts and the new ideas) to ease its reading. In Chapter 2 the state of the art is presented. Firstly, the assumptions of the structural modeling and the main beam theories are reviewed. Then, the Structural System Identification Methods (SSI) developed by the research group where this thesis is framed are detailed. Finally, the assumptions of the other SSI methods in the literature to deal with the shear deformation effects are analyzed.

In Chapter 3, the equations of the Stiffness Matrix Method (SMM) in beams with and without shear effects are reviewed. Then, an example is presented to illustrate the inability of this method to calculate the value of shear rotations from a direct analysis. After that, a new method for calculating the shear rotation in beams is presented. In addition, a parametric analysis of different structures is presented to illustrate the important role that shear rotations might play in some geometries.

Chapter 4 reviews the SSI by the different Observability algorithms presented in the literature. A simply supported beam is analyzed to illustrate the inability of the method presented in Tomas. et al. (2018) to identify mechanical properties by measuring just vertical deflections. Later, the constrained observability method (COM) is enhanced to enable structural identification by measuring only vertical deflections. To illustrate the application of this algorithm, a step by step example of a simply supported beam is presented. In addition, another numerical example of an intermediate construction stage of a cantilever bridge is analyzed.

Chapter 5 discusses the importance of shear rotations in some structures. To illustrate this, the effects of neglecting these rotations in the inverse analysis of some structural cases with different slenderness ratios are analyzed. In addition, a new iterative method for analyzing the effects of the

shear rotations in COM is presented. Different structures are analyzed to illustrate the important role that shear rotations might play in some geometries. Moreover, the applicability and accuracy of the new method in different structural models are studied.

Finally, in Chapter 6, a summary of the thesis is provided and a pathway for future possible works is described. In addition, related works and publications derivated from the thesis are presented.

1.4. Activities

To develop this work, the following activities have been carried out:

1- Literature review (in the first year) .
2- Patch test of the OM with and without shear effects (in the first year) .
3- Patch test of the commercial structural software with shear effects (in the first year).
4- Method to include shear rotations into structural simulations (in the first and the second years).
5- Updating OM to enable SSI with only vertical deflections (in the second and the third years).
6- Updating OM to work with real rotations (in the third and fourth years).
7- Conclusions (in the fourth year).
8- International stay (in the fourth year).
9- Writing conference and SCI papers (in the third and fourth years).

5

Chapter 2: State of the art

2.1 Structural modeling and beam theories

Structural modeling is related to the simulation of the behavior of structures. It is achieved based on processes in which physical problems based on a set of simplifying assumptions are expressed mathematically. There are many studies related to modeling the structural behavior of beam-like structures (e.g. Zarga, D. et al 2019, López-Colina, C. et al. 2019, Chao, S. et al. 2019). Most of these studies are based on either the Euler-Bernoulli (Kawano, A. and Zine, A. 2019) or the Timoshenko's beam theory (Arefi, M. et al2019) According to many scholars (see e.g. Lu, Y. and Panagiotou, M. 2014, Ozdagli, A. I. et al. 2018) shear deformations are traditionally neglected in Euler-Bernoulli's beam theory approach as this theory assumes the plane section deformation. This assumption states that plane sections remain plane and perpendicular to the neutral axis during bending deformation (Dahake, A. et al 2014), and accordingly, no shear strains appear or its value is negligible.

The Euler-Bernouilli's theory fails for most loading cases, as the only loading case resulting in zero shear force is a constant bending moment alongside the beam. Hence, this theory only holds for this particular case. This assumption is traditionally used in slender beams, where shear deformations are usually smaller than flexural ones, and therefore, their effects can be neglected. In these cases, the absence of shear strains and deformations can be considered as a modeling error (Tomas, D. et al 2018). Nevertheless, in structures lacking a unidimensional geometry (such as deep beams) shear deformation might play an important role and its effects should be introduced into the structural formulation (Dym, C.L. and Williams, H.E. 2007). Eurocode EN 1992-1-1 characterizes deep beams as those which span is three times smaller than the overall section depth. ACI committee 318 describes these beams as beams whose spans are equal to or less than four times the depth of the beam. Shear deformation effects can also play an important role in the other two dimensional structures, such as sandwich beams and deep beams (Chen, D. et al 2016).

Timoshenko (Timoshenko, S. P. 1921, Timoshenko, S. P. 1922) was the first one dealing with the study of shear deformations in beams. In fact, he included the effects of both shear vertical deflections and shear rotations into this theory. In this approach (known as Timoshenko's beam theory or first-order shear deformation theory) two different rotations are considered: (1) Rotations due to the bending, w_b, and (2) Rotations due to the shear, w_r. The difference assumptions of Euler-Bernouilly and Timoshenko methods are illustrated in the simply supported beam presented in Figure 1. This figure includes the assumed rotations in a support in both theories.
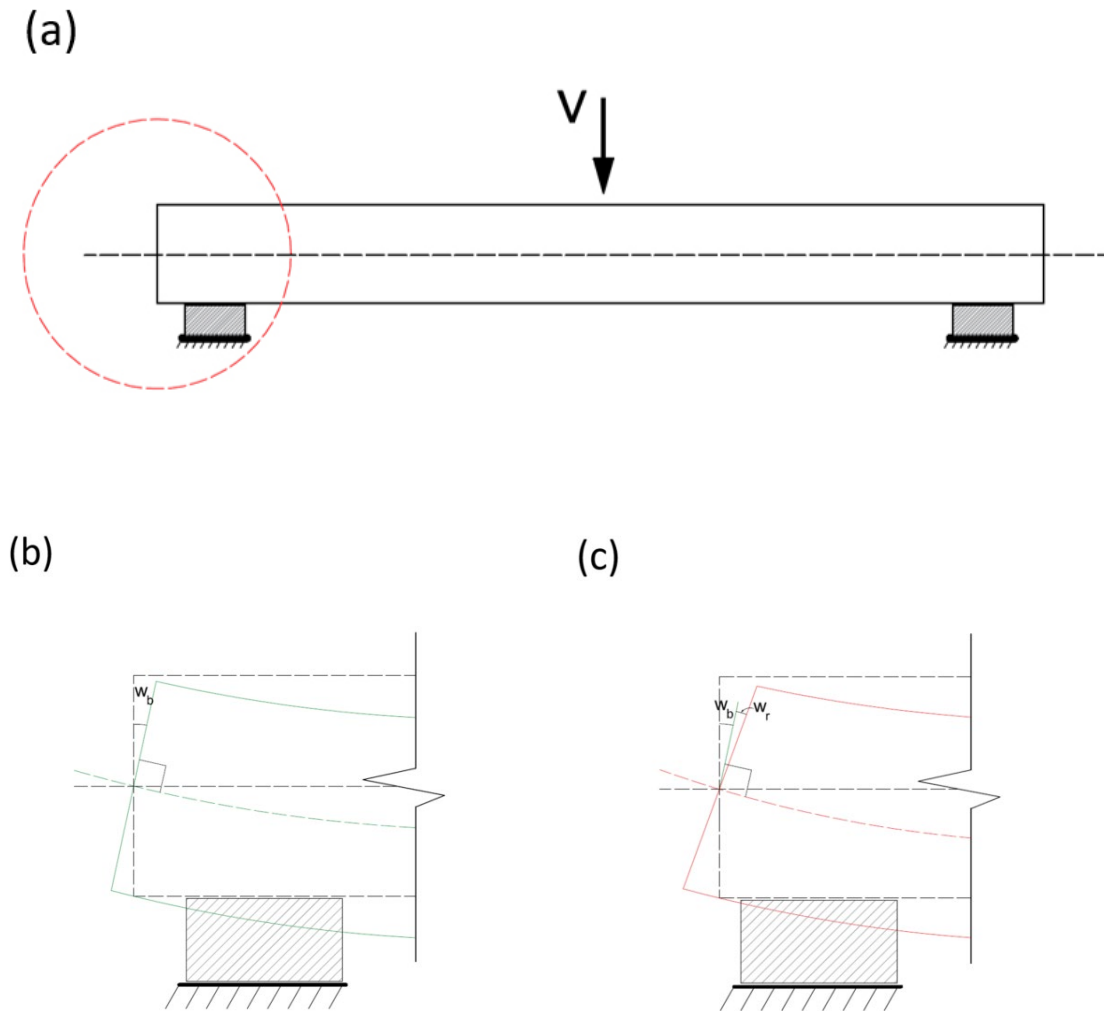
Figure 2.1: Beam theory at a beam support. (a) A simply supported beam with a zoomed support. (b) Rotations of the Euler-Bernoulli's beam theory. (c) Rotations of the Timoshenko's beam theory.

Timoshenko's theory was later improved by Mindlin (1951), who simplified the transverse shear strain as a constant distribution through the beam thickness. In this approach, a shear coefficient was used to appropriately represent the strain deformation energy in real structures. This shear coefficient can be used to include the effects of the non-constant shear stresses and strains in the members' cross-sections.

2.2 Stiffness matrix method

The Finite Element Method (FEM) is a numerical problem-solving method (Meier, C. et al 2019, Zeng, W. et al 2018, Dixit, P. and Liu, G.R, 2017) commonly used to calculate the structural response of all kind of structures. In this method, large equations are divided into smaller and

simpler ones. The concept of the FEM was first developed by Clough (1960) for solving problems in solid-state mechanics (specifically in plate-bending). Turner et al. (1956) described the application of finite elements for the analysis of aircraft structures and is pointed to as one of the main contributions to the growth of the FEM. The FEM approach allows the continuum to be discretized into a finite number of elements and ensures that the characteristics of the continuous domain can be determined by combining the properties of the different elements in the nodes. Hutton (2004) refers to FEM as the most powerful and common technique for computer-based analysis in engineering. In addition, this procedure can be used for both simple and complex structures (Bathe, K.J. 2016, CSI, 2016, Rapp E. 2017). Consequently, the FEM has been thoroughly implemented to solve a broad range of problems in different fields of science and engineering and it has grown rapidly over the years (Rao, S. 2018, Dixit, P. and Liu, G.R, 2017) which makes FEM a numerically universal tool for solving differential equations. Indeed, the fast-growing recognition of finite element methodologies is associated with the computer's growth. This led to the rapid development of the process, which now offers the key for rational structural design and the analysis of aeronautical fluid dynamics and electric magnetism required for physics through various commercial and research codes (Zienkiewicz, O. C. 1996). All of the information concerning these finite elements methods were presented, along with numerous correspondents at a meeting held in Swansea in January 1964 and 1965 formally published (Zienkiewicz, O. C. (1965)) and several other seminars such as Fraeijs de Veubeke (1965).

A common FEM model for the analysis of beam-like structures is the stiffness method. In this method, the nodal equilibrium equations of a structure loaded in its plane are correlated with the nodal forces (Zienkiewicz, O. 2004). This method was initially proposed by Louis Navier (1826) then, Alfred Clebsch (1862) developed the method and studied more details. Clebsch (1862) presented a succinct technique for the linear analysis to evaluate a moment-free 3D truss. Barr´e de Saint Venant (1883) studied the same problem (a French translation of Clebsch (1862) with more detailed discussions).

Before the advent of computers, only a small number of unknown variables could be calculated by the stiffness method. Therefore, to deal with this problem Southwell, RV (1935), developed the use of relaxation methods. Although this method was not practical to solve a complex problem manually, the iterative process of elimination proposed in his further studies (Southwell, RV. 1946, Southwell RV. 1956), increased the applicability of the method, enabling to solve very complex problems. In addition, Turner, MJ. (1962), contributed to developing the stiffness method and formulated it in more detail. The main inconvenience for the more complex structures is that hand methods of analysis become excessively inapplicable.

Standard engineering methods can be employed in other areas of engineering. For example, electrical components can be assembled to form a circuit the same as the structure assembling bars. This concept was already proven in Kirchhoff GR. (1847). In the analysis of designing aircraft which is described by Levy, S. (1937), it is believed that all normal stresses are taken up by the spars and ribs and all shear stresses by the panels. The analogous approach was employed by

Falkenheiner, H. (1950), Lang, AL. and Bisplinghoff, RL. (1951), as well. Hrenikoff, A. (1941) proposed a system for solving problems of linear elasticity. A rectangular arrangement of the trusses model is presented by McHenry, D. (1943). Related equations of SMM arised in electrical networks, and these follow similar formulations to structural engineering problems (Megson, T.H.G. 2019). Similar to Kirchhoff and Maxwell, Gabriel Kron (1944) explained a close comparison between electrical and mechanical networks for the solution of 3D frames in a complete matrix algorithm. He was the first one who considered these stiffness matrices along the diagonal of a large-scale matrix. Argyris made considerable progress in the use of matrices in structural engineering (Argyris JH. 1955) applying the methods proposed by Kron. Clearly, the particular computational advantage of the SMM refers to the local definition of the shape function (known as stiffness matrix). The local assembly of the structure in terms of matrix equations was firstly presented in Walter, R. (1909). The purpose of this approach relies on the formation of a relationship between forces imposed at nodes of an element of a structure, and the displacement related to the force.

The SSM is traditionally used to calculate nodal deflections from applied loads assuming the terms in the stiffness matrix as known. This approach is known as the direct analysis and it is particularly suitable for the computer-automated analysis of complex structures (Rocas, M. et al. 2020). In fact, there is a wide range of software packages (such as SAP2000 (CSI, 2016), Midas/ Civil. 2015) that enable the calculation of structures with this structural approach. In these software the stiffness matrix [K] is traditionally based in the Euler–Bernoulli's beam theory and the shear effects are neglected (Sayyad, A.S. 2011). The [K] matrix of a 2D beam element is presented in Figure 1.1a. This matrix is independent for each beam element and it contains its length L, Young's Modulus, E, Inertia, I, Area, A.

The [K] matrix obtained by the Euler-Bernouilli's beam theory can be successfully applied to slender beams. Nevertheless, this is not the case in other structures (such as deep beams), where shear deformations might play an important role and these effects cannot be ignored (see e.g. Tomas, D. et al. 2018). Shear deformation in beams can be analyzed by the sum of two components: (1) Vertical and axial deflections, and (2) Rotations. Some authors proposed innovative stiffness matrices to include the shear effects into the SMM formulations (Lu, Y. and Panagiotou, M. 2014, Heyliger, P.R.and Reddy, J.N. 1988, Nickel, R.E. and Secor, G.A. 1972, Prathap, G. and Bhashyam, G.R. 1982, Tessler, A. and Dong, S. B. 1981). In order to include the effects of the shear rotation into the SMM, some authors developed their own mathematical model (Davis, R. et al. 1972, Archer, J.S. 1965, Kapur, K. K. 1966, Severn, R. T. 1970, Carnegie, W. et al. 1969, Ali, R. et al. 1971, Ali, R. et al. 1971). In these models, SMM formulations were too simple to consider shear rotation effects and they were only based on the analysis of vertical and axial deflections. To deal with the shear effects, specific boundary conditions were considered to remove unnecessary equations from the beam equilibrium system. But these methods have limited applicability as they can only be used in simple cases and their equations are different for each case. The first FEM for Timoshenko beam theory was proposed by McCalley (1963), who

developed a two-node, four-degree of freedom element (transverse displacement and cross-section rotation at every node). This FEM was extended to a tapered beam by Archer, J.S. (1965). The values of the shear coefficient for different cross-sections were proposed by Cowper G.R. (1966). At the time Kapur, K. K. (1966) found that in a clamped-end element (such as the fixed end of a cantilever beam), Archer's formulation could not represent the exact boundary conditions (as the rotation due to shear is constrained to be zero). To deal with this problem, Kapur developed a new element based on a cubic displacement function for both the bending and the shear displacements. In this formulation both effects (shear rotation and bending rotation) were analyzed separately, resulting in an eight degree of freedom beam element. The FEM presented by Kapur works properly when there are four unknowns per node (such as in simply-supported beams and cantilevers). However, in complex structures, where adjacent elements are not collinear, Kapur's element does not work properly. Other authors used slightly different approaches for their FEM's and achieved almost the same results as Kapur. Various types of FEMs for Timoshenko's beam elements are proposed in the literature. These methods are based on similar assumptions with small differences (Augarde, C.E. 1997, Astley, R.J. 1992, Pickhaver, J.A. 2006). Thomas et al. (1973) described many of the early models presented in the literature to deal with shear. He categorized the elements of these models into two classes: simple and complex. On the one hand, a simple element is considered with only two degrees of freedom at each of its two nodes. On the other hand, a complex element has more than four degrees of freedom (having nodes with more than two degrees of freedom or more than two nodes per element).

According to the literature, a number of different SMM approaches can be found to include shear rotations into the simulation of simple and complex elements. But complex structural cases which have discontinuities in cross-sections or non-collinear elements can only be analyzed by the FEM's whose nodal variables are bending rotation and transverse displacement (Thomas et al. 1973). It is important to notice that the effect of shear rotation is neglected in this SMM formulation. A detailed formulation of this type of common Timoshenko's beam theory SMM can be found in many works, such as, for example, in Przemieniecki, J.S. (1968). On the other hand, where, there are continuous cross-section or beam-column, several SMM based on Timoshenko's beam theory are proposed by different authors (Sapountzakis, E. J. and Kampitsis, A. E., 2010, Sapountzakis, E. 2011, Sapountzakis, E. J. & Kampitsis, A.E., 2011, Dikaros, I. & Sapountzakis, E. 2014).

2.3 Deformations in the Structural System Identification

System Identification (SI) is a process of modeling an unknown system that has been employed in a number of engineering fields (Sirca et al. 2012, Altunişik et al. 2017) .The discipline of SI aims to create mathematical models that characterize properly the system behavior. One of the pioneers in this approach was Friedrich Gauss who developed the Gauss-Newton method to find the values of parameters in a model of the trajectory to calculate the dwarf planet trajectories. SI began in the area of electronic engineering and, after a while, it has been extended to other fields of engineering (Gevers 2006, and Pisano 1999). Structural system identification (SSI) is a part of the SI dealing

with the construction of mathematical models to identify the structural parameters (such as flexural stiffnesses, axial stiffnesses, or damping parameters) from the structural response (Pajonk 2009).

The SSI analysis enables the calibration of parameters in the stiffness matrix [K] from the structural response, this simulation is also known as an inverse analysis. A number of methods are proposed for SSI in the literature (Liao, 2012, Lozano-Galant 2013, Yan, 2005). The SSI methods can be classified according to the excitation test type as dynamic (Breuer, et al. 2015, Dowling et al, 2012, Li et al. 2017, Górski et al. 2018) or static (Thirumalaiselvi et al. 2016, Walsh et al. 2009, Lee et al. 2010). SSI methods might be also classified as a parametric (Lozano-Galant et al. 2013, Gracia-Palencia et al. 2015) or non-parametric methods (Karabelivo et al. 2015, Mei et al. 2016). Parametric methods rely on the physical-based models, while in non-parametric ones, parameters do not have any physical meaning. In fact, in non-parametric methods, parameters are identified directly with optimization procedures that minimize the difference between the predicted structural response and the measured ones. For parametric SSI methods, a mathematical representation of the structural behavior is required. The most common way to do this modeling is based on the SSM (Hou et al. 2015, Kahya et al. 2018, Li et al. 2017, Khayat et al. 2017, Khayat, et al. 2017, Li et al. 2014, Araki et al.2005). The details of some of the main SSI methods proposed in the literature are presented in (American Society of Civil Engineers, Reston, VA 2013).

Despite the importance of shear deformation in some structures, this phenomenon is usually overlooked by most of SSI methods as shear deformations are traditionally smaller than the bending ones. In these cases, shear effects are considered as modeling errors in the mathematical models (such as any property in the model assumed with a wrong value). Nevertheless, in some structures (such as deep beams, shear walls, short span beams, or thin-web bridges) shear effects might play an important role. In this case, they should not be neglected and should be introduced into the formulation.

Most traditional SSI methods are not able to observe correctly the parameters of a structure (such as bending stiffness) when shear deformation is not negligible. SSI methods based on SMM normally use elementary beam theory, underestimating deflections, and overestimating the natural frequencies since the shear deformation effect is disregarded (Sayyad 2011). SSI models are mostly based on Euler–Bernoulli beam theory which includes axial and flexural deformations and neglects shear effects are. Some authors studied the effect of shear deformation in their SMM models of composite structures (Kumar et al. 2018, Nguyen et al.2018, Singh et al. 2017). Moreover, Soto et al. (2017) proposed a new SMM's formulation including shear effects for the modeling fixed–end moments of I-sections. The effects of shear deformations in the recursive matrix method for the sandwich plate were also studied by (Huoet al. 2017). The impact of shear effects in steel-concrete composite structures was also studied by (Yang et al. 2018) and (Wang et al. 2018).

2.4 Observability Method

Mechanical properties (such as bending, EI, or axial, EA, stiffness) of actual structures on site might differ from theoretical values due to damage (e.g. by carbonation, corrosion, accidental actions, fires, impacts or material degradation) or other uncertainties (e.g. lack of knowledge of the material or its variation over time). The Structural System Identification (SSI) enables the estimation of these unknown parameters from the structural response on tests. To do so, the system of equations in the Stiffness Matrix Method (SMM) must be analyzed from an inverse approach. Parametric analysis of this system is not a straight forward task as it leads to a polynomial system of equations where the unknown variables are coupled to the deformations in the non-measured degrees of freedom. As stated in Castillo et al. (2015) the Observability Method (OM) is the first method that enables efficient analysis of this kind of system of equations. This method is based on the observability techniques already validated in many engineering fields (such as Lozano-Galant et al. 2013).

In the structural engineering field, the OM has proved its efficiency in different structural typologies (such as trusses, beams, frame structures and cable-stayed bridges) (see e.g. Lozano-Galant et al. 2014, Nogal et al. 2015, Castillo et al. 2007, Castillo et al. 2016, Lozano-Galant et al. 2015, Lei et al. 2016, Lei et al.2017, Lei et al. 2019). The different works dealing with the application of observability techniques to SSI in the literature are reviewed in Table 1.1. This table includes information of the following characteristics: (1) Test: Type of test used for monitoring the structural response on-site, Static: S, or Dynamic: D, (2) Analysis: Type of analysis used to deal with the system of equations Parametric: P, or Numerical, N, (3) Optimization: If a numerical optimization tool was used to define the value of the parameters, and (4) Shear: If the effects of shear deformations are included into the system of equations or not.

Table 2.1: Characteristics of the observability methods presented in the literature: S: Static, D: Dynamic, P: Parametric, and N: Numerical.

	Test	Analysis	Optimization	Shear
Lozano-Galant et al. (2013)	S	P		
Lozano-Galant et al. (2014)	S	P		
Castillo et al. (2015)	S	P		
Castillo et al. (2016)	S	P		
Nogal et al. (2016)	S	N		
Lei et al. (2017)	S	N		
Lei et al. (2018)	S	P+N	■	
Tomás et al. (2018)	S	P+N		■
Emadi et al. (2019)	S	N	■	■
Lei et al. (2019)	S	N	■	
Peng et al. (2020)	D	N	■	

The analysis of Table 1.1 shows that up to now, all studies in the literature but one (Peng et al. 2020) are based on the monitored response on static tests. This table also evidences an evolution in the analysis methods. In fact, to enable the application of the OM to real structures the parametric simulation introduced into the first applications has been successively changed to a

numerical one. To deal with the numerical errors in the system of equations, most of the latter studies use the optimization tool named Constrained Observality Method, COM introduced by Lei et al. (2018). A more detailed explanation of this method is presented in Chapter 4. Finally, two works studied the shear deformation effects. The first of these studies (Tomás et al. 2018) introduced the Timoshenko theory into the stiffness matrix of the system of equations to include the shear effects on vertical deflections. Nevertheless, as indicated this method fails to deal with shear rotation effects. To fill this gap the second paper (Emadi et al. 2019) was published in the frame of this thesis. A detailed review of this work is presented in Chapter 4.

Chapter 3: Introducing shear rotations into the SMM

3.1 Introduction

According to the Stiffness Matrix Method (SMM), the nodal equilibrium equations might be written in the matrix form as:

$$[K] \cdot \{\delta\} = \{f\} \tag{1}$$

where the displacements vector $\{\delta\}$ contains the horizontal, u_i, vertical deflections, v_i, and rotations, w_i, the external force vector $\{f\}$ contains the horizontal forces, H_i, vertical forces, V_i, and moments, M_i and the global stiffness matrix $[K]$ contains the stiffness of all the beam elements in the structure.

The traditional application of the SSM enables the calculation of nodal deflections from the loads applied to the structure assuming all the parameters in $[K]$ as known. This simulation is also known as the direct analysis of the SSM.

The $[K]$ matrix of a 2D beam element from the Euler-Bernouilli is presented in Figure 3.1a. This matrix is defined in terms of the length L_j, Young's Modulus, E_j, Inertia, I_j, and Area, A_j of each j_{th} element. An alternative stiffness matrix is presented in the literature (Tomas, et al. 2018) to deal with the shear deformation effects. This matrix is presented in Figure 3.1b and it is based on the Timoshenko theory. Stiffness matrices of both theories (Figures 3.1a and 3.1b) have the same axial stiffness coefficients. This is because the shear and flexural stiffnesses are uncoupled from the axial stiffness. However, for the rest of the non-null elements of the matrix, shear and flexural stiffnesses are coupled. In this case, the shear effects are defined by the shear parameter $\emptyset$. This coefficient was introduced by Przemieniecki, J.S. (1968) and it can be expressed as:

$$\emptyset = \frac{12EI}{GA_v L^2}, \tag{2}$$

where A_v is the shear area and G is the shear modulus that can be calculated in terms of the poisons ratio, ν, as:

$$G = \frac{E}{2(1 + v)} \tag{3}$$

a)

$$[K] = \begin{bmatrix} \frac{EA}{L} & 0 & 0 & -\frac{EA}{L} & 0 & 0 \\ 0 & \frac{12EI}{L^3} & \frac{6EI}{L^2} & 0 & -\frac{12EI}{L^3} & \frac{6EI}{L^2} \\ 0 & \frac{6EI}{L^2} & \frac{4EI}{L} & 0 & -\frac{6EI}{L^2} & \frac{2EI}{L} \\ -\frac{EA}{L} & 0 & 0 & \frac{EA}{L} & 0 & 0 \\ 0 & -\frac{12EI}{L^3} & -\frac{6EI}{L^2} & 0 & \frac{12EI}{L^3} & -\frac{6EI}{L^2} \\ 0 & \frac{6EI}{L^2} & \frac{2EI}{L} & 0 & -\frac{6EI}{L^2} & \frac{4EI}{L} \end{bmatrix}$$

b)

$$[K_s] = \begin{bmatrix} \frac{EA}{L} & 0 & 0 & -\frac{EA}{L} & 0 & 0 \\ 0 & \frac{12EI}{L^3(1+\emptyset)} & \frac{6EI}{L^2(1+\emptyset)} & 0 & -\frac{12EI}{L^3(1+\emptyset)} & \frac{6EI}{L^2(1+\emptyset)} \\ 0 & \frac{6EI}{L^2(1+\emptyset)} & \frac{EI(4+\emptyset)}{L(1+\emptyset)} & 0 & -\frac{6EI}{L^2(1+\emptyset)} & \frac{EI(2-\emptyset)}{L(1+\emptyset)} \\ -\frac{EA}{L} & 0 & 0 & \frac{EA}{L} & 0 & 0 \\ 0 & -\frac{12EI}{L^3(1+\emptyset)} & -\frac{6EI}{L^2(1+\emptyset)} & 0 & \frac{12EI}{L^3(1+\emptyset)} & -\frac{6EI}{L^2(1+\emptyset)} \\ 0 & \frac{6EI}{L^2(1+\emptyset)} & \frac{EI(2-\emptyset)}{L(1+\emptyset)} & 0 & -\frac{6EI}{L^2(1+\emptyset)} & \frac{EI(4+\emptyset)}{L(1+\emptyset)} \end{bmatrix}$$

Figure 3.1: Stiffness Matrix of a beam element: (a) Euler-Bernouilli's theory, (b) Timoshenko theory.

The latter formulation (Figure 3.1b) is traditionally used by most computer software to deal with shear effects in beam-like structures. To enable a direct simulation in this approach the shear rotations are neglected and the shear effects are only included into the horizontal and vertical deflections. Nevertheless, real structures do not behave that way. In fact, according to Timoshenko's beam theory, nodal rotations are produced by both bending and shear effects. On the one hand, bending rotations can be easily calculated by the Euler-Bernoulli SMM. On the other hand, shear rotations are traditionally neglected as their effects are practically negligible in most structures. This simplification assumption might lead to significant errors in the simulation of the structural response of actual structures. This chapter aims to illustrate the importance of shear rotations in some structures (such as deep beams). In addition, a new method is presented to calculate shear rotations. In this method, the shear rotations are calculated separately and added to the bending rotations computed from the SMM. In order to illustrate the structures where shear rotations cannot be neglected, a set of guidelines is proposed for different structures.

3.2 Detected gap 1: Analysis of shear rotations with the SMM

The analysis of the system of equations in the SMM shows that the shear rotations are systematically neglected in all kinds of beam-like structures. Many authors tried to develop methods to add the effects of these rotations to their stiffness matrices, but none of these methods can be applied in complex structural cases.

Nowadays, even commercial simulation programs based on the SMM (such as SAP 2000 (CSI, 2016) or Midas/ Civil. 2015) also neglect shear rotations. In these software total rotations are equal to the bending rotations and shear effects are only considered in the horizontal and vertical deflections. To show the inability of these methods to calculate the total value of the rotations, an illustrative example is presented in the following section.

3.2.1 Example 3.1: Simply supported beam

Consider the 10 m long and 0.2 m wide simply supported beam modeled with 3 nodes and 2 beam elements depicted in Figure 3.2.a. This structure can be considered as a deep beam, where shear effects are not negligible. This beam has a constant cross-section and the value of its young modulus, shear area, cross-sectional area, and inertia along the beam are 30 GPa, 0.833 m^2, 1 m^2, and 2.083 m^4, respectively. Dimensions of the beam cross-section are presented in Figure 3.2.b and its mechanical properties are listed in Table 3.1. The boundary conditions of the structure are horizontal and vertical displacements restricted in node 1 and vertical displacement restricted in node 3 (this is to say, $u_1=v_1=v_3= 0$). The beam is subjected to a concentrated vertical force in node 2 of 100kN (V_2=-100kN).

(a)

(b)
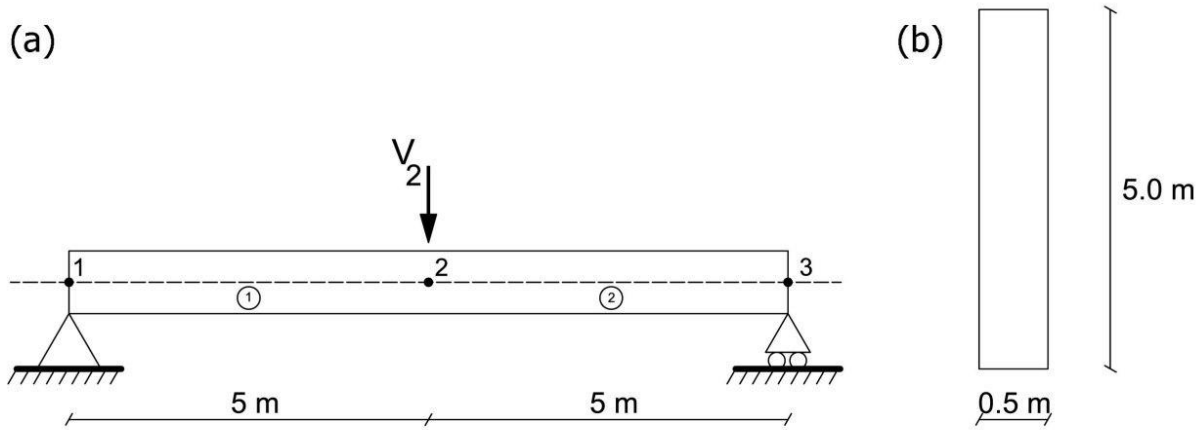
Figure 3.2: Example 3.1: Simply supported beam:) a) FEM and (b) Cross-section.

Table 3.1. Properties of the FEM of the simply supported beam.

Properties (unit)	Values
Area [m2]	1.000
Shear Area [m2]	0.833
Inertia [m4]	2.083
Concrete Young's Modulus [GPa]	30.000
Poisson's Ratio γ	0.250

To calculate the bending and shear response of the structure in this simple example, formulations based on Timoshenko beam theory can be used. The value of bending vertical deflections for the loading case presented in Figure 3.2.a, v_b at mid-span might be expressed by Equation (4). From Timoshenko [15], the value of vertical deflection due to shear, v_s at mid-span of this structure is calculated as in Equation (5). Also, the value of bending rotation w_b at node 1 is presented in Equation (6). Where V1 is the shear force at node number 1. Shear rotation w_s at the node number 1 can be calculated from Timoshenko's assumptions as it is presented in Equation (7).

$$v_b = \frac{V_2 \cdot L^3}{3 \cdot E \cdot I} \tag{4}$$

$$v_s = \frac{V_2}{2 * A_v * G} \cdot L \tag{5}$$

$$w_b = \frac{V_1 \cdot L^2}{4 \cdot E \cdot I} \tag{6}$$

$$w_s = \frac{V_1}{A_v \cdot G}$$

<div align="right">(7)</div>

To show the inability of different structural analysis methods to calculate the shear rotations, the vertical deflections and total rotations (sum of rotation due to shear and bending) of Example 3.1 obtained from the commercial software SAP2000, common Timoshenko SMM (Przemieniecki, J.S. 1968) and formulations based on Timoshenko beam theory are compared in Table 3.2.

<div align="center">Table 3.2: Properties of the FEM of the simply supported beam.</div>

Methods	Total rotation in node 1 (rad)	Bending rotation in node 1(rad)	Total vertical deflection in node 2 (m)
SAP2000	0.010	0.010	-0.058
Common Timoshenko SMM	0.010	0.010	-0.058
Formulation based on Timoshenko beam	0.015	0.010	-0.058

As can be seen in Table 3.2, the value of total rotation and bending rotation obtained by SAP2000 are equal to each other. This means that the effects of the shear rotations are neglected by this software. This table also shows that the effects of shear rotations are disregarded in common Timoshenko SMM. In this particular case, the results of hand calculation for total rotations (0.015 rad) are 50 % higher than those obtained by the other analyzed methods. These results illustrate the important role that shear rotations might play and the fact that they are systematically neglected (independently of the beam geometry) in all structural analysis methods based on the SMM.

In the case of the vertical deflections, Table 3.2 shows that all methods include properly the shear effects as the same results are obtained by all the analyzed procedures. Obviously, the magnitude of the shear rotations depends greatly on the beam geometry. To show in which cases shear rotation can be considered negligible and when it should be introduced into the simulation, a new simulation method is proposed in the following section and a parametric analysis is performed.

3.3 New simulation method for the analysis of shear rotations in beams

To introduce the effects of shear rotation into the common Timoshenko's SMM, a new procedure is developed in this section. In this procedure, firstly, the bending rotation of each node can be computed by the SMM. Then, the shear rotation of each element is calculated by the formulations based on the Timoshenko beam method presented in Equation (7). According to this equation, the shear rotation for each element can be calculated only by shear forces, shear areas, and shear modulus. The latter two terms (shear area and shear modulus) can be directly obtained from the mechanical properties of the structure, while the shear forces are obtained from the results of the SMM analysis. By summing up the value of shear and bending rotation the total rotation of each node can be obtained. The new method is presented in Figure 3.3 and summarized by the following steps:

- **Step 1:** Compute the bending rotation of each node by the SMM.

- **Step 2:** Calculate the shear rotations of each element with the shear forces obtained in (1).

- **Step 3:** Obtain the total rotation at the beam edges by summing up the value of the shear and the bending rotations obtained in Steps (1) and (2). It is to highlight that shear rotations are proportional to the shear diagram. Hence, discontinuities in the shear diagram introduced by point loads or reactions imply discontinuities in the shear rotations. Elements converging to the same node can have different rotations at these points.
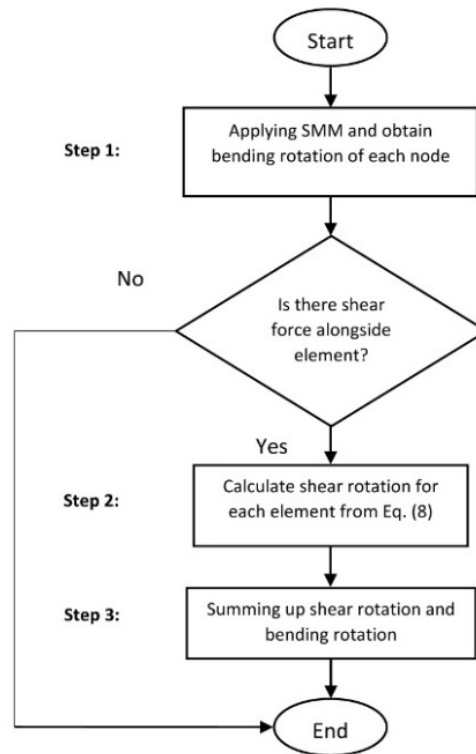
Figure 3.3: Flow chart of the procedure of adding shear rotation into the common SMM.

The optimization algorithm used for the COM is the "fmincon" function of MATLAB (2018). This function is a minimum finder of a constrained nonlinear multivariable function in MATLAB program. MATLAB (2018) is a multi-paradigm numerical computing environment and MathWorks developed proprietary programming language. This program helps to manipulate matrixes, to map functions and results, to apply algorithms, to construct user interfaces, and to communicate with programs written in other languages.

In the following sections, a set of parametric analyses using the new method is performed on beams with different geometry, to evaluate when the effect of the shear rotation is significant. This study is included into the paper presented in Appendix 1 recently submitted for publication.

3.3.1 Example 3.2: Simply supported beam with a concentrated load

Consider the cross-section of the simply supported beam presented in Figure 3.2.b. Material properties of the simply supported beam can be found in Table 3.1. The boundary conditions of the structure are horizontal and vertical displacements due to bending restricted in node 1 and vertical displacement restricted in node 3 (this is to say, $u_1=v_1=v_3=0$), and the only external force applied in this numerical loading test is a concentrated vertical force of 100kN at node 2 ($V_2=-100kN$). To evaluate the effect of the shear rotations at node number 1, a parametric analysis is carried out. In this analysis, the length of the beam (L) varies from 1 to 15 meters while the height (h) remains constant.

As expected, Figure 3.4 illustrates how the slenderer the beam, the lower the effect of the shear deformation is. As presented in Figure 3.4a, the shape of the shear rotation variation is linear which means that this parameter is independent of the length of the beam. In fact, the value of shear rotation for different L/h ratios is always equal to 0.005 radians. The values of the bending rotations vary from 0.0025 to 0.5625 rad where the L/G ratios range between 1 and 15. The percentage of error when shear rotations are neglected for different L/h ratios is shown in Figure 3.4.b. For illustrative purposes, the limits of 2 % and 5% are also indicated in this figure. The ratio limits for deep beams proposed by the Eurocode EN and by the ACI Committee 318 are also highlighted.
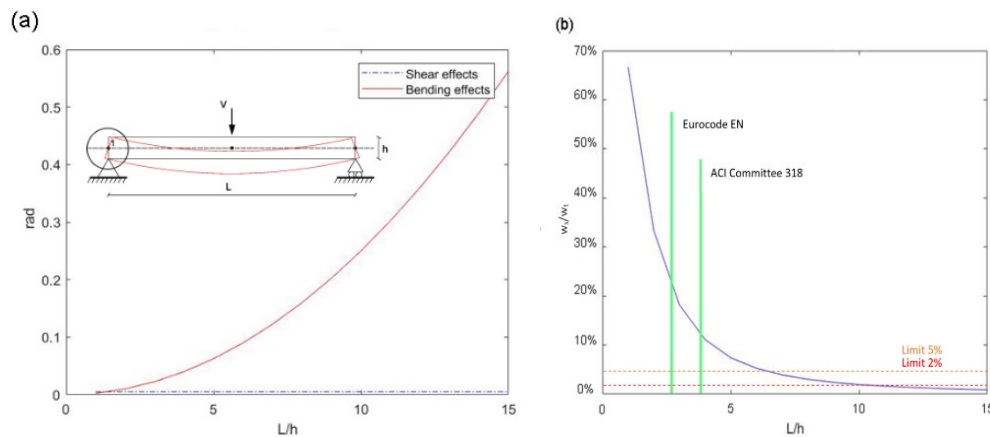
Figure 3.4: Example 3.2: (a) Rotation due to bending and shear at node 1. (b) Percentage of error in the rotation in node 1 when the shear rotations are neglected.

In Figure 3.4b, a 5 % error is gained when L/h ratio is equal to 6.197. In the same way, a 2 % error corresponds to a beam L/h ratio of 9.914. In addition, the measurement error in node 1 is 18.185 percent where the ratio of L/h is 3 (deep beam limitation by Eurocode EN) and it is 11.113 percent when the L/h ratio is 4 (ACI Committee 318 proposed limitation).

3.3.2 Example 3.3: Simply supported beam with a distributed load

Consider a beam with the same material properties and boundary conditions of the simply supported beam presented in Example 3.1. The external force in this numerical loading test is a distributed vertical force of 100/L kN applied alongside the beam, in such a way that the total load in the beam equals 100 kN. A parametric analysis is carried out to illustrate the role of the shear rotations in a beam with different geometries. The length (L) of this beam is varied from 1 to 15 meters and its height (h) is considered constant. As presented in Figure 3.5a, the value of shear rotation in terms of the L/h ratio is constant with an equal to 0.005 rad. The values of bending rotations vary from 0.001 to 0.409 rad when the L/h ratios range between 1 and 15. The percentage of error when shear rotation is neglected for different L/h ratio is shown in Figure 3.5b. The ratio limits for deep beams proposed by the Eurocode EN and by the ACI Committee 318 are also highlighted together with the 2 % and 5% error limits.
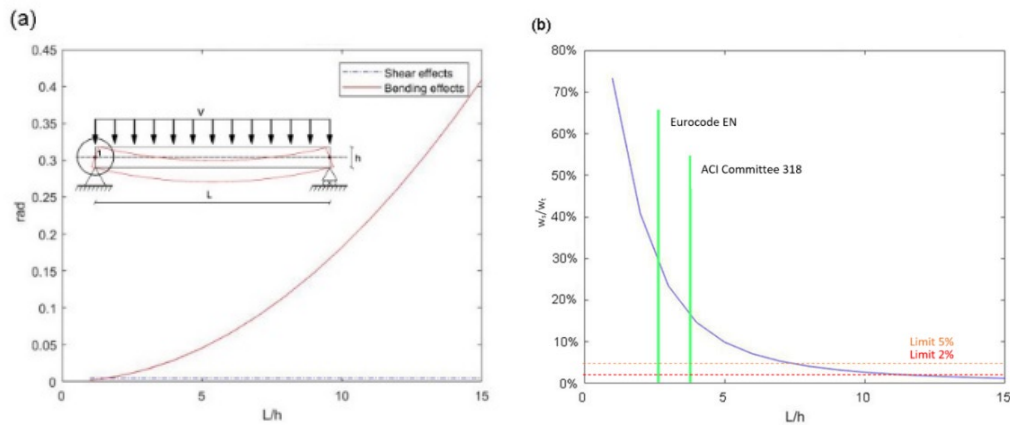
Figure 3.5: Example 3.3: (a) Rotation due to bending and shear at node 1. (b) Percentage of error in measurement in node 1 when shear rotations are neglected.

As expected, Figure 3.5a shows in deep beam effects of shear rotations are higher than in slender ones. In Figure 3.5b, errors in rotations in different lengths of elements for node 1 are presented. A 5 % error is gained when the L/h ratio is equal to 7.265. In the same way, a 2 % error corresponds to a L/h ratio of 11.639. In addition, the measurement error in node 1 is 23.409 % when the ratio of L/h is 3 (deep beam limitation by Eurocode EN) and 14.670 % when the L/h ratio is 4 (ACI Committee 318 proposed limitation).

3.3.3 Example 3.4: Cantilever Beam

Consider a cantilever beam with the same cross-section and same properties as in Example 3.1 modeled with a single beam element and two nodes. The boundary conditions of the structure are horizontal and vertical displacements and rotation due to bending restricted in node 1 (this is to say, $u_1=v_1=w_{b1}=0$). The only external force applied in this numerical loading test is a concentrated vertical force at node 2 of 100kN ($V_2=-100$kN). A parametric analysis is carried out to evaluate

the role of the shear rotations on node 2. In this analysis, the length of the beam (L) is varied from 1 to 15 meters and its height (h) is considered constant.

As presented in Figure 3.6a, the shape of the shear rotation variation is constant and the value of shear rotation in different L/h is equal to 0.010 rad. But the values of bending rotations vary from 0.020 to 4.501 rad when the L/h ratios change between 1 and 15. As expected, Figure 3.6.a shows how in deep cantilever beams the effects of shear rotations are greater than those obtained in slender ones. The percentage of error when shear rotation is neglected for different L/h ratio is shown in Figure 3.6.b. As in previous figures, the ratio limits for deep beams proposed by the Eurocode EN and by the ACI Committee 318 are highlighted together with the 2% and 5% limits.
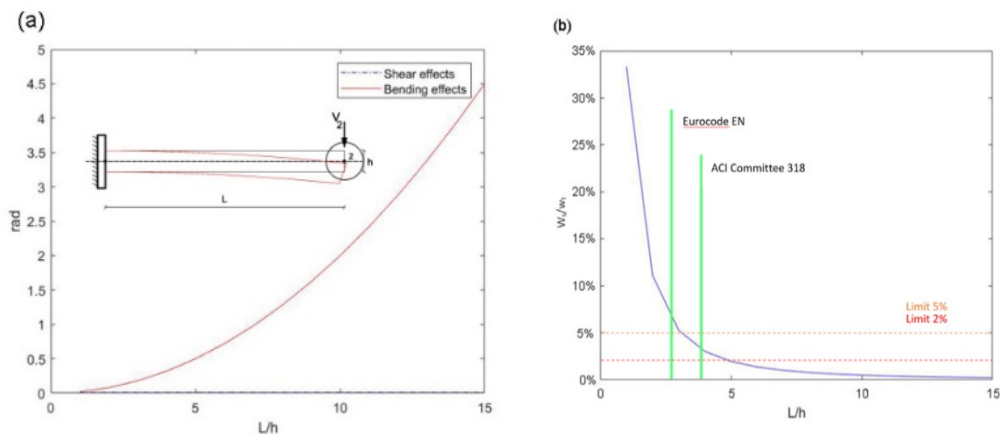
Figure 3.6: Example 3.4: (a) Rotation deflection due to bending and shear at node 2. (b) Percentage of error in measurement in node 2 when shear rotations are neglected.

In Figure 3.6b, a 5 % error is expected when L/h ratio is equal to 3.118. In the same way, a 2 % error corresponds to a L/h ratio of 4.964. Also, the measurement error in node 2 is 5.264 % when the ratio of L/h is 3 (deep beam limitation by Eurocode EN) and 3.031 % when the L/h ratio is 4 (ACI Committee 318 proposed limitation).

3.4. Example of application

To show the applicability of the new method in complex structures, the problem of bridge construction by the balanced cantilever method is analyzed in this section. In this kind of erection technique, the deflections of different segments have to be forecasted, to build the new segments with the proper precamber. Precamber is updated for each step of construction after a thorough topographical survey. This data can be used by inverse analysis for model updating to increase the accuracy of the precamber calculations. Although shear deflections may not be very important for a fully developed cantilever, the modeling error due to the neglecting of shear effects for the first segments may lead to inaccurate estimations of bending stiffnesses (Valerio, P. et al. 2011).

The structure chosen for this example is a simplified model of an intermediate construction stage of the Yunbao Bridge over the Yellow River in China (see Figure 3.7a). The bridge includes a series of spans of 48m+9×90m+48m. This structure is a rigid frame-continuous composite bridge 906 meters long. The height of the box girder beam ranges 5.5m to 2.7m from the supported end to the mid-span with a parabola curve of 1.8 power (Dong, X. et al. 2017). The analyzed construction stage of the balanced cantilever method is 29.5 m long and contains 3 segments on each side of the stage (2.5 m). The formwork traveler at the end of each span is presented in Figure 3.7b.
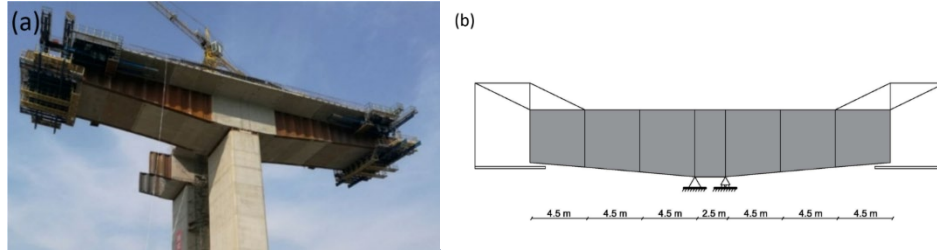
Figure 3.7: Example of application: (a) Yunbao Bridge under construction in China (Dong, X. et al. 2017) (b) Sketch of the analyzed construction stage.

The connection between the concrete and the steel is assumed as rigid (total connection), and the relative slip between both materials is neglected. A typical cross-section of the composite deck is presented in Figure 3.8a. The FEM of the analyzed structure is composed of 8 nodes and 7 beam elements as presented in Figure 3.8b. The mechanical and material properties of this structure (EA, GA_v and EI) are listed in Table 3.3.
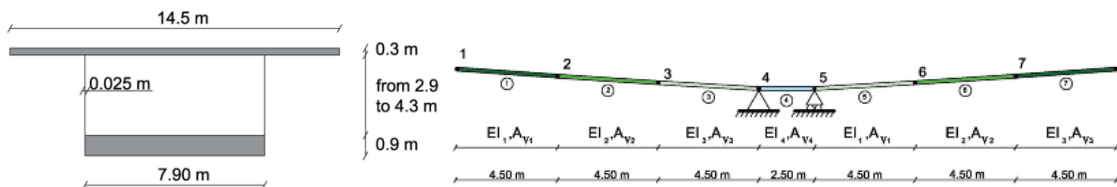
Figure 3.8: Numerical analysis: (a) Cross-section of Yunbao Bridge in China. (b) FEM of the bridge.

Table 3.3: Properties of the Finite Element Model of the Bridge.

Parameters	Elements 1 and 5	Elements 2 and 6	Elements 3 and 7
EA [m^2]	4.33E+11	4.38E+11	4.43E+11
GA_v [m^2]	1.10E+10	1.25E+10	1.43E+10
EI [m^4]	1.34E+12	1.69E+12	2.13E+12

The analyzed loading case is presented in Figure 3.9, where the weight F of the formwork traveler (1041 kN) (presented in Figure 3.7b) is assumed as 60% of the maximum weight of the bridge segment. The effect of each form traveler in the deck is assumed as a pair of vertical forces of

values 0.25F and 1.25F (226 kN, upwards and 1267 kN, downwards) as presented in Figure 3.9a the analyzed loading case results from the combination of the loads applied by form traveler and the weight of the bridge segments. The segment's loads are considered distributed loads alongside segments. The resultant loading case introduced in the simulation is shown in Figure 3.9b.
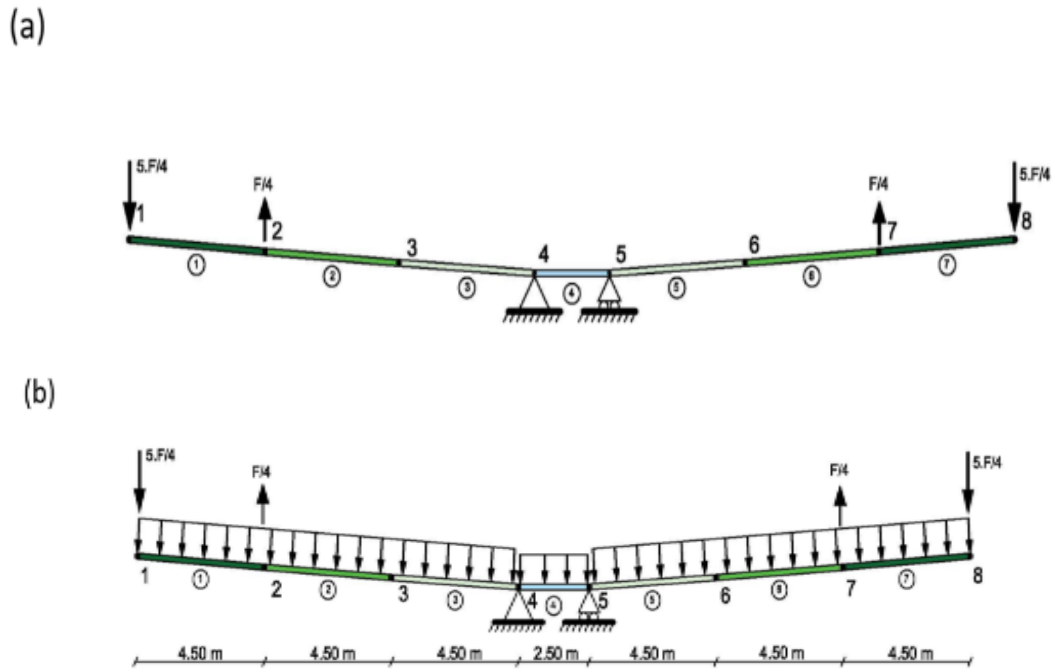
Figure 3.9. Loading case: (a) Loads applied by formwork traveler. (b) Loading case used for the analysis.

The rotations in the nodes of the structure were calculated by the proposed method. The results obtained from the new method and the ratio between the shear rotation and bending rotation are presented in Table 3.4.

Table 3.4: Rotation in nodes calculated by the new method.

Node number	Shear rotation w_s (rad)	Bending rotation w_b (rad)	Percentage of error in the model (w_s/w_t)
1	-1.23E-04	-1.29E-04	48.93%
2	-1.68E-04	-1.16E-04	59.08%
3	-2.17E-04	-7.90E-05	73.28%

In this example, the maximum error in the calculations of shear rotations is obtained at nodes 3 and 6. This will lead to an error in the calculation of the total nodal rotation of 73.420%. In comparison with results from other Timoshenko's beam methods, obtained results prove the potential power of the proposed method. In addition, they show the applicability of the new method where cross-sections are discontinued, elements are non-collinear and there are external loads applied in the different elements. It is important to highlight that no other Timoshenko beam theory

FEM in literature is able to calculate total rotation (including both shear and bending effects) in structural schemes with such features.

3.5. Conclusions

Stiffness Matrix Methods (SMM) are the most common analysis tool in beam-like structures. In fact, most commercial computer software is based on this procedure. The literature review showed that the SMM only introduces shear effects in axial and vertical deflections. Nevertheless, these methods usually neglect the shear rotations as the magnitude of this deformation is usually less significant than the bending one. Despite the important role that this rotation might play in structural members with a low span-to-depth ratio, no detailed study of the shear rotations is presented in the literature. To fill this gap, this chapter proposes a new general method for the direct calculation of shear rotations in beams. It is important to highlight that no other Timoshenko beam theory method in literature is able to calculate total rotation (including both shear and bending effects) in a structural model including the same features.

To illustrate the important role of shear rotations in some structures, different beams (a simply supported beam with a concentrated load, a simply supported beam with a distributed load, and a cantilever with a concentrated load) with different length to height ratios are studied. In fact, these examples illustrate that the difference between Timoshenko's theory and Euler-Bernoulli's theory in terms of rotation is higher for deep beams with low length-to-height ratio. In addition, the geometries (length-to-height ratio) where the shear rotations can be neglected are identified.

Chapter 4: Observability Method including shear effects without rotations

4.1. Introduction

In the inverse analysis of structures with the Observability Method (OM), the stiffness matrix [K] is partially unknown and its parameters are obtained from the deflections and rotations measured on-site. To determine the unknown stiffnesses (EA_j and EI_j) of this matrix, Equation (1) might be reordered into the following system of equations:

$$[K^*] \cdot \{\delta^*\} = \{f\}, \tag{8}$$

in which the products of unknowns are located in the modified vector of displacements $\{\delta^*\}$ and the modified stiffness matrix [K*] is a matrix of known coefficients with different dimensions than the initial stiffness matrix [K]. The new system leads to a non-linear problem due to the fact that unknown parameters, such as axial stiffness EA_j and flexural stiffness EI_j of the cross-sections are multiplied by the unknown horizontal displacements (u_i), vertical displacements (v_i), and rotations at the ith node (w_i) of vector $\{\delta^*\}$. This fact implies that non-linear products of variables (polynomial terms), such as EA_{jui}, EA_{jvi}, EI_{jui}, EI_{jvi}, and EI_{jwi} might appear. Depending on the known information, the unknown variables of vector $\{\delta^*\}$ may be the non-linear products presented above, as well as other factors of single variables, such as EI_j, EA_j, or nodal deflections and rotations.

Once the boundary conditions and the applied forces in the nodes have been defined, an inverse analysis can be performed to identify the unknown parameters. To do so, some deflections and rotations are measured in a known static test. This known information is clustered in a subset δ_1^* of $\{\delta^*\}$ and a subset f_1 of $\{f\}$, respectively. In this way, the remaining subset δ_0^* of $\{\delta^*\}$ and f_0 of $\{f\}$ are unknown. Hence, Equation (8) might be written as follows:

$$[K^*] \cdot \{\delta^*\} = \begin{bmatrix} K_{00}^* & K_{01}^* \\ K_{10}^* & K_{11}^* \end{bmatrix} \cdot \begin{Bmatrix} \delta_0^* \\ \delta_1^* \end{Bmatrix} = \begin{Bmatrix} f_0 \\ f_1 \end{Bmatrix} = \{f\}, \tag{9}$$

In order to join the unknown variable in the left-hand side and the known variable in the right-hand side, the Equation (9) is rearranged as:

$$[B] \cdot \{z\} = \begin{bmatrix} K_{10}^* & 0 \\ K_{00}^* & -I \end{bmatrix} \cdot \begin{Bmatrix} \delta_0^* \\ f_0 \end{Bmatrix} = \begin{Bmatrix} f_1 - K_{11}^* \delta_1^* \\ -K_{01}^* \delta_1^* \end{Bmatrix} = \{D\}, \tag{10}$$

where 0 and I are the null and the identity matrices, respectively. In this system, the vector of unknowns, $\{z\}$, appears on the left-hand side and the vector of observations, $\{D\}$, on the right-hand side. Both vectors are related by a matrix of known coefficients [B].

To evaluate if the system has a solution, the null space $[V]$ of matrix $[B]$ should be calculated and check that $[V]^T\{D\} = 0$. If the equation holds, the system is compatible; otherwise, it has no solution. The general solution (the set of all solutions) of the system (10) has the structure (Castillo, E. et al.2000, Castillo, E. et al.2002):

$$\{Z\} = \{Z_{\mathrm{p}}\} + [V] \cdot \{\rho\}, \tag{11}$$

where $\{Z_{\mathrm{p}}\}$ is a particular solution of the system (11). This term can be obtained in MATLAB by two alternative routines: (1) Backslash function (/) and (2) Moore-Penrose pseudoinverse (pinv). $[V].\{\rho\}$ is the set of all solutions of the associated homogeneous system of equations (a linear space of solutions, where the columns of $[V]$ are a basis of this linear space and the elements of the vector $\{\rho\}$ are arbitrary real values that describe the coefficients of all possible linear combinations). It should be noted that a variable has a unique solution not only when matrix $[V]$ has zero dimension (it does not exist), but when the associated row in the matrix $[V]$ is null. Thus, the examination of the matrix $[V]$ and identification of its null rows leads to the identification of the subset of variables with a unique solution in vector $\{Z\}$. It is interesting to note that if all parameters of vector $\{Z\}$ are not observed from the null space, any deflection, force, or parameter observed after the initial OM analysis will be used to observe new parameters by using a recursive process. For more information about this process, the reader is addressed to Lozano-Galant JA. et al. (2013).

As showed in Table 1.1, the shear deformation effects were first introduced into the OM by Tomás et al. (2018). This formulation is based on Timoshenko's beam theory and it uses the stiffness matrix [K] presented in Figure 3.1.b. Analysis of this stiffness matrix shows that shear parameter Ø appears in the denominator of most terms. To solve this problem, Tomas et al. (2017) proposed the following change of variable Q:

$$Q = \frac{\text{Ø}}{1 + \text{Ø}} \tag{12}$$

After replacing the shear parameter Ø by OM shear parameter Q, the stiffness matrix [K] in Figure 3.1.b can be written as:

$$[K] = \begin{bmatrix} \dfrac{EA}{L} & 0 & 0 & -\dfrac{EA}{L} & 0 & 0 \\[2mm] 0 & \dfrac{12EI}{L^3} - \dfrac{12EIQ}{L^3} & \dfrac{6EI}{L^2} - \dfrac{6EIQ}{L^2} & 0 & -\dfrac{12EI}{L^3} + \dfrac{12EIQ}{L^3} & \dfrac{6EI}{L^2} - \dfrac{6EIQ}{L^2} \\[2mm] 0 & \dfrac{6EI}{L^2} - \dfrac{6EIQ}{L^2} & \dfrac{4EI}{L} - \dfrac{3EIQ}{L} & 0 & -\dfrac{6EI}{L^2} + \dfrac{6EIQ}{L^2} & \dfrac{2EI}{L} - \dfrac{3EIQ}{L} \\[2mm] -\dfrac{EA}{L} & 0 & 0 & \dfrac{EA}{L} & 0 & 0 \\[2mm] 0 & -\dfrac{12EI}{L^3} + \dfrac{12EIQ}{L^3} & -\dfrac{6EI}{L^2} + \dfrac{6EIQ}{L^2} & 0 & \dfrac{12EI}{L^3} - \dfrac{12EIQ}{L^3} & -\dfrac{6EI}{L^2} + \dfrac{6EIQ}{L^2} \\[2mm] 0 & \dfrac{6EI}{L^2} - \dfrac{6EIQ}{L^2} & \dfrac{2EI}{L} - \dfrac{3EIQ}{L} & 0 & -\dfrac{6EI}{L^2} + \dfrac{6EIQ}{L^2} & \dfrac{4EI}{L} - \dfrac{3EIQ}{L} \end{bmatrix} \tag{13}$$

When this new stiffness matrix is introduced into the OM a new variable has to be calculated in addition to the axial (EA) and flexural (EI) stiffness. This new variable is named shear stiffness (EIQ) and it is related to the shear deflections and the shear parameter Ø.

4.2: Detected gap: Rotations are required for inverse analysis of the OM including shear effects

According to the literature, more reliable information can be produced from measuring vertical displacement than rotation and most of international standards deal with vertical deformation (Vicente, M.A. et al. 2018, AASTHO.2017, European Committee for Standardization 2005). So it is useful to provide a method that allows SSI from measured vertical deflections. Unfortunately, the OM proposed by Tomas et al. 2018 fails to identify structural parameters with measurement sets including only vertical deflections. In fact, the measurement of both deflections and rotations is always required to observe any parameter. This limitation comes from a basic feature of the OM: the linearization of the unknown variables (for example the product of the variables E, I and Q is defined as a new linear variable named EIQ). This assumption might result in a significant loss of information that leads to wrong estimation values. The limitation of the OM to enable the identification of structural parameters with only vertical deflections is illustrated in the following academic example.

4.2.1 Example 4.1: Simply supported beam with vertical deflections

Consider the 0.6 m long simply supported beam modeled with 7 nodes and 6 Timoshenko beam elements in the FEM of Figure 4.2a, where, v_j, with j (1 to 7) represents the vertical deflection for each node. The beam has a constant cross-section and the value of Young modulus, E, Poisson's ratio, ν, shear area, A_v, cross-sectional area, A, and inertia, I, of all elements along the beam are constant. Properties of this simply supported beam are listed in Table 4.1. The boundary conditions of the structure are horizontal and vertical displacements restricted in node 1 and vertical displacement restricted in node 7 (this is to say, $u_1=v_1=v_7= 0$), and the only external force applied in this numerical loading test is a concentrated vertical force in node 3 of 100kN ($V_3= 100$kN). The vertical deflections obtained from the software Midas/Civil of this structure are presented in Figure 4.2b.
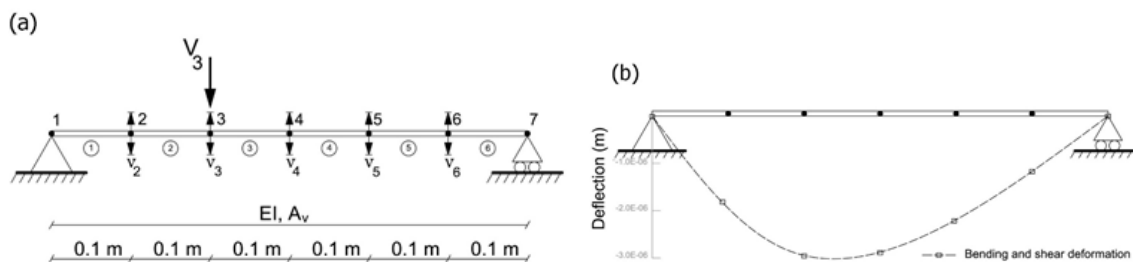
Figure 4.1: Example 4.1: (a) FEM for a simply supported beam with vertical deflections. (b) Vertical nodal deflections including flexural and shear deformation.

Table 4.1: Properties of the FEM of the simply supported beam.

Property	Value
Area [m^2]	0.1
Shear Area [m^2]	0.0833
Inertia [m^4]	0.0083
Young's Modulus [GPa]	27
Poisson's Ratio γ	0.25

For this inverse analysis of the structure, V3, the length, L, Poisson's ratio, v and Young modulus, E, of all elements are assumed as known, while the inertia I and the shear area A_v are assumed as unknown. Since no horizontal forces are applied to the structure, the axial resistant mechanisms are not activated. So the terms associated with axial behavior are removed from the general SMM system of equations.

Since the only two unknown parameters assumed in Example 4.1 are A_v and I, the measurement of at least two deformations is required to identify their values. Nevertheless, no set of vertical deflections enables the proper identification of the unknown parameters. To illustrate this inability of the method, the results of the SSI obtained with the measurement set consisting of all 5 possible vertical deflections (this is v_2 to v_6 from Figure 4.2b) are presented. In this example, after the change of variable, the vector of unknowns {Z}, as it is presented in Eq. (11), include the unknown targeted parameters I and Q and some coupled unknown variables as I_{wj} and Q_w, as well as the boundary reactions (H_1, V_1, V_7). The general solution can be written as follows:

$$
\begin{bmatrix} I \\ Iw_1 \\ Iw_2 \\ Iw_3 \\ Iw_4 \\ Iw_5 \\ Iw_6 \\ Iw_7 \\ Q \\ Qw_1 \\ Qw_2 \\ Qw_3 \\ Qw_4 \\ Qw_5 \\ Qw_6 \\ Qw_7 \\ H_1 \\ V_1 \\ V_7 \end{bmatrix} = \begin{Bmatrix} 8.0E-07 \\ 5.0E-12 \\ 4.0E-12 \\ 2.0E-13 \\ 4.0E-12 \\ 7.0E-12 \\ 9.0E-12 \\ 1.0E-11 \\ 0.0 \\ 0.0 \\ 2.0E-11 \\ 0.0 \\ 0.0 \\ 0.0 \\ 0.0 \\ 0.0 \\ 0.0 \\ -6.7E04 \\ -3.3E04 \end{Bmatrix} + \begin{bmatrix} 1 & \frac{L}{20*(v_5-2*v_6)} & 0 & \frac{-L}{20*(v_5-2*v_6)} \\ 0 & \frac{-v_6}{2*(v_5-2*v_6)} & \frac{1}{2} & \frac{v_5-v_6}{2*(v_5-2*v_6)} \\ 0 & \frac{-v_6}{2*(v_5-2*v_6)} & \frac{1}{2} & \frac{v_5-v_6}{2*(v_5-2*v_6)} \\ 0 & \frac{-v_6}{2*(v_5-2*v_6)} & \frac{1}{2} & \frac{v_5-v_6}{2*(v_5-2*v_6)} \\ 0 & \frac{-v_6}{2*(v_5-2*v_6)} & \frac{1}{2} & \frac{v_5-v_6}{2*(v_5-2*v_6)} \\ 0 & \frac{-v_6}{2*(v_5-2*v_6)} & \frac{1}{2} & \frac{v_5-v_6}{2*(v_5-2*v_6)} \\ 0 & \frac{-v_6}{2*(v_5-2*v_6)} & \frac{1}{2} & \frac{v_5-v_6}{2*(v_5-2*v_6)} \\ 0 & \frac{-v_6}{2*(v_5-2*v_6)} & \frac{1}{2} & \frac{v_5-v_6}{2*(v_5-2*v_6)} \\ 1 & 0 & 0 & 0 \\ 0 & \frac{-2*(v_2-v_3+v_4-v_5+v_6)}{(v_5-2*v_6)} & 0 & \frac{2*v_2-2*v_3+2*v_4-v_5}{(v_5-2*v_6)} \\ 0 & \frac{(v_2-2*v_3+2*v_4-2*v_5+v_6)}{(v_5-2*v_6)} & 1 & \frac{-(v_2-2*v_3+2*v_4-2*v_5+v_6)}{(v_5-2*v_6)} \\ 0 & \frac{(v_3-2*v_4+2*v_5-2*v_6)}{(v_5-2*v_6)} & 0 & \frac{-(v_3-2*v_4+v_5)}{(v_5-2*v_6)} \\ 0 & \frac{(v_4-2*v_5+v_6)}{(v_5-2*v_6)} & 1 & \frac{-(v_4-2*v_5+v_6)}{(v_5-2*v_6)} \\ 0 & 1 & 0 & 0 \\ 0 & 0 & 1 & 0 \\ 0 & 0 & 0 & 1 \\ 0 & 0 & 0 & 0 \\ 0 & 0 & 0 & 0 \\ 0 & 0 & 0 & 0 \end{bmatrix} \cdot \begin{bmatrix} \rho_1 \\ \rho_2 \\ \rho_3 \\ \rho_4 \end{bmatrix} \quad (14)
$$

According to the definitions of the observability techniques, when the associated row in the matrix $[V]$ (the null space matrix) is null, the variable has a unique solution. In this example, the three rows of the null space (the ones corresponding with reactions H_1, H_7 and V_7) are null. The general solution of these variables corresponds with the particular one and therefore, their solution is unique. In the next recursive step, the observed parameters are incorporated into the input of SSI by OM. Although these new inputs will update Equation (14), the updated system of equations cannot observe any new variable. Hence, the recursive steps end, and no additional information is observed. It is to remark that the only observed parameters correspond with the reactions of an isostatic structure which can be identified by equilibrium equations. This is not the case of the Inertia and the OM shear parameter, I and Q, as they appear strongly coupled with the rotations. These parameters cannot be observed as their null space is not null. This example illustrates the inability of OM to identify parameters when rotations are not included into the measurement set (even if as in this case the number of measurements exceeds the number of unknowns). As variables are strongly coupled, those equations dealing with including the effect of rotation cannot be used to solve the system, unless some rotations are included in the measurement set. In order to uncouple the variables in the system of equations properly, vertical deflection and rotation should be measured together. Otherwise, the system cannot be solved by OM. A mathematical explanation

of this fact is that the null space rows associated with the inertia will not be zero, meaning that the parameters have not a unique solution. In order to enable the observability to identify structures without measuring rotations, a new procedure is presented in the following section.

4.3: New method for the inverse analysis from vertical deflections

Lei et al. (2017) found that in OM, the nonlinear constraints among product variables are lacking. According to this work, the reduced observability produced by these characteristics is due to the following reasons: (a) the immature end of the recursive steps and (b) the ineffective measurements because of redundancy in the measurement sets (the same problem appearing in Example.4 1). The Constraint Observability Method (COM) finds a solution to the OM adding some nonlinear constraints: the value of the solution of the coupled unknowns (e.g. EI_{wj} or EQ_{vj}) has to be equal to the product of the single parameters (such as $E \cdot I \cdot w_j$ or $E \cdot Q \cdot v_j$, respectively). Hence, the system of equations is solved numerically by minimizing numerical errors after including the nonlinear constrains.

In comparison with the original OM, this new approach does not provide any symbolic solution and initial numerical values of the unknown parameters are required. Any number can be used as initial values, but in order to ease the convergence in the optimization process, a ratio with the theoretical values (e.g. between 0.5 to 1.5) is traditionally used.

In the COM variables are classified in one of the following three categories: (1) Coupled variables V_c (such as I_{wj} or Q_{wj}) ; (2) Single variables V_{s1} (such as I or Q), which already exist in the unknown $\{Z\}$ vector; (3) Single variables V_{s2} (such as w_j), which did not exist in the unknown vector $\{Z\}$ from OM. All these variables are introduced into a new vector $\{Z\}$ named $\{Z^*\}$ that is a combination of the original $\{Z\}$ and the new single variables V_{s2}.

In order to create an objective function for a numerical optimization process and take into account, the new unknowns V_{s2}, Equation (10) can be rewritten as:

$$\{\in\} = [B^*] \cdot \{Z^*\} - \{D\}, \tag{15}$$

where $\in$ is the residuals of the equations which is a vector with the same number of rows of the original matrix B and $B^* = [B^{N_{eq} \times N_z} | \Omega^{N_{eq} \times N_{s2}}]$ is obtained by adding a null matrix Ω to the matrix B calculated from the last recursive step of SSI by OM. The size of this null matrix Ω is $N_{eq} \times N_{s2}$. N_{eq} and N_z, explain the number of equations and the number of unknowns in $\{Z\}$ respectively. N_{s2} explains the number of new single unknowns in V_{s2}.

The objective function of the minimization problem is determined by minimizing the square sum of the residuals in Equation (15). In order to reach a certain level of efficiency in the COM optimization process, the variables in this equation should be normalized.

Originally, COM method is not able to consider the effect of shear in measurements. To include this phenomenon, in this work, equations are updated to the procedure proposed by Tomás et al. (2018). With this new updated method, the problem of linearization in OM variables is solved and equations related to shear stiffnesses are taken into account. This new procedure enables to identify structural parameters in structures with shear deformation by only measuring vertical deflections. The results of this work were published in Emadi et al. (2019). This work is included in Appendix 2.

The proposed application of the COM is as follows:

- **Step 1**: Apply the OM to check whether any unknown is observed (the parameters can be identified with a unique solution). If so, update the input and reinitiate OM until no new unknowns are observable. If full observability (all the pursued parameters are observed) is achieved, there is no need to go to the COM process, otherwise, go to step 2.

- **Step 2**: Obtain Equation (16) from the last step of OM recursive process then generate the new unknown vector of Z* included Coupled variables V_c; as well as single variables V_{s1} and V_{s2}.

- **Step 3**: Add a null matrix $[\Omega]$ to the matrix $[B]$ to generate $[B^*]$, in order to contain V_{s2} in Z* guaranteeing that the system of equations is satisfied.

- **Step 4**: Obtain the normalized unknown parameters.

- **Step 5**: Guess the initial values of unknowns parameters of Z* vector, set the bound for the solution and solve the optimization process to find the minimized value for the residual vector, $\in$.

A summary of the procedure is shown in the flow chart in Figure 4.2. For more information about the COM, the reader is addressed to (Lei. et al. 2017). In the proposed optimization, the optimal solution of the objective function was obtained by the optimization toolbox of Matlab (MATLAB and Optimization Toolbox Release 2018). In order to limit the computational expense and the time of the optimization process, the stopping criterion has been defined based on the value of the norm of the residual vector, $\in$ (Equation (15)). When this is smaller than 1e-8 the iterations stop.
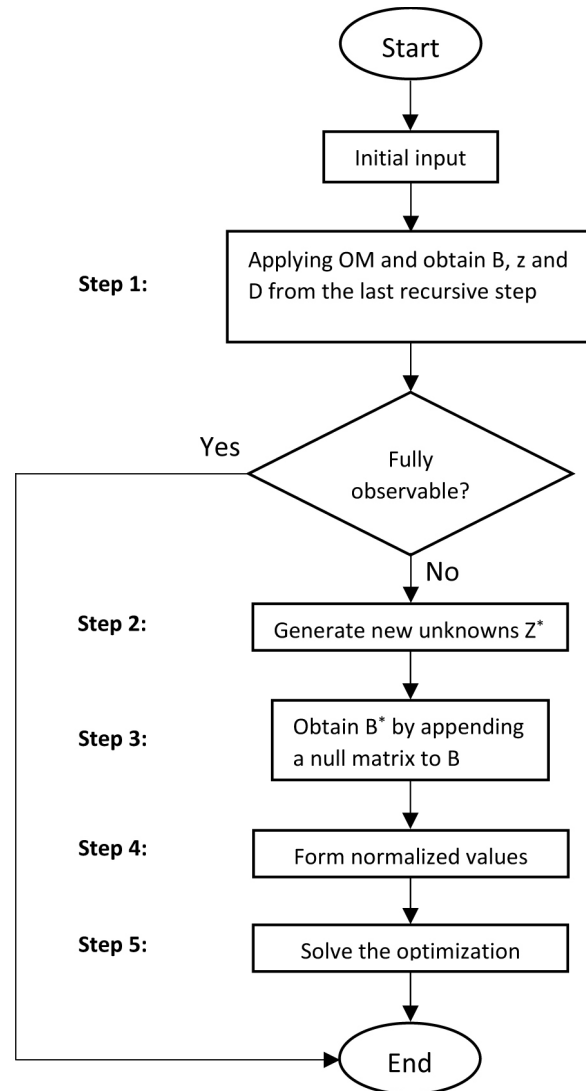
Figure 4.2: Flow chart of structural system identification by COM.

In order to illustrate the applicability of the method, the same structure in Example 4.1 is analyzed below with the new method.

4.3.1 Example 4.2 revisited: simply supported beam with vertical deflections (COM)

The beam of Example 4.1 is recalculated by the COM with the same parameters. The unknown inertia and shear parameter can be obtained not only with all possible vertical deflections (5 degrees of freedom) but also just with 2 deflections (e.g. v_2 and v_3). The {Z} vector including just measuring v_2 and v_3 is presented in Equation (16) but in order to apply COM, {Z*} should be calculated. The vector {Z*} with a measured vertical deflection in nodes 2 and 3 is presented in Equation (17).

$$Z = \begin{bmatrix} I \\ Iv_4 \\ Iv_5 \\ Iv_6 \\ Iw_1 \\ . \\ . \\ . \\ Iw_7 \\ Q \\ Qv_4 \\ Qv_5 \\ Qv_6 \\ Qw_1 \\ . \\ . \\ . \\ Qw_7 \\ H_1 \\ V_1 \\ V_7 \end{bmatrix} \tag{16}$$

$$Z^* = \begin{bmatrix} I \\ I.v_4 \\ I.v_5 \\ I.v_6 \\ I.w_1 \\ . \\ . \\ . \\ I.w_7 \\ Q \\ Q.v_4 \\ Q.v_5 \\ Q.v_6 \\ Q.w_1 \\ . \\ . \\ . \\ Q.w_7 \\ H_1 \\ V_1 \\ V_7 \end{bmatrix} \tag{17}$$

As highlighted in the previous section, in the COM, terms of {Z*} vector (Equation (17)) should satisfy certain nonlinear constrains, e.g. $Q_1 w_1 = Q_1.w_1$, these constraints are neglected in OM due to the linearity of equations which lead to a failure of the identification of the mechanical properties.

Numerical information from Table 4.1 is multiplied by different random coefficients ranging from 0.5 to 1.5 to generate initial values for COM process. According to the results, the optimization converges to the exact values of inertia and OM shear parameter after few iterations. In the following comparison, the evolution of shear area and inertia ratio throughout the iterative process for different initial values (0.5 for shear area and 1.5 for inertia) are presented in Figures 4.3a. and 4.3b, respectively.

(a)

(b)
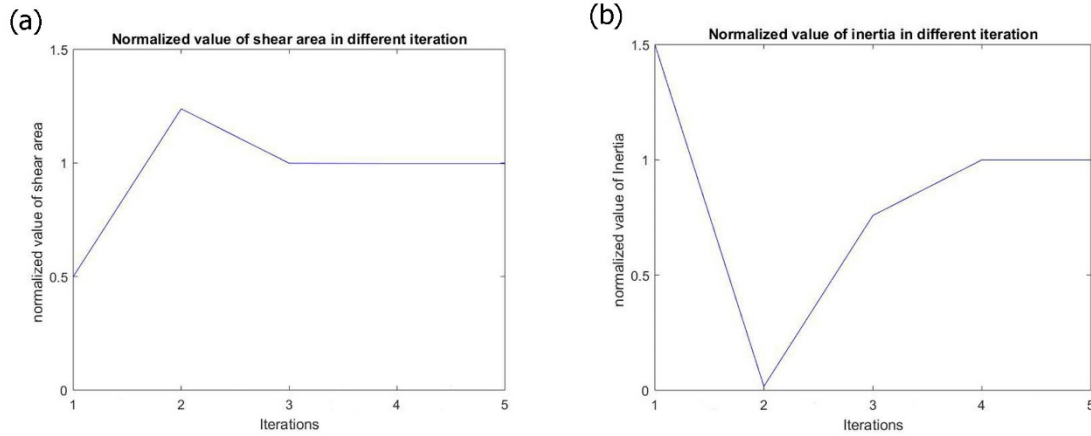
Figure 4.3: Evaluation of shear area and inertia ratio throughout the iterative process, where $\bar{x}$ is the estimated and $\hat{x}$ is the exact value of the shear area $_{Av}$ and the Inertia I. (a) Evolution of shear area parameter ratio throughout the iterative process. (b) Evolution of inertia ratio throughout the iterative process.

The analysis of Figure 4.3 shows how the exact values of both the shear area and the inertias are obtained at the end of the iterative process (5 iterations). In the following section, a more complex example is presented to illustrate the potential of the developed tool.

4.4 Application to a composite bridge

To illustrate the possible application of the COM to an actual structure, the problem of the construction of a bridge by the balanced cantilever presented in Section 3.4 is studied. In such a construction method, deflections have to be anticipated in advance to calculate the precamber with which the different segments of the structure have to be built. In order to update this precamber for every step during construction, thorough topographic surveying is usually performed. This information can be used for model updating via an inverse analysis. Even though shear deflections might not play a very important role for a full developed cantilever, modeling error of not taking into account shear effects for the first segments might lead to an inaccurate estimation of the bending stiffness. To illustrate this and the possible application of this method, a simplified model of the Yunbao Bridge over the Yellow River in China (see Figure 3.7a) is studied in this section. The structure span is 90m long. This model includes the construction of two symmetric cantilevers. The length of the standard deck segments is 4.5m and the length of the segment over the pile, 2.5m. The total length of the studied construction stage is 29.5 m. The mechanical and material properties defined by the method of the transformed section (Chen et al. 1980) are listed in Table 4.2.

Table 4.2: Properties of the Finite Element Model of the Bridge

Property	Value
Area [m^2]	12.52
Shear Area [m^2]	9.83
Inertia [m^4]	35.62
Steel Young's Modulus [GPa]	210
Concrete Young's Modulus [GPa]	35
Poisson's Ratio γ	0.3

Actual site data is not considered in this structure and the structural response is simulated numerically. The effects of creep and shrinkage in concrete are overlooked. The load test used simulates the movement of the formwork traveler (Fig. 4.4). The weight F of the formwork traveler (weight of formwork included) is considered as the 60 % of the weight of the segment (1041 kN). The effect of each form traveler in the deck is considered as two vertical forces. The values of these two forces are 0.25F and 1.25F (226 kN, upwards and 1267 kN, downwards). The load case of the bridge model is calculated by reducing the effects of the stage i (Figure 4.4.a), from stage i+1 (Figure 4.4.c), wherein the formwork traveler is moved forward to the next segment. Load cases of the stages i and i+1 are expressed in Figures 4.4.b and 4.4.d, respectively. The consequent load case introduced in the simulation is shown in Figure 4.4.e. It is to highlight that the vertical resultant of such forces in each side of the cantilever is zero.
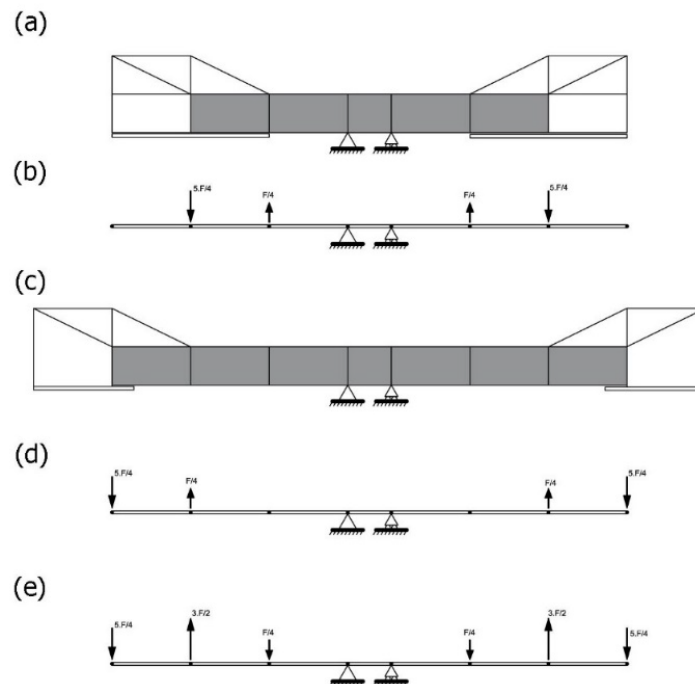
Figure 4.4: Definition of the load case: (a, b) Stage i. (c, d) Stage i+1. (e) Load case used for the inverse analysis

This structure is simulated by the simplified FEM presented in Figure 4.5.a. This FEM includes 7 elements and 6 point loads. Software Midas/Civil is used in order to calculate the vertical deflections in the nodes of the structure presented in Figure 4.5.b. For brevity, in the inverse

analysis, young modulus of all elements are considered as known parameters. Due to the fact that axial stiffness is not activated in this example, only flexural behavior is analyzed. For this reason, the terms related to the axial behavior are removed from equations (as axial stiffness are not activated with vertical forces). Because of loading case, shear area in elements numbers 3, 4 and 5 are not activated, so shear area in these elements cannot be observed in the inverse analysis. The shear area and inertia of all other beam elements (that is to say I_1, I_2, I_3, I_4, I_5, I_6, I_7, A_{v1}, A_{v2}, A_{v6}, and A_{v7}) are assumed as unknowns.
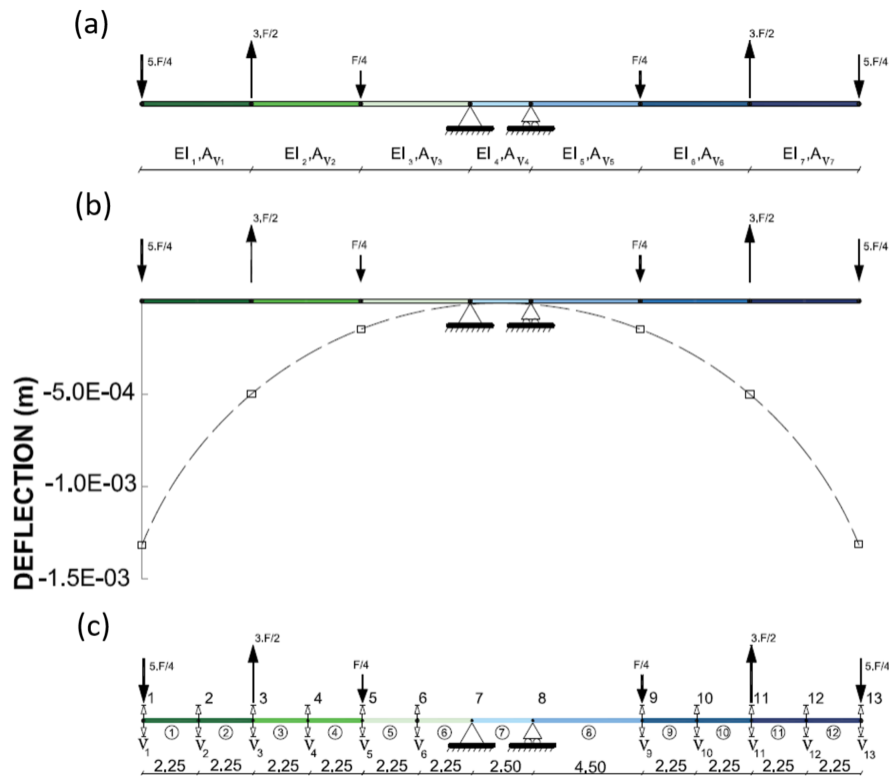
Figure 4.5: Example 4.2: (a) FEM of the bridge with load case used for inverse analysis. (b) Variation of vertical deflections in this loading case with shear deformation. (c) FEM with 13 nodes and 12 elements used for inverse analysis (dimensions in m).

To identify the 11 unknown mechanical properties at least, 11 measurements are required. As it was showed before, OM is not able to identify mechanical properties only with vertical deflections. However, it is examined and it is confirmed that no results were obtained with the measurement set of all possible vertical deflections (it is to say v_1, v_2, v_3, v_4, v_5, v_6, v_9, v_{10}, v_{11}, v_{12}, v_{13}, v_{14}, v_{15}, v_{16}) proposed for FEM presented in Figure 4.5c when the traditional OM is applied. To observe parameters with OM, the variation of deflection and rotation should be taken into account. In order to observe parameters just by vertical deflection in the bridge example, COM is applied. Table 4.3 presents the initial value coefficient of different unknown inertia and shear area which is randomly chosen between 0.5 and 1.5 for the optimization process.

Table 4.3: Initial random value of the bridge unknown properties

Parameter	Initial Random Value
I_1	0.791
I_2	0.688
I_3	1.078
I_4	1.486
I_5	0.963
I_6	0.941
I_7	1.230
Q_1	1.312
Q_2	1.255
Q_6	0.944
Q_7	0.618

COM managed to observe the unknown shear area and inertia in 14 iterations, the evolution of shear area and inertia ratio throughout the iterative process, are presented in Figure 4.6a and Figure 4.6b, respectively.

(a) Evolution of shear area parameters ratio throughout the iterative process

(b) Evolution of inertia ratio throughout the iterative process
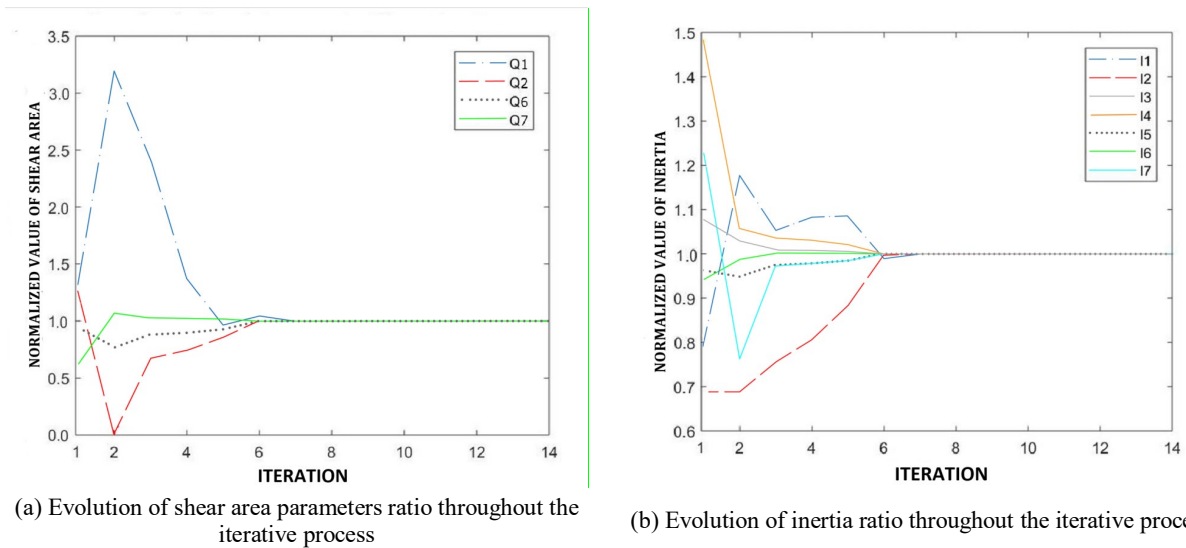
Figure 4.6: Evolution of shear area and inertia ratio throughout the iterative process.

To prove the consistency of the new method, 200 analyses with random initial value coefficients between 0.5 and 1.5 are conducted for the bridge. In 62 of these simulations, the optimization process was not convergent to the solution and no result was acquired, the results of the other 37 simulations of the optimization process were removed, due to the lack of physical meaning (e.g. negative values of the inertias). The normalized average, standard deviation and coefficient of variation of the remaining results as well as the mode is presented in Table 4.4.

Table. 4.4: Obtained results from random initial values

Inertia	Average	CoV	Standard deviation
I_1	1.000	0.001	0.000
I_2	1.000	0.002	0.001
I_3	0.975	2.279	0.791
I_4	0.993	12.229	4.324
I_5	0.969	2.888	0.996
I_6	0.999	0.004	0.002
I_7	1.000	0.001	0.001

Tomas et al. (2018) compared the differences between the estimated flexural stiffnesses ($E\bar{I}$) and the actual values (EI) in the seven elements of the bridge example without including the shear effects into the stiffness matrix of OM. According to this work when shear deformations are included into the measurements (error-free measurements), significant errors (e.g. -65,5% in segments 1 and 7 or +26,7% in segments 2 and 6) appear in the observed flexural stiffnesses in OM. As it can be seen for Table 4.4, these differences are greatly reduced with COM. Inertia in elements 1, 2, 6 and 7 can be observed with less than 0.005 CoV and the average normalized observed values of 1 with 0.000, 0.001, 0.999 and 0.001 standard deviations, respectively. For I_3, CoV, average and standard deviation are 2.29, 0.975 and 0.791, respectively. Since the shear area is not activated in the element associated with I_4 (less accurate result), there is no shear area, the average observed value is 0969, CoV of 12.229 and 4.324 for standard derivation. The observed average, CoV and standard deviation for the I5 are 2.888, 0.969 and 0.996, respectively. However, the shear area of some elements is not activated due to the loading case, making impossible the observation of shear areas of elements 5, 6, 7 and 8.

This example proves the efficiency of the proposed COM to estimate inertia when shear effects are taken into account.

4.5. Conclusions

Most Structural System Identification (SSI) methods neglect shear deformation as this phenomenon is usually negligible in comparison with flexural deformation. However, it can play a significant role in some structures, as deep beams. According to the literature, the only detailed study which addressed the particular effects of this deformation in static SSI tests is the observability method (OM). However, this failed to observe parameters just using vertical deflections measured from controlled static tests due to the complexity of equations. OM always required measurement sets that combined rotations and deflections to take into account shear deformations. However, many infrastructure control usually relies on deflection measurement (e.g. surveying through topography), being rotation measurement and the use of clinometers much more scarce. So it might be practical to have a method that only requires vertical deflections. To fill this gap, this chapter introduces the effects of shear deflections on the constrained observability method (COM). This method adds some nonlinear constraints to OM and, hence, the complex system of analytical equations is solved numerically after including the nonlinear constrains.

In the Chapter, a simply supported beam is studied in order to show the inability of the OM to observe any parameter just by vertical deflections when shear effects are considered. In addition, to illustrate the applicability of the COM on a thin-web structure, a simplified model of an intermediate construction stage of a cantilever composite bridge in China is studied. The results of this study show how the value of material properties can be observed by COM when the shear effects are taken into account in the equations and the measurement sets only include vertical deflections. The robustness of the numerical method is also validated.

Chapter 5: Observability Method with shear rotations

5.1. Introduction

Finite Element Method (FEM) is a numerical problem-solving method based on a concept in which large equations are divided into smaller and simpler equations. This technique is a common method for computer-based analysis in engineering (CSI, 2016). The Stiffness Matrix Method (SMM) is one of the major methods of the FEM approach for analyzing the structural Response of beam-like structures (Pisano, A.A (1999), Enokida, R. (2019), Zhang, F. et al (2019), Fu, Y. et al (2019)). The literature review showed that a number of SMM approaches included shear rotation into their SMM's formulations. However, most of these methods fail to simulate structural cases with discontinuities in the cross-sections, with non-collinear elements or with non-uniform loads. The only SMM that is able to analyze these models is the FEM's in which nodal variables are bending rotation and transverse displacement (the effects of shear rotation are neglected in this SMM formulation). Many works, for instance, in Przemieniecki (1968), contain a detailed formulation of the common Timoshenko beam theory SMM. The stiffness matrix presented in this approach overlooks the effect of shear rotation. In Chapter 3 it is illustrated how the shear rotation effects are neglected in some of the most common commercial simulation software based on the stiffness matrix (such as SAP 2000, CSI, 2016), and Midas Civil, 2015). In fact, these programs only include the shear effects into the vertical deflections.

System Identification (SI) represents a modeling process for unknown variables in a certain system of equations used in numerous engineering fields (Sirca Jr, G.F., & Adeli, H. (2012), Altunisik, A. C., et al. (2017)). The SI goal is to be able to characterize adequately the parameters of a certain system. Since its introduction, SI has been extended to most of the engineering fields (Gevers, M. (2006), Pisano, A.A (1999)). Structural System Identification (SSI) can be framed in the context of the SI that deals with the design of mathematical models for identifying structural parameters (such as the flexural or the axial stiffnesses) (Hoang, T. 2018).

In the literature, many methods for SSI are proposed (e.g. Zhang, F. et al (2019), Fu, Y. et al (2019), Enokida, R. (2019)). Most of them are based on the SMM (see e.g. Boumechra, N. (2017), Casciati, S., & Elia, L. (2017), Chatzieleftheriou, S., & Lagaros, N. D. (2017), Shafieezadeh, A., & Ryan, K. L. (2011)). The details of the main SSI methods are shown in the literature and addressed in (Catbas, N. (2013)). Most of SSI methods are not able to quantify correctly the structural parameters when shear effects are not negligible. This can be explained by the fact that most SSI methods based on SMM normally use Euler-Bernoulli's beam theory (see e.g. Dincal, S., & Stubbs, N. (2014), Caddemi, S. et al. (2018)), this assumption underestimates deflections and overestimating the natural frequencies since the shear effects are disregarded (Sayyad, A.S. (2011). The effects of shear deformations in their SMM models are studied by some authors (Leblouda, M., et al. (2017), Liu, S. et al (2018)). As illustrated in Chapter 3, the effects of shear rotations are neglected in the SMM's; therefore, these effects are neglected in SSI methods based on SMM. Although the assumption of neglecting shear rotations may lead to wrong estimations

for mechanical properties in SSI methods, normally these effects are overlooked. Nevertheless, in some structures (such as deep beams) shear effects might play an important role. In these cases, shear effects should be introduced into the formulation in order to reduce the errors of SSI methods, and the inability of considering these effects should be considered modeling error (error in the modeling of structures). The observability method (OM) is an SSI method based on the system of equations of the SMM. In this procedure, the mechanical properties (e.g. Flexural stiffness EI) can be quantified from the deformations measured in static tests. In Chapter 4, the effects of shear deformations are into the Constrained Observability Method (COM). Unfortunately, this application (like other SSI methods based on SMM in the literature) is not able to take into account the shear rotations as shear effects are only considered in the vertical deflections. Because of the inability of this method to consider shear rotations in SMM, COM is not able to observe the value of mechanical properties correctly when actual rotations are included into the measurement sets. For this reason, this procedure is not suitable for actual structures as wrong results are obtained even when noise-free measurements are considered. In this Chapter the effects of considering shear rotations in SSI methods based on SMM are studied. To do so, the theoretical rotations (sum of shear rotation and bending rotations) were calculated in beams with different length to height ratios in different boundary conditions (simply supported beams and cantilever beams) and different loading cases (distributed and concentrated vertical forces).

This chapter aims to fill this gap by presenting a new method based on OM to observe the structural properties from actual rotations measured on-site for any kind of structure (even in those where shear rotations are not negligible). To do so, the use of an iterative process is proposed. In this process, estimated shear rotations are subsequently subtracted from the actual rotations on site. Then the normal COM can be performed in terms of bending rotations and bending and shear vertical deflections. Also, throughout iterative steps, the structural properties are successively updated from the inverse observations.

5.2 Detected gap: No SSI method includes shear rotations

A major concern in Structural System Identification (SSI) methods in actual structures is related to the errors in measurements. As SSI methods based on Stiffness Matrix Method (SMM) systematically neglect shear rotation effects. For example, this is the case of the Observability Method (OM) proposed by Tomás et al. (2018). The numerical optimization approach (Constrained Observability Method (COM)) proposed in Jun et al. (2017) does not consider this effect either. This simplification can lead to modeling errors (Sanayi et al. (2001) as rotation measured on-site will not correspond with the one considered by the model. Depending on the structure, these modeling errors can surpass measurement errors. These errors will appear even in noise-free measurements and they will affect the estimation of structural properties in SSI methods.

In the following section, three academic examples are presented to illustrate the important role that shear rotations play in some beam geometries.

5.2.1 Academic examples

To illustrate the role of the shear rotations in the inverse analysis of structures a sensitivity analysis is developed in this section for the simple structures presented in Examples 3.2 (simply supported beam with a concentrated load at mid-span), 3.3 (simply supported beam with a uniform load) and 3.4 (cantilever beam with a concentrated load at its edge). In these analyses, the total rotation (sum of shear rotation and bending rotation) in different length (L) to height (h) ratio (1 to 15) are evaluated. Effects of these errors in estimating the inertia are presented in Figure 5.1. The ratio limits for deep beams proposed by the Eurocode EN and by the ACI Committee 318 are also indicated in this figure.
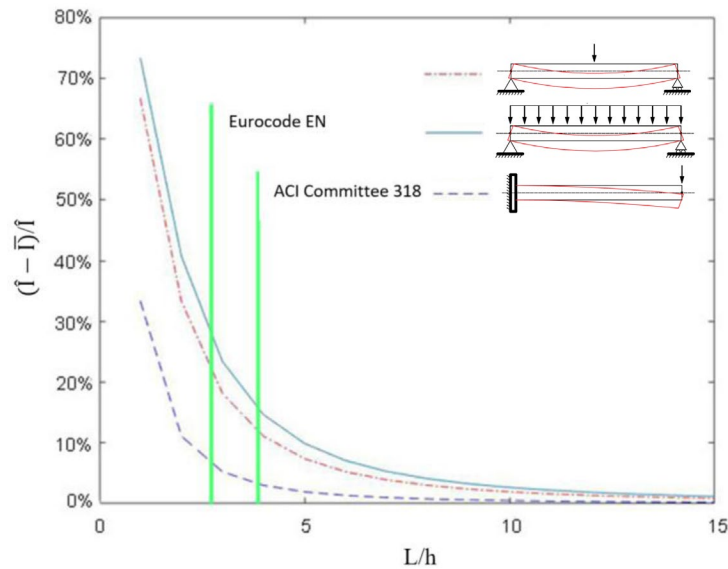
Figure 5.1: Percentage of error in inertia estimation based on depth to the length ratio, when shear rotation is not formulated in SMM. (structure as a legend)

The results of these analyses illustrate the cases where the calculation of shear rotation in SSI methods is important. When the L/h ratio is 3 (deep beam limitation by Eurocode EN), the error in inertia estimation in Examples 3.2, 3.3 and 3.4 are 18.179%, 23.401% and 5.262%, respectively. When the L/h ratio is 4 (ACI Committee 318 proposed limitation) the errors in these structures are reduced to 11.101%, 14.665% and 3.030%, respectively. The results from Figure 5.1 shows the fact that the effects of shear rotation on inverse analysis are even more important than in the direct one and they should not be neglected.

5.3. Proposed methodology

In this section, a new procedure is developed to take into account the effects of shear rotations in the SSI of 2-dimensional structures modeled with beam elements.

Providing that a static load test is performed in a structure and measurements are taken from some nodal displacements (total deflections and rotations including bending and shear displacements and rotations), the first step will be trying to separate the bending and shear rotations. Then, firstly, direct analysis is performed assuming those beam elements have their theoretical mechanical properties. Then, the shear rotation of each element is calculated based on the assumed mechanical properties. Equation (18) can be used to calculate shear rotation, v_s in each element based on Timoshenko's beam theory (Timoshenko, S. P. 1921, Timoshenko, S. P. 1922).

$$w_s = \frac{Q}{A_v * G},$$

(18)

where A_v is the shear area, Q is the shear force and the shear modulus G might be written as:

$$G = \frac{E}{2(1+v)},$$

(19)

where the coefficient v refers to the Poisson's ratio. According to Equation (18), the shear rotation for each element only depends on shear forces, shear area and shear modulus. On the other hand, shear area and shear modulus are directly obtained from the assumed mechanical properties of the structure, while the shear forces can be obtained from the results of the direct SMM analysis. By subtracting the value of shear rotation from the measured rotation of each node the bending rotation can be obtained (it is important to highlight that the measured rotation can be expressed as the sum of shear and bending rotations). Therefore, the COM process can be used as it is based on neglecting shear rotation effects. Once COM provides an estimate of the mechanical properties of the structure, these can be used to calculate new shear rotations. In this way, an iterative process should be performed until the adequate structural response of all the elements is satisfied. In order to limit the computational cost of the optimization process, the stopping criteria are defined: 1) when the iterative process is performed more than 200 times without getting improvement of the solution, and 2) when the difference between values of the observed structural properties in 2 subsequent iterative steps are less than 1^{e-3}.

The main steps of this procedure are described as follows:

- **Step 1:** Assumption of the initial values of structural properties, as the theoretical ones

- **Step 2:** Calculate the shear rotation of each element from the assumed structural properties and static loads. It is important to highlight that the stiffness properties can be obtained through either theoretical values (for the first time) or observed structural properties provided by the COM optimization (in the iterative process).

- **Step 3:** Obtain the bending rotation from the calculated shear rotation in step 2 and perform COM analysis. It is to say that the value of bending rotation for the measured nodes is calculated by subtracting the actual value (measured on-site) from theoretical shear rotation calculated in step 2.

- **Step 4:** Check the stopping criteria. If one of them is satisfied, the process stops, otherwise go to step 2.

A summary of the procedure is shown in the flow chart in Figure 5.2. In the following sections, a set of structures are analyzed to illustrate the applicability and potential of the proposed method. This will be called 2COM as COM is applied in two steps.
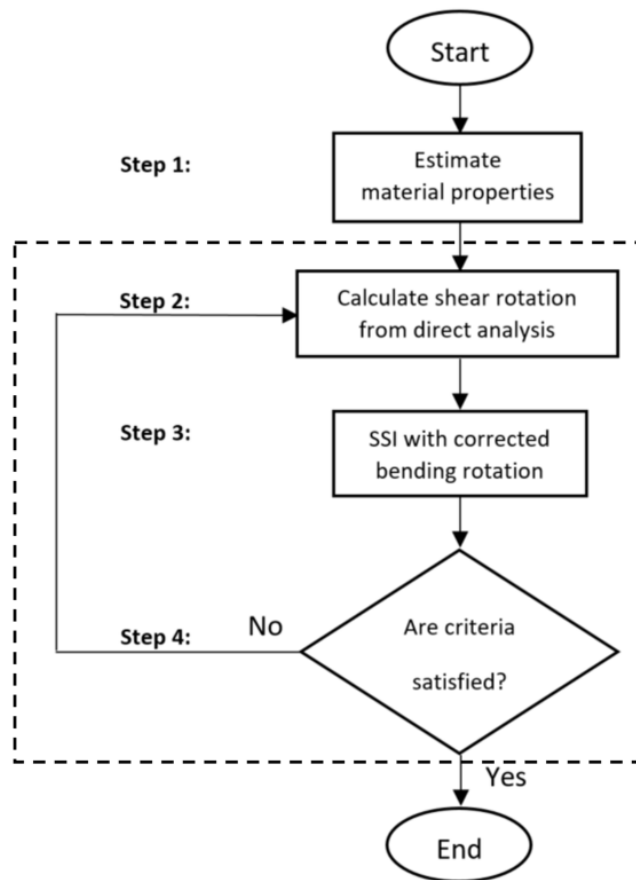
Figure 5.2. Flow chart of 2COM

To show the applicability of the new method, several academic examples are analyzed in this section. It is important to highlight that in these simulations no horizontal forces are considered and therefore, the axial resistant mechanisms are not studied as they are not excited. In addition, measurement errors are neglected in the simulations.

5.3.1. Example 5.1: simply supported beam with 2 iteration processes

Consider the 4 m long and 0.2 m wide simply supported beam modeled with 3 nodes and 2 beam elements depicted in Figure 5.3.a. This beam has a constant cross-section and its mechanical properties are listed in Table 5.1. The boundary conditions of the structure are horizontal and vertical displacements restricted in node 1 and vertical displacement restricted in node 3 (this is to say, $u_1=v_1=v_3=0$). The beam is subjected to a concentrated vertical force in node 2 of 100kN ($V_2=$ 100kN).
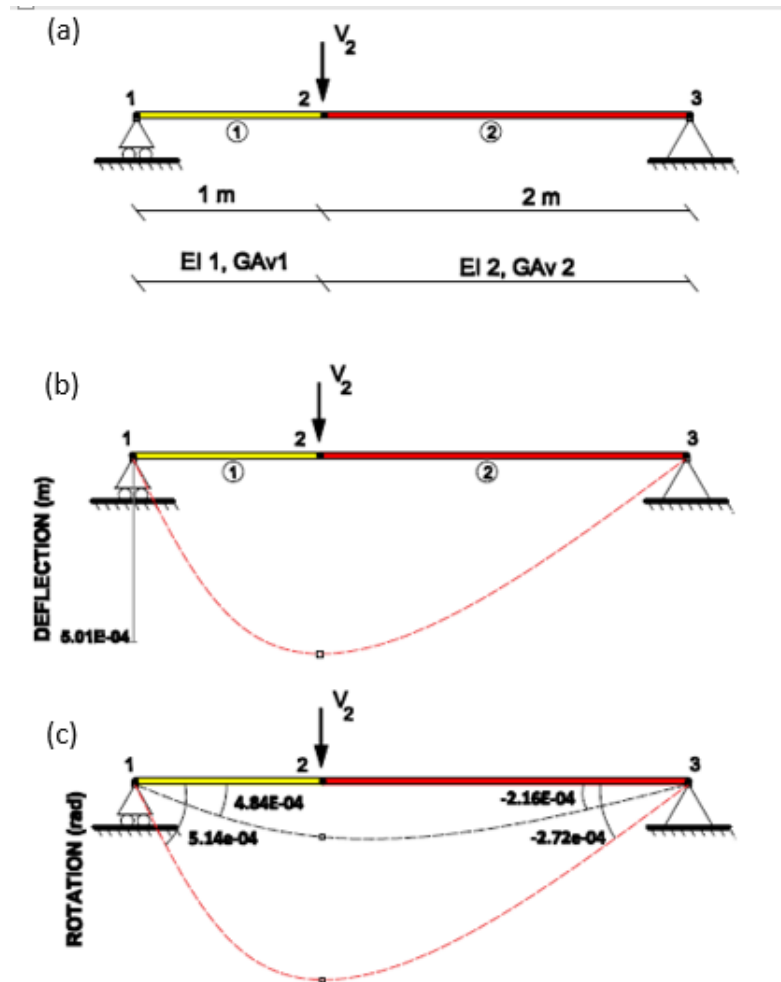
Figure 5.3: Example 1. (a) FEM for a simply supported beam. (b) Deformed shape with the value of bending vertical deformation and with bending and shear vertical deformation at Node 2. (c) Deformed shape with bending rotation and with bending and shear rotation at Node 1.

Table 5.1: *Properties of the FEM of the simply supported beam.*

Axial stiffness [GPa·m²]	440.65
Shear stiffness for node 1 [GPa·m²]	344.05
Shear stiffness for node 2 [GPa·m²]	385
Flexural stiffness for node 1 [GPa·m⁴]	1,246.7
Flexural stiffness for node 2 [GPa·m⁴]	1,120

For the inverse analysis of the structure, the load V_2, the length of the elements, Poisson's ratio and Young modulus E are assumed as known, while the inertia, I and the shear area A_v for both elements are assumed as unknown. To identify the two unknown parameters (A_v and I) a measurement set of at least four rotations is required to identify the values of unknowns. Nevertheless, the analysis of the traditional OM of this model proves that no set of four rotations in OM enables the proper identification of the unknown parameters. Therefore, a set of a vertical deflection and a rotation should be measured together (it is to say w_1, w_2, w_3 and v_2). The values of the measurement set are obtained from Timoshenko's beam theory simulation can be seen in Figure 5.3.b and Figure 5.3.c.

To check the robustness of the method, a set of random values is chosen for Inertia and Shear area to be used to calculate the hypothetical site measurements. 50 different random sets of the initial value coefficients for the inertia and the shear area were randomly chosen between 0.8 and 1.2 of the theoretical values. These initial parameters are successively updated throughout the iterative process. From 50 analyses, in 3 analyses the optimization process was not convergent to the solution and no result was acquired. The normalized average, standard deviation and coefficient of variation of the remaining results as well as the mode is presented in Table 5.2.

Table. 5.2: Obtained results from random initial values

Parameter	Average	CoV	Standard deviation
EI_1	1.000	$8.791e^{-7}$	$8.791e^{-7}$
EI_2	1.000	$9.114e^{-7}$	$9.114e^{-7}$
GA_{v1}	1.000	0.000	0.000
GA_{v2}	0.910	0.128	0.116

These results prove the adequate convergence of the proposed methodology in simply supported beams for random initial values of the Inertia. The reason for the flaw in the observed value of GA_{v2} is that the measuring on node 2 cannot provide sufficient information for covering the shear area of beam number 2. Therefore, the value of the shear area cannot be observed properly. It should be said that even in this situation the new method is able to observe Inertia properly. the shear area in For the same measurement set, the results of traditional COM (without the ability to consider shear rotations) in this example lack physical meaning. These values illustrate the inability of traditional COM to identify the correct value of parameters as it is not able to identify shear rotations.

5.3.2. Example 2: Cantilever beam

Consider a cantilever beam with the same cross-section and same properties as in Example 5.1 modeled with one beam element and 2 nodes as it is presented in Figure 5.4. The boundary conditions of the structure are total horizontal and vertical displacements and rotation due to bending restricted in node 1 (this is to say, $u_1=v_1=w_{b1}=0$). The only external force applied is assumed as a concentrated vertical force in Node 3 of 100kN ($V_3=$ 100kN). As in the previous example, the length of the elements, L, the Poisson's ratio and the Young modulus E are assumed

as known in the inverse analysis, while the inertia I and the shear area A_v for elements 1 and 2 are assumed as unknown. To obtain these four unknown parameters the measurement set should include at least four rotations. Nevertheless, the analysis of the traditional OM proves that no set of two rotations in COM enables the proper identification of the unknown parameters. Therefore, a set of vertical deflection and rotation should be measured together in this example. To perform the COM2, a measurement set that consists of two rotations and two vertical deflections (w_2, w_3 and v_2, v_3) is employed. The rotations and the vertical deformations including shear effects of this structure are presented in Figure 5.4.
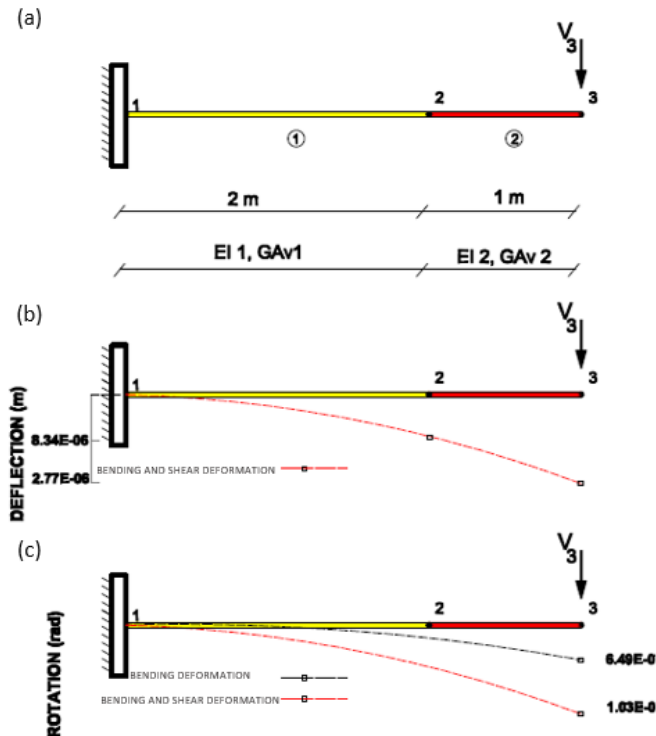
**Figure 5.4**: Example 2. (a) FEM for a cantilever beam. (b) Deformed shape with the value of bending vertical deformation and with bending and shear vertical deformation at Node 2. (c) Deformed shape with bending rotation and with bending and shear rotation at Node 2.

To check the robustness of the method, a set of random values is chosen for Inertia and Shear area to be used to calculate the hypothetical site measurements. 50 different random sets of the initial value coefficients for the inertia and the shear area were randomly chosen between 0.8 and 1.2 of the theoretical values. Also, no matter what set of the initial value is chosen, in all circumstances, the obtained values of 2 iterative process have proper convergence to real values of mechanical properties. The normalized average, standard deviation and coefficient of variation of the remaining results as well as the mode is presented in Table 5.3.

Table. 5.3: *Obtained results from random initial values*

Parameter	Average	CoV	Standard deviation
EI_1	1.000	$8.783e^{-7}$	$8.783e^{-7}$
EI_2	1.000	$9.118e^{-7}$	$9.117e^{-7}$
GA_{v1}	1.000	0.000	0.000
GA_{v2}	1.000	0.000	0.000

These results prove the adequate convergence of the proposed methodology in cantilever beams for random initial values of the unknown parameters. These results show the applicability of the proposed methodology in cantilever structures. It is important to highlight that obtained results of the original COM process for this example lack physical meaning as ratios of 0.562 and 3.000 were obtained for the Inertia in I_1 and I_2, respectively.

5.4. Application to a composite bridge

To show the application of the proposed methodology to a real structure, the problem of the construction of a bridge by the balanced cantilever method is studied in section 4.4.

The simplified FEM of this structure is presented in Figure 5.5. This FEM includes 7 elements and 6 concentrated loads Since there is no axial load, the axial stiffness is not activated in this example; therefore, only flexural and shear behavior is analyzed. As shear stiffness and bending stiffness from elements 2, 3, 4, 5 and 6 are supposed to be observed from the previous construction steps, such properties are considered as knowns. Hence, shear and bending stiffness of the new built elements are the targets of the analysis (this is to say I_1, I_7 and A_{v1}, A_{v7}) and are assumed as unknowns.
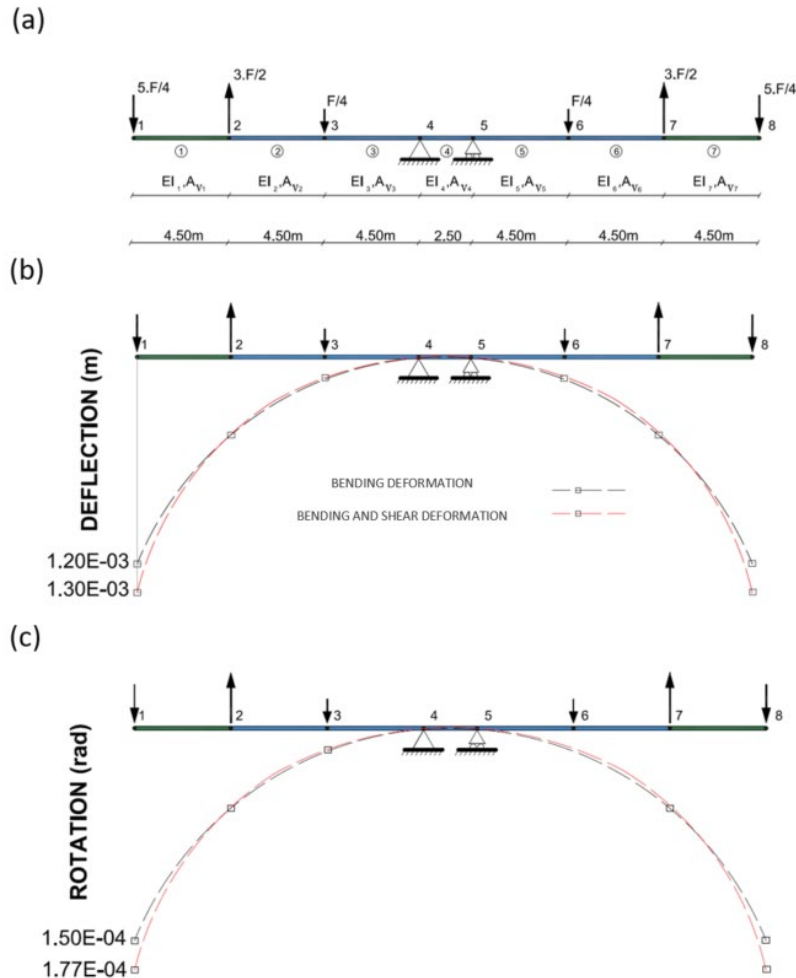
Figure 5.5: *Example 3. FEM of the bridge with load case used for inverse analysis. (b) Deformed shape with the value of bending vertical deformation and with bending and shear vertical deformation at Node 1. (c) Deformed shape with bending rotation and with bending and shear rotation at Node 1.*

In this example, there are 4 unknowns (it is to say EI_1, GA_{v1} and EI_7, GA_{v7}). In order to identify the 4 unknown mechanical properties, a set of at least 4 measurements are required. The analysis of the OM proves that the COM is not able to observe any structural properties by only measuring rotations in this example. To observe the structural parameters with the proposed methodology, the variation of deflection and rotation should be taken into account (it is to say, w_1, v_2 and w_7, v_6). The value of theoretical rotation and vertical deflection of node 1 are presented in Figure 5.5.b and c. Timoshenko's beam theory is used to calculate the values of measured variables in the node number 1 (the value at node number 7 is the same).

The initial value coefficients of unknown inertia and shear area (I_1, I_7 and A_{v1}, A_{v7}) were randomly chosen between a ratio of 0.8 and 1.2 of the theoretical values. The 50 analyzed random initial values are performed.

To check the robustness of the method, a set of random values is chosen for Inertia and Shear area to be used to calculate the hypothetical site measurements. 50 different random sets of the initial

value coefficients for the inertia and the shear area were randomly chosen between 0.8 and 1.2 of the theoretical values. Also, no matter what set of the initial value is chosen, in all circumstances, the obtained values of 2 iterative process have proper convergence to real values of Inertia. The normalized average, standard deviation and coefficient of variation of the remaining results as well as the mode is presented in Table 5.3.

Table. 5.3: *Obtained results from random initial values*

Parameter	Average	CoV	Standard deviation
EI_1	1.000	$8.237e^{-7}$	$8.237e^{-7}$
EI_2	1.000	$8.903e^{-7}$	$8.903e^{-7}$
GA_{v1}	0.617	0.740	0.456
GA_{v2}	0.256	0.305	0.078

These results prove the adequate convergence of the proposed methodology in a bridge structure for random initial values of the unknown parameters. These results prove the efficiency of the proposed COM to estimate the inertia when the effects of shear rotations are considered, in case that the shear area cannot be observed by the proposed method. In addition, it is important to highlight that, as far as the authors know, no other SSI method based on SMM in literature is able to include the effects of these rotations in the inverse simulation.

5.5 Conclusions

All Structural System Identification (SSI) methods in the literature neglect shear rotations. This limitation might lead to significant errors when the structural parameters of some structures (such as deep beams) are obtained from actual rotations on site. To fill this gap, the formulation of the Constrained observability method (COM) is updated to include the effects of the shear rotations. This application leads to an iterative process where the initial values of the estimates are successively updated. The applicability of the proposed methodology is illustrated by several academic examples. In addition, to illustrate the applicability of the proposed method on actual structures, a simplified model of an intermediate construction stage of a cantilever composite bridge in China is studied. The results of this study show how the value of structural properties can be observed by COM when the actual rotations are included into the measurement set.

Chapter 6: Conclusions and future research

6.1. Conclusions

Stiffness matrix methods are used normally to analyze complex structures neglecting shear rotations. Based on the literature review, which thoroughly studied different SMM, these are not able to calculate shear rotations in models no collinear, discontinued and with external loads. Also, all Structural System Identification (SSI) methods reviewed in the literature neglect rotation due to shear in their formulation as this phenomenon is usually less significant than the bending rotation. Despite the important role that this rotation might play especially in members with a low span-to-depth ratio, no detailed study addressing the particular effects of this rotation in inverse analysis can be found in the literature.

To show how important the role of shear rotation might be, several different structures (a simply supported beam with a concentrated load, a simply supported beam with a distributed load, and a cantilever with a concentrated load) with different length to height ratios are studied in section 3. In fact, these examples illustrate that the difference between Timoshenko's theory and Euler-Bernoulli's theory in terms of rotation is higher for members with low length-to-height ratio. For deep beams ratio between the shear rotation and bending rotation can be significant. Also, a model of a bridge built in cantilever is analyzed to show the applicability of the proposed method. It should be mentioned that no other Timoshenko beam theory FEM in literature is able to calculate total rotation (including both shear and bending effects) in a structural model.

OM always required measurement sets that combined rotations and deflections to take into account shear deformations. However, many infrastructure control usually relies on deflection measurement (e.g. surveying through topography), being rotation measurement and the use of clinometers much more scarce. So it might be practical to have a method that only requires vertical deflections. To fill this gap, in section 5 the effects of shear deflections on the constrained observability method (COM) are introduced. This method adds some nonlinear constraints to OM and, hence, the complex system of analytical equations is solved numerically after including the nonlinear constrains.

According to the literature, the only detailed study which addressed the particular effects of shear deformation in static SSI tests is the observability method (OM). However, this failed to observe parameters just using vertical deflections measured from controlled static tests due to the complexity of equations. In section 4, a simply supported beam is studied in order to show the inability of OM to observe any parameter just by vertical deflections when shear effects are considered. To solve this problem, the formulation of constrained observability method (COM) is updated to include shear deformation. The COM performance in a simply supported beam shows the power of the new method to observe the value of the structural parameters just by vertical deflections. To show the applicability of the COM on a thin web structure, a simplified model of

an intermediate construction stage of a cantilever composite bridge in China is studied. The results of this study show how the value of material properties can be observed by COM when the shear effects are taken into account in the equations and the measurement sets only include vertical deflections. The robustness of the numerical method is also evaluated.

As it is explained, shear rotation is not included into the SSI methods based on SMM, to fill this gap, the formulation of the Constrained observability method (COM) is updated to include the effects of shear rotations in section 5. This leads to an iterative process where the initial values of the estimates are successively updated. The applicability of the proposed methodology is presented in several academic examples. To illustrate the applicability of the proposed method on actual structures, a simplified model of an intermediate construction stage of a cantilever composite bridge in China is studied. The results of this study show how the value of structural properties can be observed by 2COM when the actual rotations are included into the measurement set. It is important to highlight that the result of the original COM method in all analyzed cases lacks physical meaning. Also, for the first time in literature, the sensitivity of the SSI methods to this modeling error is performed in section 5. The study of this sensitivity analysis might provide some insight into which structures rotation due to shear should be taken into account and in which cases these effects can be neglected.

6.2. Related works and publication

This thesis has led to the following SCI papers:

- Appendix 1: Emadi, S., Lozano-Galant, J. A., Xia, Y., Ramos, G., & Turmo, J. (2019). Structural system identification including shear deformation of composite bridges from vertical deflections. Steel and Composite Structures, 32(6), 731-741. doi:10.12989/scs.2019.32.6.731

- Appendix 2: Emadi, S., Lozano-Galant, J. A., Xia, Y., Ramos, G., & Turmo, J. (2020). Shear rotation analysis in stiffness matrix methods: A state of the art and application in the direct and inverse analyses. Computers and Composite Structures, (under review)
- Appendix 3: Emadi, S., Lozano-Galant, J. A., Xia, Y., & Turmo, J (2021). Observing material properties in beams from actual rotations. To be submitted

6.3. Future research

The following works can be addressed in the future:

1. New optimization method: Although the MATLAB's "Fmincon" function which has been used for solving the non-linear problem of COM works well in most cases, there is room for improvement. Other optimization tools such as heuristic optimization methods or genetic algorithms can be taken into account to have faster convergence in results in more complicated cases.

2. Study of modeling errors: The effect of modeling errors (such as changes in the supports' stiffness, or the assumption or wrong parameters) should be studied to validate the robustness of the procedure in real structures.

3. Application with actual measurement sets: The application of the methods in this thesis is based on error-free measurement sets so it is advised the application to actual monitoring data obtained on-site.

Bibliography

1. AASTHO (2017), LRFD Bridge Design Specifications, (8th Edition), American Association of State Highway and Transportation Officials; Washington, DC, USA.

2. Abdo, M. (2012). Parametric study of using only static response in structural damage detection. Engineering Structures. 34. 124–131. 10.1016/j.engstruct.2011.09.027.

3. ACI committee 318 Building code requirements for structural concrete and commentary. American Concrete Institute, Detroit, 2000, USA

4. Ali, R., Hedges, J.L., Mills, B. (1971) The Application of Finite Element Techniques to the Analysis of an Automobile Structure: First Paper: Static Analysis of an Automobile Chassis Frame. Automobile Division 185 665-674.

5. Ali, R., Hedges, J.L., Mills, B. (1971) Dynamic analysis of an automobile chassis frame, Automobile Division. 185 683-690.

6. Altunisik, A. C., Gunaydin, M., Sevim, B., & Adanur, S. (2017). System identification of arch dam model strengthened with CFRP composite materials. *Steel and Composite Structures*, 25(2), 231-244.

7. American society of Civil engineers, Structural Identification of Constructed Systems, American Society of Civil Engineers, Reston, VA 2013.

8. Aquino, W., & Erdem, I. (2007) Implementation of the modified compression field theory in a tangent stiffness-based finite element formulation. Steel and Composite Structures, 7(4) 263-278. doi:10.12989/scs.2007.7.4.263

9. Araki, Y., Miyagi, Y (2005), "Mixed integer nonlinear least-squares problem for damage detection in truss structures", *Journal of Engineering Mechanics*, **131**(7) (2005), 659–667.

10. Archer, J.S. (1965) Consistent matrix formulations for structural analysis using finite-element techniques. American Institute of Aeronautics and Astronautics Journal. 3 1910-1918.

11. Arefi, M., Pourjamshidian, M., & Ghorbanpour Arani, A. (2019) Dynamic instability region analysis of sandwich piezoelectric nano-beam with FG-CNTRCs face-sheets based on various high-order shear deformation and nonlocal strain gradient theory. Steel and Composite Structures, 32(2) 157-171. doi:10.12989/scs.2019.32.2.151

12. Argyris, J., Dunne, P.C. (1952), "Structural Analysis, Structural Principles and Data, Part 2", Handbook of Aeronautics No. 1, The New Eva Publ. Co. Ltd, London

13. Astley, R.J. (1992). Finite elements in solids and structures: an introduction. Chapman and Hall, London

14. Augarde, C.E. (1997). Numerical modelling of tunneling processes for assessment of damage to buildings. DPhil thesis, University of Oxford.

15. Bathe, K.J. Finite Element Procedures. K.J. Bathe Watertown MA,2016 ISBN 978-0-9790049-5-7.

16. Breuer, P., Chmielewski, T., Górski, P., Konopka, E., Tarczyński, L (2015), "Monitoring horizontal displacements in a vertical profile of a tall industrial chimney using Global Positioning System technology for detecting dynamic characteristics", *Structural Control and Health Monitoring*, **22** (7), 1002-1023.

17. Boumechra, N. (2017). Damage detection in beam and truss structures by the inverse analysis of the static response due to moving loads. Structural Control and Health Monitoring, 24(10) doi:10.1002/stc.1972

18. Caddemi, S., Caliò, I., Cannizzaro, F., & Morassi, A. (2018). A procedure for the identification of multiple cracks on beams and frames by static measurements. Structural Control and Health Monitoring, 25(8) doi:10.1002/stc.2194

19. Carnegie, W., Thomas, J., Dokumaci, E. (1969) An improved method of matrix displacement analysis in vibration problems. The Aeronautical Quarterly 20 321-332.

20. Casciati, S., & Elia, L. (2017). Damage localization in a cable-stayed bridge via bio-inspired metaheuristic tools. Structural Control and Health Monitoring, 24(5) doi:10.1002/stc.1922

21. Castillo, E., Conejo,A. J., Pruneda, R. E., Solares, C (2007), "Observability in linear systems of equations and inequalities: applications", *Computers and Operations Research*, **34** (6) 1708–20.

22. Castillo, E., Nogal, M., Lozano-Galant, J.A., Turmo, J (2016), "Solving Some Special Cases of Monomial-Ratio Equations Appearing Frequently in Physical and Engineering Problems", *Mathematical Problems in Engineering*.

23. Castillo, E., Cobo, A., Jubete, F., Pruneda, R.E. and Castillo, C (2000), "An orthogonally based pivoting transformation of matrices and some applications", *SIAM Journal on Matrix Analysis and Applications*, **22**(3),666-681.

24. Castillo, E., Jubete, F., Pruneda, R.E. and Solares, C (2002), "Obtaining simultaneous solutions of linear subsystems of equations and inequlities", *Linear Algebra and its Applications*, **364** (1-3),131-154.

25. Catbas, Necati & kijewski-correa, tracy & Aktan, A. (2013). Structural Identification of Constructed Systems: Approaches, Methods, and Technologies for Effective Practice of St-Id. 10.13140/2.1.1218.1761.

26. Çavdar, Ö., Bayraktar, A., Çavdar, A., & Adanur, S. (2008) Perturbation based stochastic finite element analysis of the structural systems with composite sections under earthquake forces. Steel and Composite Structures, 8(2) 129-144. doi:10.12989/scs.2008.8.2.129

27. Chatzieleftheriou, S., & Lagaros, N. D. (2017). A trajectory method for vibration based damage identification of underdetermined problems. Structural Control and Health Monitoring, 24(3) doi:10.1002/stc.1883

28. Chao, S., Wu, H., Zhou, T., Guo, T., & Wang, C. (2019) Application of self-centering wall panel with replaceable energy dissipation devices in steel frames. Steel and Composite Structures, 32(2) 265-279. doi:10.12989/scs.2019.32.2.265

29. Chaudhary, S., Pendharkar, U., & Nagpal, A. K. (2007) An analytical-numerical procedure for cracking and time-dependent effects in continuous composite beams under service load. Steel and Composite Structures, 7(3) 219-240. doi:10.12989/scs.2007.7.3.219

30. Chen, D. Kitipornchai, S.; Yang, J. Nonlinear free vibration of shear deformable sandwich beam with a functionally graded porous core, Thin-walled structures, 107 (2016) 39-48.

31. Chen, Y.S. and Yen, B. T. (1980), Analysis of Composite Box Girders, Report N0 380.12, Fritz Engineering Laboratory Library.

32. Clough, R.W.: The Finite Element Method in Plane Stress Analysis. Second ASCE Conference on Electronic Computation, Pittsburgh, PA, p. 345-378 (1960)

33. CSI, CSI Analysis Reference Manual for SAP2000, ETABS, SAFE and CSiBridge, Berkeley, California, USA, 2016.

34. Cowper, G.R. (1966) The shear coefficient in Timoshenko's beam theory. Journal of Applied Mechanics 33 335-340. doi:10.1115/1.3625046

35. Emadi, S., Lozano-Galant, J. A., Xia, Y., Ramos, G., & Turmo, J. (2019). Structural system identification including shear deformation of composite bridges from vertical deflections. Steel and Composite Structures, 32(6), 731-741. doi:10.12989/scs.2019.32.6.731

36. Dahake, A., Ghugal, Y., Uttam, B., Kalwane, U.B. (2014) Displacements in Thick Beams using Refined Shear Deformation Theory. Proceedings of 3 rd International Conference on Recent Trends in Engineering & Technology.

37. Davis, R., Henshell, R.D., Warburton, G. B. (1972) A Timoshenko beam element, Journal of Sound and Vibration. 22 (4) 475-48.

38. Deretić-Stojanović, B., Kostic, S.M (2017), "A simplified matrix stiffness method for analysis of composite and prestressed beams", *Steel and Composite Structures*, **24** (1), 53-63. doi:10.12989/scs.2017.24.1.053

39. Dikaros, I. & Sapountzakis, E. (2014). Generalized Warping Analysis of Composite Beams of an Arbitrary Cross Section by BEM. I: Theoretical Considerations and Numerical Implementation. Journal of Engineering Mechanics. 10.1061/(ASCE)EM.1943-7889.0000775.

40. Dixit, P., Liu, G.R. A Review on Recent Development of Finite Element Models for Head Injury Simulations. Arch Computat Methods Eng 24, 979–1031 (2017). https://doi.org/10.1007/s11831-016-9196-x

41. Dowling, J., Obrien, E. J., González, A (2012), "Adaptation of Cross Entropy optimization to a dynamic Bridge WIM calibration problem", *Engineering Structures*, **44** ,13-22.

42. Dincal, S., & Stubbs, N. (2014). Nondestructive damage detection in euler-bernoulli beams using nodal curvatures - part I: Theory and numerical verification. Structural Control and Health Monitoring, 21(3), 303-316. doi:10.1002/stc.1562

43. Dong, X. Zhao, L. Xu, Z. Du, S. Wang, S. Wang, X. and Jin, W (2017), "Construction of the Yunbao Bridge over the yellow river", EASEC-15. 2017, Xi'an, China.

44. Duncan WJ, Collar AR. A method for the solution of oscillation problems by matrices. Philosophical Magazine 1934; 17(Series 7):865.

45. Duncan WJ, Collar AR. Matrices applied to the motions of damped systems. Philosophical Magazine 1934; 19(Series 7):197.

46. Dym, C.L., Williams, H.E. (2007) Estimating Fundamental Frequencies of Tall Buildings. Journal of Structural Engineering. 133 1479-1483.

47. EN 1992-1-1: Eurocode 2: Design of concrete structures - Part 1-1: General rules and rules for buildings. CEN, Brussels, 2002, Belgium.

48. Enokida, R. (2019). Stability of nonlinear signal-based control for nonlinear structural systems with a pure time delay. Structural Control and Health Monitoring, 26(8) doi:10.1002/stc.2365

49. Emadi, S., Lozano-Galant, J. A., Xia, Y., Ramos, G., & Turmo, J. (2019). Structural system identification including shear deformation of composite bridges from vertical deflections. Steel and Composite Structures, 32(6), 731-741. doi:10.12989/scs.2019.32.6.731

50. Emadi, S., Lozano-Galant, J. A., Xia, Y., Ramos, G., & Turmo, J. (-). Shear rotation analysis in stiffness matrix methods: A state of the art and application in the direct and inverse analyses. Computers and Composite Structures, (under review)

51. Eurocode (2005), Design of Concrete Structures—Concrete Bridges—Design and Detailing Rules, European Committee for Standardization: Brussels, Belgium.

52. Falkenheiner H. Calcul syst´ematique des caracteristiques elastic des syst´emes hyperstatiques. La Recherche A´eronautique 1950; 17:17.

53. Fang, G., Wang, J., Li, S., & Zhang, S. (2016) Dynamic characteristics analysis of partial-interaction composite continuous beams. Steel and Composite Structures, 21(1) 195-216. doi:10.12989/scs.2016.21.1.195

54. Fraser RA, Duncan WJ, Collar AR. Elementary Matrices and some Applications to Dynamics and Differential Equations. Cambridge University Press: Cambridge, 1938.

55. Frazer RR, Duncan WJ, Collar AR. Elementary Matrices. Cambridge University Press: Cambridge, MA, 1960.

56. Fu, Y., Peng, C., Gomez, F., Narazaki, Y., & Spencer, B. F., Jr. (2019). Sensor fault management techniques for wireless smart sensor networks in structural health monitoring. Structural Control and Health Monitoring, 26(7) doi:10.1002/stc.2362

57. Garoni, C., Speleers, H., Ekström, S. et al. Symbol-Based Analysis of Finite Element and Isogeometric B-Spline Discretizations of Eigenvalue Problems: Exposition and Review. Arch Computat Methods Eng 26, 1639–1690 (2019). https://doi.org/10.1007/s11831-018-9295-y

58. Greiner, D., Periaux, J., Emperador, J.M. et al. Game Theory Based Evolutionary Algorithms: A Review with Nash Applications in Structural Engineering Optimization Problems. Arch Computat Methods Eng 24, 703–750 (2017). https://doi.org/10.1007/s11831-016-9187-y

59. Gevers, M. (2006). A personal view of the development of system identification: A 30-year journey through an exciting field. IEEE Control Systems, 26(6), 93-105.

60. Górski, P., Stankiewicz, B., Tatara, M (2018), "Structural evaluation of all-GFRP cable-stayed footbridge after 20 years of service life", Steel and Composite Structures, 29 (4),527-543.

61. Gracia-Palencia, A.J., Santini-Bell, E., Sipple, J.D. Sanayi, M (2015), "Structural model updating of an in-service bridge using dynamic data", Structural Control and Health Monitoring, 22 (10), 1265-1281.

62. Heyliger, P.R., Reddy, J.N. (1988) A higher-order beam finite element for bending and vibration problems, J. Sound Vib. 126(2), 309-326

63. Hrenikoff A. Solution of problems of elasticity by the framework method. Journal of Applied Mechanics 1941; A8(1):169–175.

64. Hoang, T., Foret, G., Duhamel, D. Dynamical response of a Timoshenko beams on periodical nonlinear supports subjected to moving forces. Engineering Structures. 176 (2018) 673-680. 10.1016/j.engstruct.2018.09.028.

65. Hou, Z., Xia, H., Y, W., Zhang, Y., Zhang, T (2015), "Dynamic analysis and model test on steel-concrete composite beams under moving loads", Steel and Composite Structures, 18 (3) ,565-582.

66. Huo, R., Liu, W., Wu, P., Zhou, D (2017), "Analytical solutions for sandwich plates considering permeation effect by 3-D elasticity theory", Steel and Composite Structures, 25 (2), 127-139.

67. Hutton, D. Fundamentals of finite element analysis Boston: McGraw-Hill, [2004].

68. Kahya, V., Turan, M (2018), "Vibration and buckling of laminated beams by a multi-layer finite element model", Steel and Composite Structures", 28 (4), 415-426.

69. Kapur, K. K. (1966) Vibrations of a Timoshenko beam, using finite element approach. Journal of the Acoustical Society of America, 40 1058-1063.

70. Karabelivo, K., Cue'llar, P., Baebler, M., Rucker, W (2015), "System identification of inverse, multimodal and nonlinear problem using evolutionary computing-application to a pile structure supported in nonlinear springs", Engineering Structure, 101, 609-620.

71. Kawano, A., Zine, A. (2019) Reliability evaluation of continuous beam structures using data concerning the displacement of points in a small region. Engineering Structures. 180 379-387. 10.1016/j.engstruct.2018.11.051.

72. Khayat, M., Poorveis, D., Moradi, S (2017), "Buckling analysis of functionally graded truncated conical shells under external displacement-dependent pressure", Steel and Composite Structures, 23 (1), 1-16.doi:10.12989/scs.2017.23.1.001

73. Kim, N. (2009) Dynamic stiffness matrix of composite box beams. Steel and Composite Structures 9(5) 473-497. doi:10.12989/scs.2009.9.5.473

74. Kirchhoff GR. Annalen der Physic und Chemie 1847; 72.

75. Kron G. Tensorial analysis of elastic structures. Journal of the Franklin Institute 1944; 238:399–442.

76. Kumar, D., & Srivastava, A. Elastic properties of CNT-and graphene-reinforced nanocomposites using RVE. Steel and Composite Structures, 21(5) (2016). 1085-1103. doi:10.12989/scs.2016.21.5.1085

77. Kumar, P., Srinivas, J (2018), "Transient vibration analysis of FG-MWCNT reinforced composite plate resting on foundation", *Steel and Composite Structures*, **29** (5), 569-578.

78. Lang AL, Bisplinghoff RL. Some results of sweptback wing structural studies. Journal of the Aeronautical Sciences 1951; 18:751.

79. Leblouda, M., Junaid, M.T., Barakat, S., Maalej, M. Shear buckling and stress distribution in trapezoidal web corrugated steel beams; Thin-walled structures, 113 (2017) 13-26.

80. Lee, J.W., Coi, K.H and Huh, Y.C (2010), "Damage detection method for large structures using static and dynamic strain data from distributed fiber optic sensor", *International Journal of Steel Structure* ,**10** (1) , 91-97.

81. Lei, J., Lozano-Galant, J.A., Nogal, M., Xu, D., Turmo, J (2016), "Analysis of measurement and simulation errors in structural system identification by observability techniques", *Structural Control and Health Monitoring*, **24**(6), e1923. doi: 10.1002/stc.1923.

82. Lei, J., Lozano-Galant, J.A., Xu, D, Turmo, J. (2019) Structural system identification by measurement error-minimizing observability method. Struct Control Health Monit, e2425. https://doi.org/10.1002/stc.2425.

83. Lei, J., Xu, D., Turmo, J (2017), "Static structural system identification for beam-like structures using compatibility conditions", *Structural Control and Health Monitoring*, **25**(1), e2062.

84. Lei, j., Nogal, M., Lozano-Galant, J.A., Xu, D. and Turmo, j (2017), "Constrained observability method in static structural system identification", *Structural Control and Health Monitoring*, **25** (1), e2040.

85. Levy S. Computation of influence coefficients for aircraft structures with discontinuities and sweepback. Journal of the Aeronautical Sciences 1937; 14:547.

86. Li, Z., Park, H. S., Adeli, H (2017), "New method for modal identification of super high-rise building structures using discretized synchrosqueezed wavelet and Hilbert transforms", *The Structural Design of Tall and Special Building*, **26** (3), e1312.

87. Li, J., Jiang, L., Li, X (2017), "Free vibration of a steel-concrete composite beam with coupled longitudinal and bending motions", *Steel and Composite Structures*, **24** (1), 79-91. doi:10.12989/scs.2017 24.1.079

88. Li, J., Huo, Q., Li, X., Kong, X., Wu, W (2014), "Dynamic stiffness analysis of steel-concrete composite beams", *Steel and Composite Structures*, **16** (6), 577-593.

89. Liao, J., Tang, G., Meng, L., Liu, H., Zhang, Y (2012), "Finite element model updating based on field quasi-static generalized influence line and its bridge engineering application", Procedia Engineering ,31, 348–353.

90. Liu, S., D Ziemian, R., Chen, L., Chan, S-L. Bifurcation and large-deflection analyses of thin-walled beam-columns withnon-symmetric open-sections; Thin-walled structures, 132 (2018) 287-301

91. López-Colina, C., Serrano, M. A., Lozano, M., Gayarre, F. L., Suárez, J. M., & Wilkinson, T. (2019) Characterization of the main component of equal width welded I-beam-to-RHS-column connections. Steel and Composite Structures, 32(3). 337-346. doi:10.12989/scs.2019.32.3.337

92. Lozano-Galant, J. A., Emadi, S. B., Ramos, G., & Turmo, J. (2018). Structural system identification of shear stiffnesses in beams by observability techniques. Paper presented at the IABSE Symposium, Nantes 2018: Tomorrow's Megastructures, S24-111-S24-118.

93. Lozano-Galant J.A, Nogal M, Castillo E, Turmo J (2013), "Application of observability techniques to structural system identification", *Computer-Aided Civil and Infrastructure Engineering*, **28** (6), 434–450.

94. Lozano-Galant, J.A., Nogal, M., Paya-Zaforteza, I., and Turmo, J (2014), "Structural system identification of cable-stayed bridges with observability techniques", *Structure and Infrastructure Engineering*, **10** (11), 1331-1344.

95. Lozano-Galant, J.A., Nogal, M., Turmo, J., Castillo, E (2015), "Selection of measurement sets in static structural identification of bridges using observability trees", *Computers and Concrete*, **15** (5), 771–794.

96. Lu, Y., Panagiotou, M. (2014) Three-Dimensional Cyclic Beam-Truss Model for Nonplanar Reinforced Concrete Walls. Journal of Structural Engineering. 140. 04013071. DOI: 10.1061/(ASCE)ST.1943-541X.0000852.

97. MATLAB and Optimization Toolbox Release 2017b, The MathWorks, Inc., Natick, Massachusetts, United States.

98. MATLAB. (2018). 9.7.0.1190202 (R2019b). Natick, Massachusetts: The MathWorks Inc.

99. McCalley, R. B. (1963) Rotary inertia ccrrectior: for mass matrices. General Electric Knolls Atomic Power Laboratory, Schenectady, New York, Report DIG/SA. 68-73.

100. McHenry D. A lattice analogy for the solution of stress problems. Journal of the Institute of Civil Engineer 1943; 21:59–82.

101. Megson, T.H.G. (2019) "Structural and Stress Analysis (Fourth Edition)" Butterworth-Heinemann, ISBN 9780081025864, https://doi.org/10.1016/B978-0-08-102586-4.09993-5.

102. Mei, L., Mita, A. and Zhou, J. (2016), "An improved substructural damage detection approach of shear structure based on ARMAX model residual", *Structural Control and Health Monitoring*, **23** (2), 218-236.

103. Meier, C., Popp, A. & Wall, W.A. Geometrically Exact Finite Element Formulations for Slender Beams: Kirchhoff–Love Theory Versus Simo–Reissner Theory. Arch Computat Methods Eng 26, 163–243 (2019). https://doi.org/10.1007/s11831-017-9232-5.

104. Midas Civil [Computer software] Midas Information Technology Co.2015, Ltd. http://en.midasuser.com/product/civil_overview.asp.

105. Mindlin, R. D. (1951) Influence of rotatory inertia and shear on flexural motions of isotropic elastic plates. ASME Journal of Applied Mechanics. 18 31–38.

106. Navier L. Resumé des lecons sur l'application de la Mécanique. Ecole de Ponts et Chaussées, Paris, 1826.

107. Nickel, R.E., Secor, G.A. (1972) Convergence of consistently derived Timoshenko beam finite elements, Int. J. Numer. Meth. Engng. 5 243-253.

108. Nodargi, N.A. An Overview of Mixed Finite Elements for the Analysis of Inelastic Bidimensional Structures. Arch Computat Methods Eng 26, 1117–1151 (2019). https://doi.org/10.1007/s11831-018-9293-0

109. Nogal, M., Lozano-Galant, J.A., Turmo, J. and Castillo, E (2015), "Numerical damage identification of structures by observability techniques based on static loading tests", *Structure and Infrastructure Engineering*, **12** (9), 1216-1227.

110. Nguyen, D.K. & Tran, T.T (2018), "Free vibration of tapered BFGM beams using an efficient shear deformable finite element model", *Steel and Composite Structures*, **29** (3) ,363-377.

111. Ozdagli, A. I., Liu, B., Moreu, F. (2018) Measuring Total Transverse Reference-Free Displacements for Condition Assessment of Timber Railroad Bridges: Experimental Validation. Journal of Structural Engineering. 144 040180471.

112. Pajonk, O (2009), "Overview of System Identification with Focus on Inverse Modeling", *Technische Universität Braunschweig*, **63**.

113. T. PENG, M. Nogal, J.R. Casas, J.A. Lozano-Galant, J. Turmo. Constrained Observability Techniques for Structural System Identification Using Modal Analysis, Journal of Sound and Vibration,Structural system identification by measurement error-minimizing observability method (2019) Structural Control and Health Monitoring 26(6) DOI: 10.1002/stc.2425

114. Pickhaver, J.A. (2006) Numerical modelling of building response to tunneling. Ph.D. thesis, University of Oxford.

115. Pisano, A.A (1999), "Structural System Identification: Advanced Approaches and Applications". PhD. Ph.D. Dissertation, Università di Pavia, Italy.

116. Prathap, G. Bhashyam, G.R. (1982) Reduced integration and the shear flexible beam element, Int. J. Numer. Methods Engrg. 18 195-210.

117. Przemieniecki, J.S. (1968) Theory of Matrix Structural Analysis. Library of Congress Catalog Card Number 67, 19151.

118. Rapp E., "Microfluidics: Modelling, Mechanics and Mathematics", Elsevier (2017) ISBN 9781455731411, https://doi.org/10.1016/B978-1-4557-3141-1.50048-4.

119. Rao, S. "The Finite Element Method in Engineering (Sixth Edition")", Butterworth-Heinemann (2018) ISBN 9780128117682, https://doi.org/10.1016/B978-0-12-811768-2.03001-7.

120. Reddy, J. N. (1984) Energy and Variational Methods in Applied Mechanics, New York: John Wiley. ISBN: 978-0-471-89673-9.

121. Reddy, J. N. (2006) An introduction to the finite element method, McGraw-Hill Education, ISBN: 9780072466850.

122. Rocas, M., García-González, A., Larráyoz, X. Nonintrusive Stochastic Finite Elements for Crashworthiness with VPS/Pamcrash. Arch Computat Methods Eng (2020). https://doi.org/10.1007/s11831-019-09397-x.

123. Saint-Venant Barré de. Course lectures Ecole Polytechnique, Paris, 1838.

124. Sanayei, Masoud & Arya, Behnam & Santini, Erin & Wadia-Fascetti, Sara. (2001). Significance of Modeling Error in Structural Parameter Estimation. Computer-Aided Civil and Infrastructure Engineering. 16. 12 - 27. 10.1111/0885-9507.00210.

125. Sapountzakis, E. J. and Kampitsis, A. E., (2010) Nonlinear dynamic analysis of Timoshenko beam-columns partially supported on tensionless Winkler foundation, Computers and Structures, 88, 1206-1219.

126. Sapountzakis, E. (2011). Nonlinear Analysis of Shear Deformable Beam-Columns Partially Supported on Tensionless Three-Parameter Foundation. Archive of Applied Mechanics. 81. 1833-1851. 10.1007/s00419-011-0521-4.

127. Sapountzakis, E. J. & Kampitsis, A.E., (2011). Nonlinear response of shear deformable beams on tensionless nonlinear viscoelastic foundation under moving loads. Journal of Sound and Vibration. 330. 5410–5426. 10.1016/j.jsv.2011.06.009.

128. Sayyad, A.S (2011), "Comparison of various refined beam theories for the bending and free vibration analysis of thick beams", *Applied and Computational Mechanics*, **5**, 217–230.

129. Severn, R. T. (1970) Inclusion of shear deformation in the stiffness matrix for a beam element. Journal of Strain Analysis 5 239-241.

130. Shafieezadeh, A., & Ryan, K. L. (2011). Demonstration of robust stability and performance of filter-enhanced H 2/LQG controllers for a nonlinear structure. Structural Control and Health Monitoring, 18(6), 710-720. doi:10.1002/stc.387

131. Sirca Jr, G.F., & Adeli, H. (2012). System identification in structural engineering. *Scientia Iranica*, **19**(6), 1355-1364.

132. Singh, S. K., & Chakrabarti, A. (2017) Hygrothermal analysis of laminated composites using C0 FE model based on higher order zigzag theory. Steel and Composite Structures, 23(1) 41-51. doi:10.12989/scs.2017.23.1.041

133. Soto, I.L., Rojas, A.L (2017), "Modeling for fixed-end moments of I-sections with straight haunches under concentrated load", *Steel and Composite Structures*, **23** (5), 597-610.

134. Southwell RV. Stress calculation in frameworks by the method of systematic relaxation of constraints. Proceedings of the Royal Society 1935; 15:36–95.

135. Southwell RV. Relaxation Methods in Theoretical Physics, vol. I. Clarendon Press: Oxford, 1946.

136. Southwell RV. Relaxation Methods in Theoretical Physics, vol. II. Clarendon Press: Oxford, 1956.

137. Tessler, A., Dong, S. B. (1981) On a hierarchy of conforming Timoshenko beam elements, Comput. Struct. l4(3-4) 335-344.

138. Thirumalaiselvi, A., Anandavalli, N., Rajasankar, J., Iyer, N.R (2016), "Numerical evaluation of deformation capacity of laced steel-concrete composite beams under monotonic loading", *Steel and Composite Structures*, **20** (1), 167-184.

139. Timoshenko, S. P (1921), "On the correction for shear of the differential equation for transverse vibrations of prismatic bars", *Philosophical Magazine*, 41 (6), 742–746.

140. Timoshenko, S. P. (1922) On the transverse vibrations of bars of uniform cross-section. Philosophical Magazine. 43 125-131.

141. Tomas, D., Lozano-Galant, J.A., Ramos, G., Turmo, J (2018), "Structural system identification of thin web bridges by observability techniques considering shear deformation", *Thin-Walled Structures*, **123**, 282-293.

142. Thomas, D.L., Wilson, J.M., Wilson, R.R. (1973) Timoshenko beam finite element. Journal of sound and vibration. 31(3) 315-330.

143. Turner. M.J. (1959) The Direct Stiffness Method of Structural Analysis. Structural and Materials Panel Paper, AGARD Meeting, Aachen.

144. Turner, M. J., Clough, R. W., Martin, H. C. and Topp, L. J. (1956). Stiffness and Deflection Analysis of Complex Structures. J. Aeron. Sci., 23, 805-824

145. Turner MJ, Martin HC, Weikel RC. Further development and applications of the stiffness method. AGARD Structures and Materials Panel, Paris, France in AGARDograph 72, 1962.

146. Valerio, P., Ibell, T. J., & Darby, A. P. (2011) Shear assessment of prestressed concrete bridges. Proceedings of the Institution of Civil Engineers: Bridge Engineering, 164(4) 195-210. doi:10.1680/bren.2011.164.4.195

147. Vicente, M.A., Gonzalez, D.C., Minguez, J., Schumacher, T (2018), "A Novel Laser and Video-Based Displacement Transducer to Monitor Bridge Deflections", *Sensors*, **18**(4), 970-985.

148. Vigliotti, A., Auricchio, F. Automatic Differentiation for Solid Mechanics. Arch Computat Methods Eng (2020). https://doi.org/10.1007/s11831-019-09396-y

149. Walter Ritz. 1909. Theorie der transversalschwingungen einer quadratischen platte mit freien Rändern. Ann. Der Physik 333, 4 (1909), 737–786. OI:https://doi.org/10.1002/andp.19093330403

150. Walsh, B. J., González, A (2009), "Assessment of the Condition of a Beam Using a Static Loading Test", *Key Engineering Materials*, 413–414, 269-276.

151. Wang, J., Li, T., Luo, L (2018), "Theoretical and experimental study on deflection of steel-concrete composite truss beams", *Steel and Composite Structures*, **29** (1), 91-106.

152. Weaver W., Gere J.M. (1990) Computer-Oriented Direct Stiffness Method. In: Matrix Analysis of Framed Structures. Springer, Boston, MA DOI:https://doi.org/10.1007/978-1-4684-7487-9_4.

153. Yan, A., Golinval, J (2005), "Structural damage localization by combining flexibility and stiffness methods", Engineering Structures, 27 (12) ,1752–1761.

154. Yang, Y., Chen, Y., Zhang, J., Xue, Y., Liu, R., Yu, Y (2018), "Experimental investigation on shear capacity of partially prefabricated steel reinforced concrete columns", Steel and Composite Structures, 28 (1), 73-82.

155. Zarga, D., Tounsi, A., Bousahla, A. A., Bourada, F., & Mahmoud, S. R. Thermomechanical bending study for functionally graded sandwich plates using a simple quasi-3D shear deformation theory. Steel and Composite Structures, 32(3). (2019) 389-410. doi:10.12989/scs.2019.32.3.389

156. Zeng, W., Liu, G.R. Smoothed Finite Element Methods (S-FEM): An Overview and Recent Developments. Arch Computat Methods Eng 25, 397–435 (2018). https://doi.org/10.1007/s11831-016-9202-3.

157. Zhang, F. -., Yang, Y. -., Xiong, H. -., Yang, J. -., & Yu, Z. (2019). Structural health monitoring of a 250-m super-tall building and operational modal analysis using the fast bayesian FFT method. Structural Control and Health Monitoring, 26(8) doi:10.1002/stc.2383

158. Zienkiewicz, O. C. (1996). Origins, milestones and directions of the finite element method-A personal view doi:10.1016/S1570-8659(96)80002-0

159. Zienkiewicz OC. (1965) Displacement and equilibrium models in the finite element method by B. Fraeijs de Veubeke, Chapter 9, pages 145–197 of Stress Analysis, Edited by O. C. Zienkiewicz and G. S. Holister, Published by John Wiley & Sons,. Int J Numer Methods Eng

160. Zienkiewicz, O. (2004). The birth of the finite element method and of computational mechanics. International Journal for Numerical Methods in Engineering. 60. 3 - 10. 10.1002/nme.951.

161. Zohdi, T.I. Rapid Voxel-Based Digital-Computation for Complex Microstructured Media. Arch Computat Methods Eng 26, 1379–1394 (2019). https://doi.org/10.1007/s11831-018-9284-1

Appendix 1

Structural System Identification Including Shear Deformation of Composite Bridges from Vertical Deflections

Seyyed B. Emadi[1], Jose A. Lozano-Galant[2], Ye Xia*[3], Gonzalo Ramos[1], Jose Turmo[3]

[1]Department of Civil and Environmental Engineering, Universitat Politècnica de Catalunya (UPC) BarcelonaTECH, Barcelona, Spain.
[2]Department of Civil Engineering, University of Castilla-La Mancha, Ciudad Real, Spain.
[3]Department of Bridge Engineering, Tongji University, Shanghai, China

Abstract. Shear deformation effects are neglected in most structural system identification methods. This assumption might lead to important errors in some structures like built up steel or composite deep beams. Recently, the observability techniques were presented as one of the first methods for the inverse analysis of structures including the shear effects. In this way, the mechanical properties of the structures could be obtained from the nodal movements measured on static tests. One of the main controversial features of this procedure is the fact that the measurement set must include rotations. This characteristic might be especially problematic in those structures where rotations cannot be measured. To solve this problem and to increase its applicability, this paper proposes an update of the observability method to enable the structural identification including shear effects by measuring only vertical deflections. This modification is based on the introduction of a numerical optimization method. With this aim, the inverse analysis of several examples of growing complexity is presented to illustrate the validity and potential of the updated method.

Keywords: Structural system identification; Observability; Shear deformation; Vertical deflection; Composite structures

1. Introduction

System Identification (SI) is a process of modeling an unknown system that has been employed in a number of engineering fields (Sirca, G.F *et al.* 2012, Altunişik, A.C *et al.* 2017) .The discipline of SI aims to create mathematical models that characterize properly the system behavior. One of the pioneers in this approach was Friedrich Gauss who developed the Gauss-Newton method to find the values of parameters in a model of the trajectory to calculate the dwarf planet trajectories. SI began in the area of electronic engineering and, after a while, it has been extended to other fields of engineering (Gevers, M. 2006, Pisano, A.A. 1999). Structural system identification (SSI) is a part of the SI dealing with the construction of mathematical models to identify the structural parameters (such as flexural stiffnesses, axial stiffnesses or damping parameters) from the structural response (Pajonk, O. 2009).

---

[1] Ph.D., seyyed.behrad.emadi@upc.edu

[2] Associate Professor, joseantonio.lozano@uclm.es

* Corresponding Author, Associate Professor, P.E., yxia@tongji.edu.cn

[3] Professor, jose.turmo@upc.edu

A number of methods are proposed for SSI in the literature (Liao, J. 2012, Lozano-Galant JA. 2013, Yan, A., 2005). These methods can be classified according to the excitation test type as dynamic (Breuer, P. *et al*. 2015, Dowling, J. *et al*, 2012, Li, Z. *et al*.2017, Górski, P. *et al*. 2018) or static (Thirumalaiselvi, A. *et al*.2016, Walsh, B. J. *et al*.2009, Lee, J.W. *et al*.2010). SSI methods might be also classified as a parametric (Lozano-Galant JA. *et al*.2013, Gracia-Palencia, A.J. *et al*.2015) or non-parametric methods (Karabelivo, K. *et al*. 2015, Mei, L. *et al*. 2016). Parametric methods rely on the physical based modes, while in non-parametric ones, parameters do not have any physical meaning. In non-parametric methods, parameters are identified directly with optimization procedures that minimize the difference between the predicted structural response and the measured ones. For parametric SSI methods, a mathematical representation of the structural behavior is required. The most common way to do this modeling is based on the Stiffness Matrix Method (SMM) (Hou, Z. *et al*. 2015, Kahya, V. *et al*.2018, Li, J. *et al*.,2017, Khayat, M. *et al*. 2017, Khayat, M. *et al*. 2017, Li, J. *et al*.2014, Araki, Y. *et al*.2005). The details of the main SSI methods proposed in the literature is presented in (American Society of Civil Engineers, Reston, VA 2013).

Despite the importance of shear deformation in some structures, it is overlooked by most of SSI methods. For most structures, deflection due to the shear is much smaller than the deflection due to the bending, thus this phenomenon can be ignored. In these cases, shear effects are considered as modeling errors in the mathematical models (such as any property in the model assumed with a wrong value). Nevertheless, in some structures (such as deep beams, shear walls, short span beams, or thin-web bridges) shear effects might play an important role. In this case, they should not be neglected and should be introduced into the formulation.

Most traditional SSI methods are not able to observe correctly the parameters of a structure (such as bending stiffness) when shear deformation is not negligible. SSI methods based on SMM normally use elementary beam theory, underestimating deflections and overestimating the natural frequencies since the shear deformation effect is disregarded (Sayyad, A.S .2011). Timoshenko (1921) was the first one who included shear effects into the beam theory. This approach is known as Timoshenko beam theory. Due to the complexity of this theory, SSI models are mostly based on Euler–Bernoulli beam theory which only includes axial and flexural deformation and shear effects are neglected in the analysis. Some authors studied the effect of shear deformation in their SMM models of composite structures (Kumar, P. *et al*. 2018, Nguyen, D.K. *et al*.2018, Singh, S.K. *et al*.2017). Moreover, Soto et al. (2017) proposed a new SMM's formulation including shear effects for the modeling fixed–end moments of I-sections. The effects of shear deformations in recursive matrix method for sandwich plate were also studied by (Huo, R. *et al*.2017)). The impact of shear effects in steel-concrete composite structures is studied by (Yang, Y. *et al*.2018) and (Wang, J. *et al*. 2018). Tomas et al. (2018) included the effects of shear deformations in Observability Method (OM). This method introduced the shear formulation into the SMM. Among the advantages of the method, it is to highlight the fact that it provided for the first time in the literature parametric equations of the shear estimates by the OM. The main inconvenience of this methods is that the measurement set requires both rotations and vertical deflections to identify mechanical properties. OM is a parametric SSI method based on the system of equations of the SMM. In this procedure, the axial and flexural stiffnesses are obtained from the static deformations measured in a static test. OM has proved its efficiency in different structural typologies (such as trusses, beams, frame structures and cable-stayed bridges) (Lozano-Galant, J.A. *et al*.2014, Nogal, M. *et al*.2015, Castillo, E. *et al*. 2007, Castillo, E. *et al*. 2016, Lozano-Galant, J.A. *et al*. 2015, Lei, J. *et al*.2016, Lei, J. *et al*.2017).

Among the many parameters that can be monitored in structures, vertical displacement is one of the parameters that is more valuable than others. This is due to the fact that material degradation processes, corrosion, and changes of the mechanical properties of the steel structure because of aging (e.g. fatigue in steel bridges) have a direct effect on the static vertical deflections (Vicente, M.A. *et al*. 2018). Moreover, for the bridge service loads, all international standards specifically use the maximum allowable vertical deflections to authenticate its performance (AASTHO.2017, European Committee for Standardization.

2005). The aim of this paper is to avoid the need for including rotations in the measurement sets used for structural identification of parameters when shear behavior is taken into account. This application is not as straightforward as it might look because the equations are strongly coupled. To solve this problem, constrained observability method (COM) (Lei, j. *et al*.2017) is applied. This new method is a numerical optimization approach, where the coupled linearized variables are numerically decoupled.

This article is organized as follows: In Section 2, the SSI including shear deformations with OM is briefly presented. A simply supported beam is analyzed to illustrate the inability of the method presented in (Tomas, D. *et al*.2018) to identify mechanical properties by measuring just vertical deflections. Section 3 introduces COM to enable the structural identification by measuring only vertical deflections. To illustrate the application of this algorithm, a step by step example of a simply supported beam is presented. In addition, another numerical example of an intermediate construction stage of a cantilever bridge is analyzed. Finally, the conclusions are drawn in Section 4.

2. Observability Method including shear effects

From 2D beam element direct SMM of a structure loaded in its plane, the nodal equilibrium equations might be written as:

$$[K] \cdot \{\delta\} = \{f\} \tag{1}$$

where the displacements vector $\{\delta\}$ contains the horizontal, vertical, and rotational displacements, the external force vector $\{f\}$ contains the horizontal forces, vertical forces, and moments and the global stiffness matrix $[K]$ contains the stiffness of the beam elements. According to the literature, in 1968, Przemieniecki added shear deformation to the stiffness matrix for the very first time. Stiffness matrix including shear stiffness is as follows:

$$[K] = \begin{bmatrix} \dfrac{EA}{L} & 0 & 0 & -\dfrac{EA}{L} & 0 & 0 \\ 0 & \dfrac{12EI}{L^3(1+\emptyset)} & \dfrac{6EI}{L^2(1+\emptyset)} & 0 & -\dfrac{12EI}{L^3(1+\emptyset)} & \dfrac{6EI}{L^2(1+\emptyset)} \\ 0 & \dfrac{6EI}{L^2(1+\emptyset)} & \dfrac{EI(4+\emptyset)}{L(1+\emptyset)} & 0 & -\dfrac{6EI}{L^2(1+\emptyset)} & \dfrac{EI(2-\emptyset)}{L(1+\emptyset)} \\ -\dfrac{EA}{L} & 0 & 0 & \dfrac{EA}{L} & 0 & 0 \\ 0 & -\dfrac{12EI}{L^3(1+\emptyset)} & -\dfrac{6EI}{L^2(1+\emptyset)} & 0 & \dfrac{12EI}{L^3(1+\emptyset)} & -\dfrac{6EI}{L^2(1+\emptyset)} \\ 0 & \dfrac{6EI}{L^2(1+\emptyset)} & \dfrac{EI(2-\emptyset)}{L(1+\emptyset)} & 0 & -\dfrac{6EI}{L^2(1+\emptyset)} & \dfrac{EI(4+\emptyset)}{L(1+\emptyset)} \end{bmatrix} \tag{2}$$

The stiffness matrix $[K]$ contains the information of flexural stiffness EI, axial stiffness EA and length L, where E, I and A are Young modulus, inertia and area, respectively. Unlike traditional stiffness matrix, a coefficient $\emptyset$ known as the shear parameter appears in some elements of Equation (2). This parameter is as follows:

$$\emptyset = \frac{12EI}{GA_v L^2} \ , \tag{3}$$

where A_v is the shear area and G is the shear modulus, which can be expressed as:

$$G = \frac{E}{2(1 + v)} \tag{4}$$

where the coefficient v is Poisson's ratio. Analysis of Equation (2) shows that shear parameter Ø appears in the denominator of most terms. In order to solve this problem, Tomas et al. proposed the following change of variable implying a shear parameter Q. This parameter is described as follows:

$$Q = \frac{\emptyset}{1 + \emptyset} \tag{5}$$

After replacing the shear parameter Ø by OM shear parameter Q, the stiffness matrix presented in Equation (2) can be updated as:

$$[K] = \begin{bmatrix}
\frac{EA}{L} & 0 & 0 & -\frac{EA}{L} & 0 & 0 \\
0 & \frac{12EI}{L^3} - \frac{12EIQ}{L^3} & \frac{6EI}{L^2} - \frac{6EIQ}{L^2} & 0 & -\frac{12EI}{L^3} + \frac{12EIQ}{L^3} & \frac{6EI}{L^2} - \frac{6EIQ}{L^2} \\
0 & \frac{6EI}{L^2} - \frac{6EIQ}{L^2} & \frac{4EI}{L} - \frac{3EIQ}{L} & 0 & -\frac{6EI}{L^2} + \frac{6EIQ}{L^2} & \frac{2EI}{L} - \frac{3EIQ}{L} \\
-\frac{EA}{L} & 0 & 0 & \frac{EA}{L} & 0 & 0 \\
0 & -\frac{12EI}{L^3} + \frac{12EIQ}{L^3} & -\frac{6EI}{L^2} + \frac{6EIQ}{L^2} & 0 & \frac{12EI}{L^3} - \frac{12EIQ}{L^3} & -\frac{6EI}{L^2} + \frac{6EIQ}{L^2} \\
0 & \frac{6EI}{L^2} - \frac{6EIQ}{L^2} & \frac{2EI}{L} - \frac{3EIQ}{L} & 0 & -\frac{6EI}{L^2} + \frac{6EIQ}{L^2} & \frac{4EI}{L} - \frac{3EIQ}{L}
\end{bmatrix} \tag{6}$$

Once the geometry, the boundary conditions and the applied nodal forces in a certain static load test are defined, some displacements can be measured to identify the unknown mechanical properties in the SMM. To do so, an inverse analysis is performed. The known information is clustered in a subset δ_1 and f_1 of $\{\delta\}$ and $\{f\}$, respectively and the subset δ_0 of $\{\delta\}$ and a subset f_0 of $\{f\}$ are assumed as unknown information. The equation (1) can be rewritten as follows:

$$[K^*] \cdot \{\delta^*\} = \begin{bmatrix} K_{00}^* & K_{01}^* \\ K_{10}^* & K_{11}^* \end{bmatrix} \cdot \begin{Bmatrix} \delta_0^* \\ \delta_1^* \end{Bmatrix} = \begin{Bmatrix} f_0 \\ f_1 \end{Bmatrix} = \{f\}, \tag{7}$$

In order to join the unknown variable in the left-hand side and the known variable in the right-hand side, the Equation (7) is rearranged as:

$$[B] \cdot \{z\} = \begin{bmatrix} K_{10}^* & 0 \\ K_{00}^* & -I \end{bmatrix} \cdot \begin{Bmatrix} \delta_0^* \\ f_0 \end{Bmatrix} = \begin{Bmatrix} f_1 - K_{11}^* \delta_1^* \\ -K_{01}^* \delta_1^* \end{Bmatrix} = \{D\}, \tag{8}$$

where 0 and I are the null and the identity matrices, respectively. To evaluate if the system has a solution, the null space $[V]$ of matrix $[B]$ should be calculated and check that $[V]^T\{D\} = 0$. If the equation holds, the system is compatible; otherwise, it has no solution. The general solution (the set of all solutions) of the system (8) has the structure (Castillo, E. *et al*.2000, Castillo, E. *et al*.2002):

$$\{Z\} = \{Z_p\} + [V] \cdot \{\rho\}, \tag{9}$$

where $\{Z_p\}$ is a particular solution of the system (9). $[V].\{\rho\}$ is the set of all solutions of the associated homogeneous system of equations (a linear space of solutions, where the columns of $[V]$ are a basis of this linear space and the elements of the vector $\{\rho\}$ are arbitrary real values that describe the coefficients of all possible linear combinations). It should be noted that a variable has a unique solution not only when matrix $[V]$ has zero dimension (it does not exist), but when the associated row in matrix $[V]$ is null. Thus, the examination of matrix $[V]$ and identification of its null rows leads to the identification of the subset of

variables with a unique solution in vector {Z}. It is interesting to note that if all parameters of vector {Z} are not observed from the null space, any deflection, force or parameter observed after the initial OM analysis will be used to observe new parameters by using a recursive process. For more information about this process, the reader is addressed to (Lozano-Galant JA. *et al.*.2013, Timoshenko, S. P .1921).

According to the literature, more reliable information can be produced from measuring vertical displacement than rotation and most of international standards deal with vertical deformation (Vicente, M.A. *et al.* 2018, AASTHO.2017, European Committee for Standardization.2005). So it is useful to provide a method that allows SSI from measured vertical deflections. Traditional OM including shear deformation presented in (Tomas, D. *et al.*.2018) fails identifying shear parameters with measurement sets including only vertical deflections. In fact, the measurement of rotations is required to observe any parameter by OM. To show the inability of OM to identify material properties with only measured vertical deflection an illustrative example is analyzed in the following section.

2.1 Example 1: Simply supported beam with vertical deflections

Consider the 0.6 m long simply supported beam modelled with 7 nodes and 6 Timoshenko beam elements in figure 1.a, where, vj, with j (1 to 7) represents the vertical deflection for each node. Beam has a constant cross section and the value of young modulus, Poisson ratio, shear area, cross sectional area and inertia of all elements along the beam are constant. Properties of this simply supported beam are listed on Table 1. The boundary conditions of the structure are horizontal and vertical displacements restricted in node 1 and vertical displacement restricted in node 7 (this is to say, u1=v1=v7= 0) and the only external force applied in this numerical loading test is a concentrated vertical force in node 3 of 100kN (V3= 100kN). The vertical deflections obtained from the software Midas/Civil of this structure are presented in Fig. 1 b Measurement errors in this paper are neglected.

(a) FEM for a simply supported beam with vertical deflections	(b) Vertical nodal deflections including flexural and shear deformation.
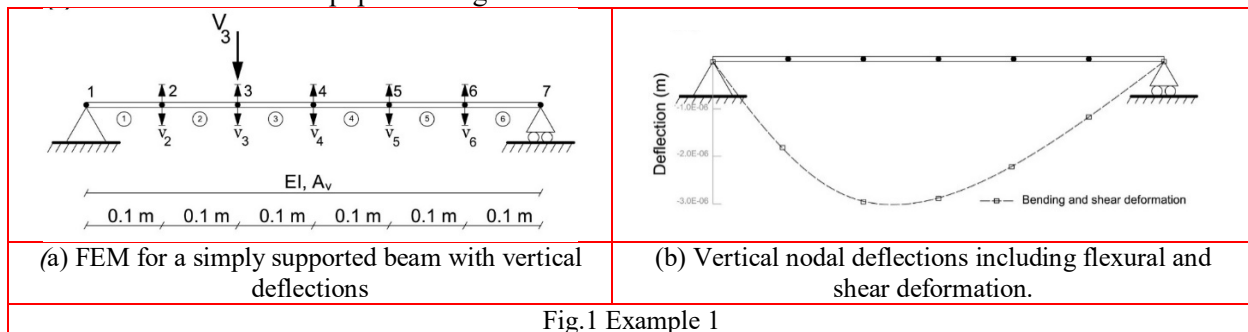
Fig.1 Example 1

Table 1 Properties of the FEM of the simply supported beam

Area [m²]	0.1
Shear Area [m²]	0.0833
Inertia [m⁴]	0.0083
Young's Modulus [GPa]	27
Poisson's Ratio γ	0.25

For this inverse analysis of the structure, V3, the length of the elements, Poisson's ratio and young modulus are assumed as known, while the inertia I and the shear area A_v are assumed as unknown. Since no horizontal force is applied in this example, the axial resistant mechanisms are not activated. So the terms associated with axial behavior are removed from general SMM system of equations. Since the only two unknown parameters assumed in example 1 are A_v and I, the measurement of at least two deformations is required to identify their values. Nevertheless, no set of vertical deflections enables the proper identification of the unknown parameters. To illustrate this inability of the method, the results of the SSI obtained with

the measurement set consisting of all 5 possible vertical deflections (this is v2 to v6 from figure 1.b) are presented. In this example, after the change of variable, the vector of unknowns $\{Z\}$, as it is presented in Eq. (9), include the unknown targeted parameters I and Q and some coupled unknown variables as I_{wj} and Q_w, as well as the boundary reactions (H1, V1, V7). The general solution can be written as follows:

As it expressed in the previous section (Eq. 9) when the associated row in matrix $[V]$ (the null space matrix) is null, the variable has a unique solution. In this example, the three rows of the null space (the ones corresponding with reactions H1, H7 and V7) are null. The general solution of these variables corresponds with the particular one and therefore, their solution is unique. In the next recursive step, the observed parameters are incorporated into the input of SSI by OM. Although these new inputs will update Eq. (10), the updated system of equations cannot observe any new variable. Hence, the recursive steps end and no additional information is observed. It is to remark that the only observed parameters correspond with the reactions of an isostatic structure which can be identified by equilibrium equations. This is not the case of the Inertia and the OM shear parameter, I and Q, as they appear strongly coupled with the rotations. These parameters cannot be observed as their null space is not null. This example illustrates the inability of OM to identify parameters when rotations are not included into the measurement set (even if as in this case the number of measurements exceeds the number of unknowns). As variables are strongly coupled, those equations dealing with including the effect of rotation cannot be used to solve the system, unless some rotations are included in the measurement set. In order to uncouple the variables in the system of equations properly, vertical deflection and rotation should be measured together. Otherwise, the system cannot be solved by OM. A mathematical explanation of this fact is that the null space rows associated with the inertia will not be zero, meaning that the parameters have not a unique solution. In order to enable the observability to identify structures without measuring rotations, a new procedure is presented in the following section.

$$
\begin{bmatrix} I \\ Iw_1 \\ Iw_2 \\ Iw_3 \\ Iw_4 \\ Iw_5 \\ Iw_6 \\ Iw_7 \\ Q \\ Qw_1 \\ Qw_2 \\ Qw_3 \\ Qw_4 \\ Qw_5 \\ Qw_6 \\ Qw_7 \\ H_1 \\ V_1 \\ V_7 \end{bmatrix} =
\begin{Bmatrix} 8.0E-07 \\ 5.0E-12 \\ 4.0E-12 \\ 2.0E-13 \\ 4.0E-12 \\ 7.0E-12 \\ 9.0E-12 \\ 1.0E-11 \\ 0.0 \\ 0.0 \\ 2.0E-11 \\ 0.0 \\ 0.0 \\ 0.0 \\ 0.0 \\ 0.0 \\ 0.0 \\ -6.7E04 \\ -3.3E04 \end{Bmatrix} +
\begin{bmatrix}
1 & \frac{L}{20*(v_5-2*v_6)} & 0 & \frac{-L}{20*(v_5-2*v_6)} \\
0 & \frac{-v_6}{2*(v_5-2*v_6)} & \frac{1}{2} & \frac{v_5-v_6}{2*(v_5-2*v_6)} \\
0 & \frac{-v_6}{2*(v_5-2*v_6)} & \frac{1}{2} & \frac{v_5-v_6}{2*(v_5-2*v_6)} \\
0 & \frac{-v_6}{2*(v_5-2*v_6)} & \frac{1}{2} & \frac{v_5-v_6}{2*(v_5-2*v_6)} \\
0 & \frac{-v_6}{2*(v_5-2*v_6)} & \frac{1}{2} & \frac{v_5-v_6}{2*(v_5-2*v_6)} \\
0 & \frac{-v_6}{2*(v_5-2*v_6)} & \frac{1}{2} & \frac{v_5-v_6}{2*(v_5-2*v_6)} \\
0 & \frac{-v_6}{2*(v_5-2*v_6)} & \frac{1}{2} & \frac{v_5-v_6}{2*(v_5-2*v_6)} \\
0 & \frac{-v_6}{2*(v_5-2*v_6)} & \frac{1}{2} & \frac{v_5-v_6}{2*(v_5-2*v_6)} \\
1 & 0 & 0 & 0 \\
0 & \frac{-2*(v_2-v_3+v_4-v_5+v_6)}{(v_5-2*v_6)} & 0 & \frac{2*v_2-2*v_3+2*v_4-v_5}{(v_5-2*v_6)} \\
0 & \frac{(v_2-2*v_3+2*v_4-2*v_5+v_6)}{(v_5-2*v_6)} & 1 & \frac{-(v_2-2*v_3+2*v_4-2*v_5+v_6)}{(v_5-2*v_6)} \\
0 & \frac{(v_3-2*v_4+2*v_5-2*v_6)}{(v_5-2*v_6)} & 0 & \frac{-(v_3-2*v_4+v_5)}{(v_5-2*v_6)} \\
0 & \frac{(v_4-2*v_5+v_6)}{(v_5-2*v_6)} & 1 & \frac{-(v_4-2*v_5+v_6)}{(v_5-2*v_6)} \\
0 & 1 & 0 & 0 \\
0 & 0 & 1 & 0 \\
0 & 0 & 0 & 1 \\
0 & 0 & 0 & 0 \\
0 & 0 & 0 & 0 \\
0 & 0 & 0 & 0
\end{bmatrix} \cdot
\begin{bmatrix} \rho_1 \\ \rho_2 \\ \rho_3 \\ \rho_4 \end{bmatrix} \quad (10)
$$

3. SSI by COM

One of the main characteristics of the OM is the linearization of the unknowns as products of unknowns are considered as new linear unknowns. For example, variable in Example 1, Iw1 corresponds in reality to the product of the inertia I and the rotation w1. Nevertheless, in the linearization it is considered as a unique Iw1, losing therefore any relation among the two multiplied terms (I and w1). This assumption, required to enable the application of OM in a linear system, might involve a significant loss of information. In order to uncouple the linearized products of unknown in traditional observability method, measurement sets have to mix rotations and deflections. Otherwise, the system cannot be solved.

Lei et al. (2017) found that in OM, the nonlinear constraints among product variables are lacking. According to this work, the reduced observability produced by these characteristics is due to the following reasons: (a) the immature end of the recursive steps and (b) the ineffective measurements because of redundancy in the measurement sets (the same problem appearing in example 1). The Constraint Observability Method (COM) finds a solution to the OM adding some nonlinear constraints: the value of the solution of the coupled unknowns has to be equal to the product of the single unknowns. Hence, the system of equations is solved numerically after including the nonlinear constrains. In comparison with OM, COM does not provide any symbolic solution. In order to obtain results from COM, initial numerical values should be assigned to the unknowns. Any number can be used as initial value, but in order to ease the

convergence in the optimization process, a ratio with the theoretical values (e.g. between 0.5 to 1.5) is advised.

In the COM (Lei.*et al.* 2017), variables are classified in one of the following three categories: (1) Coupled variables Vc (Iwj and Qwj from example 1) ; (2) Single variables Vs1 (I and Q from example 1), which already exist in the unknown {Z} vector; (3) Single variables Vs2 (wj from example 1), which did not exist in the unknown vector {Z} from OM. The new vector {Z} is named {Z*} and it is a combination of vector {Z} and the new single variables Vs2. In order to create an objective function for a numerical optimization process and take into the account the new unknowns Vs2, Eq. (8) can be rewritten as:

$$\{\in\} = [B^*] \cdot \{Z^*\} - \{D\}, \tag{11}$$

where $\in$ is the residuals of the equations which is a vector with the same number of rows of the original matrix B and $B^* = [B^{N_{eq} \times N_z} | \Omega^{N_{eq} \times N_{s2}}]$ is obtained by adding a null matrix Ω to the matrix B calculated from the last recursive step of SSI by OM. The size of this null matrix Ω is $N_{eq} \times N_{s2}$. N_{eq} and N_z, explain the number of equations and the number of unknowns in {Z} respectively. N_{s2} explains the number of new single unknowns in Vs2.
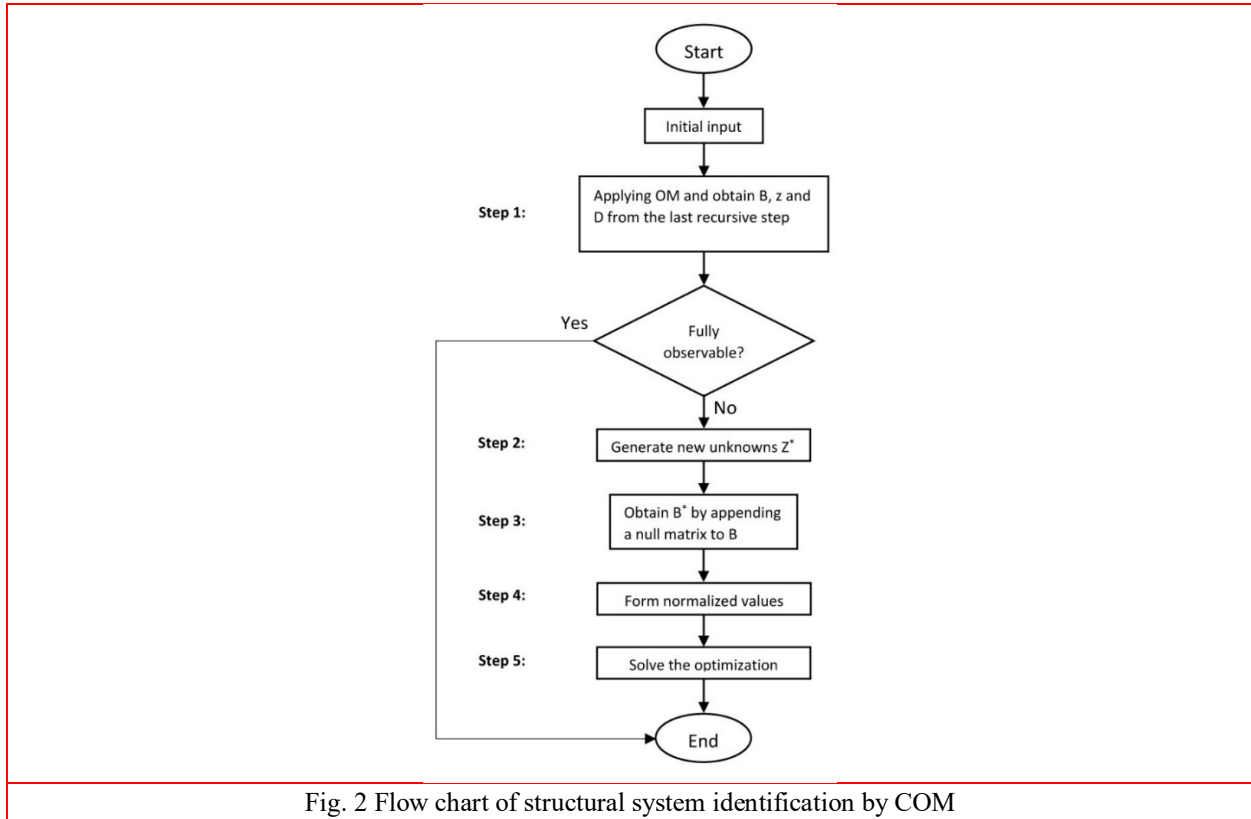

Fig. 2 Flow chart of structural system identification by COM

The objective function of the minimization problem is determined by minimizing the square sum of the residuals in Eq. (11). The optimization toolbox of Matlab (MATLAB and Optimization Toolbox Release 2017b) has been used to obtain the optimal solution of the objective function. In order to limit the computational expenses and the time of the optimization process, the stopping criterion has to be defined. In order to reach a certain level of efficiency in the COM optimization process, variables of Eq. (11) can be normalized.

The algorithm for SSI by COM is summarized as follows:
- **Step 1**: Apply SSI by OM to check whether any unknown is observed. If so, update the input and reinitiate OM until no new unknowns are observable. If full observability is achieved, there is no need to go to the COM process, otherwise go to the step 2.
- **Step 2**: Obtain the equation (8) from the last step of OM recursive process then generate the new unknown vector of Z* included Coupled variables V_c; as well as single variables V_{s1} and V_{s2}.
- **Step 3**: Add a null matrix $[\Omega]$ to the matrix $[B]$ to generate $[B^*]$, in order to contain Vs2 in Z* without violating system.
- **Step 4**: Obtain the normalized unknown parameters.
- **Step 5**: Guess the initial values of unknowns parameters of Z* vector, set the bound for the solution and solve the optimization process to find the minimized value for the residual vector, ϵ.

A summary of the procedure is shown in the flow chart in Figure 2. For more information about the COM, reader is addressed to (Lei.et al. 2017).

The majority of SSI methods, is based on the Euler-Bernoulli beam theory. Originally, COM method is not able to consider the effect of shear in measurements. To include this phenomenon, in this work, equations are updated to the procedure proposed by Tomás et al. (2018). With this new updated method, the problem of linearization in OM variables is solved and equations related to shear stiffnesses are taken into account. In order to illustrate the applicability of the method the same structure from Example 1 is analyzed below.

### 3.1 Example 1 revisited: simply supported beam with vertical deflections (COM)

$$Z = \begin{bmatrix} I \\ Iv_4 \\ Iv_5 \\ Iv_6 \\ Iw_1 \\ . \\ . \\ . \\ Iw_7 \\ Q \\ Qv_4 \\ Qv_5 \\ Qv_6 \\ Qw_1 \\ . \\ . \\ . \\ Qw_7 \\ H_1 \\ V_1 \\ V_7 \end{bmatrix} \quad (12) \qquad Z^* = \begin{bmatrix} I \\ I.v_4 \\ I.v_5 \\ I.v_6 \\ I.w_1 \\ . \\ . \\ . \\ I.w_7 \\ Q \\ Q.v_4 \\ Q.v_5 \\ Q.v_6 \\ Q.w_1 \\ . \\ . \\ . \\ Q.w_7 \\ H_1 \\ V_1 \\ V_7 \end{bmatrix} \quad (13)$$

The beam of example 1 is recalculated by the COM with the same parameters. The unknown inertia and shear parameter can be obtained not only with all possible vertical deflections (5 degrees of freedom) but also just with 2 deflections (e.g. v2 and v3). The {Z} vector of example 1 with just measuring v2 and v3 is presented in Eq. (12), but in order to apply COM, {Z*} should be calculated. The vector {Z*} of example 1 with a measured vertical deflection in nodes number 2 and 3 is presented in Eq. (13). As highlighted in the previous section, in the COM, terms of {Z*} vector should satisfy certain nonlinear constraints, e.g. $\{Q_1 w_1 = Q_1.w_1\}$, these constraints are neglected in OM due to the linearity of equations which lead to a failure of the identification of the mechanical properties.

Numerical information from Table 1 is multiplied by different random coefficients ranging from 0.5 to 1.5 to generate initial values for COM process. According to the results, the optimization converges to the

exact values of inertia and OM shear parameter after few iterations. In the following comparison, the evolution of shear area and inertia ratio throughout the iterative process for different initial values (0.5 for shear area and 1.5 for inertia) are presented in figures 3.a. and 3.b., respectively.

(a) Evolution of shear area parameter ratio throughout the iterative process	(b) Evolution of inertia ratio throughout the iterative process
Fig. 3 Evaluation of shear area and inertia ratio throughout the iterative process	
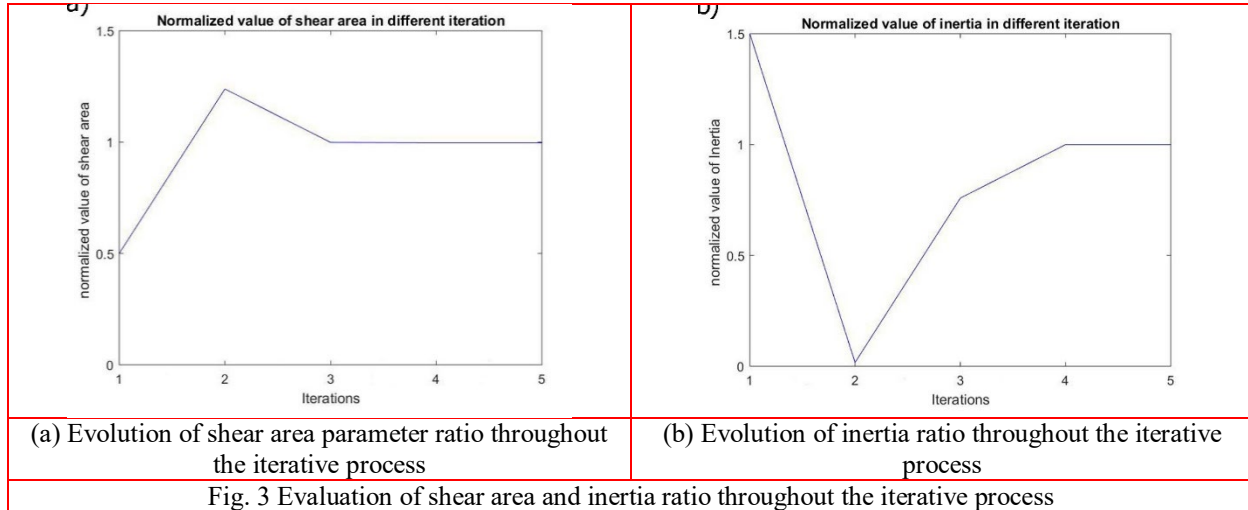
This example far from proving the strength of COM, in the following section a more complex example is presented to illustrate the potential of the developed tool.

3.2 Application to a composite bridge

To illustrate the possible application of the COM to an actual structure, the problem of the construction of a bridge by the balanced cantilever method is presented here. In such a construction method, deflections have to be anticipated in advance to calculate the precamber with which the different segments of the structure have to be built. In order to update this precamber for every step during construction, a thorough topographic surveying is usually performed. This information can be used for model updating via an inverse analysis. Even though shear deflections might not play a very important role for a full developed cantilever, modelling error of not taking into account shear effects for the first segments, might lead to an inaccurate estimation of the bending stiffness. To illustrate this and the possible application of this method, a simplified model of the Yunbao Bridge over the Yellow River in China (see Fig. 4) is studied in this section. The structure span is 90m long. An intermediate construction stage is considered in this example. This model includes the construction of two symmetric cantilevers. The length of the standard deck segments is 4.5m and the length of the segment over the pile, 2.5m. The total length of the studied construction stage is 29.5 m. The mechanical and material properties defined by the method of the transformed section (Chen, Y.S. *et al*. 1980) are listed in Table 2.

Fig. 4 Composite bridge on site (China) [53]
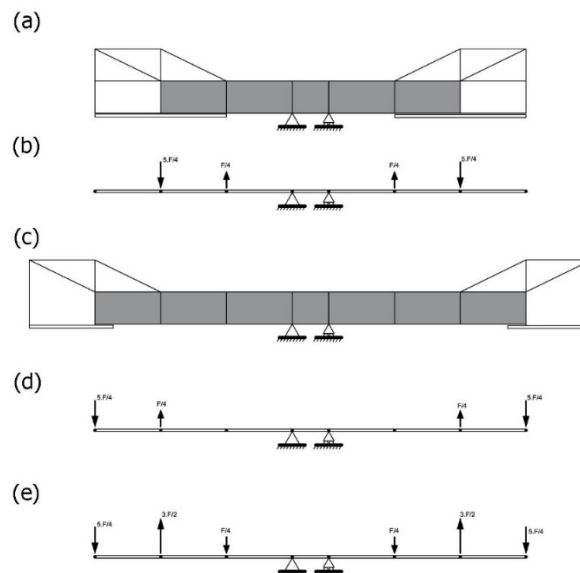
Fig. 5 Definition of the load case: (a, b) Stage i. (c, d) Stage i+1. (e) Load case used for the inverse analysis

Actual site data is not considered in this structure and the structural response is simulated numerically. Effects of creep and shrinkage in concrete are overlooked. The load test used simulates the movement of the formwork traveler (Fig. 5). The weight F of the formwork traveler (weight of formwork included) is considered as the 60 % of the weight of the segment (1041 kN). The effect of each form traveler in the deck is considered as two vertical forces. The values of these two forces are 0.25F and 1.25F (226 kN, upwards and 1267 kN, downwards). Load case of the bridge model is calculated by reducing the effects of the stage i (Fig. 5.a), from stage i+1 (Fig. 5.c), wherein the formwork traveler is moved forward to the next segment. Load cases of the stages i and i+1 are expressed in Figures 5.b and 5.d, respectively. The consequent load case introduced in the simulation is shown in Fig. 5.e. It is to highlight that the vertical resultant of such forces in each side of the cantilever is zero.

This structure is simulated by the simplified FEM presented in Fig. 6.a. This FEM includes 7 elements and 6 point loads. Software Midas/Civil is used in order to calculate the vertical deflections in the nodes of the structure presented in Fig 6.b. For brevity, in the inverse analysis, young modulus of all elements are considered as known parameters. Due to the fact that axial stiffness is not activated in this example, only

flexural behavior is analyzed. For this reason, the terms related to the axial behavior are removed from equations (as axial stiffness are not activated with vertical forces). Because of loading case, shear area in elements number 3,4 and 5 are not activated, so shear area in these elements cannot be observed in the inverse analysis. The shear area and inertia of all other beam elements (that is to say I1, I2, I3, I4, I5, I6, I7 and $A_{v1}, A_{v2}, A_{v6}, A_{v7}$) are assumed as unknowns.
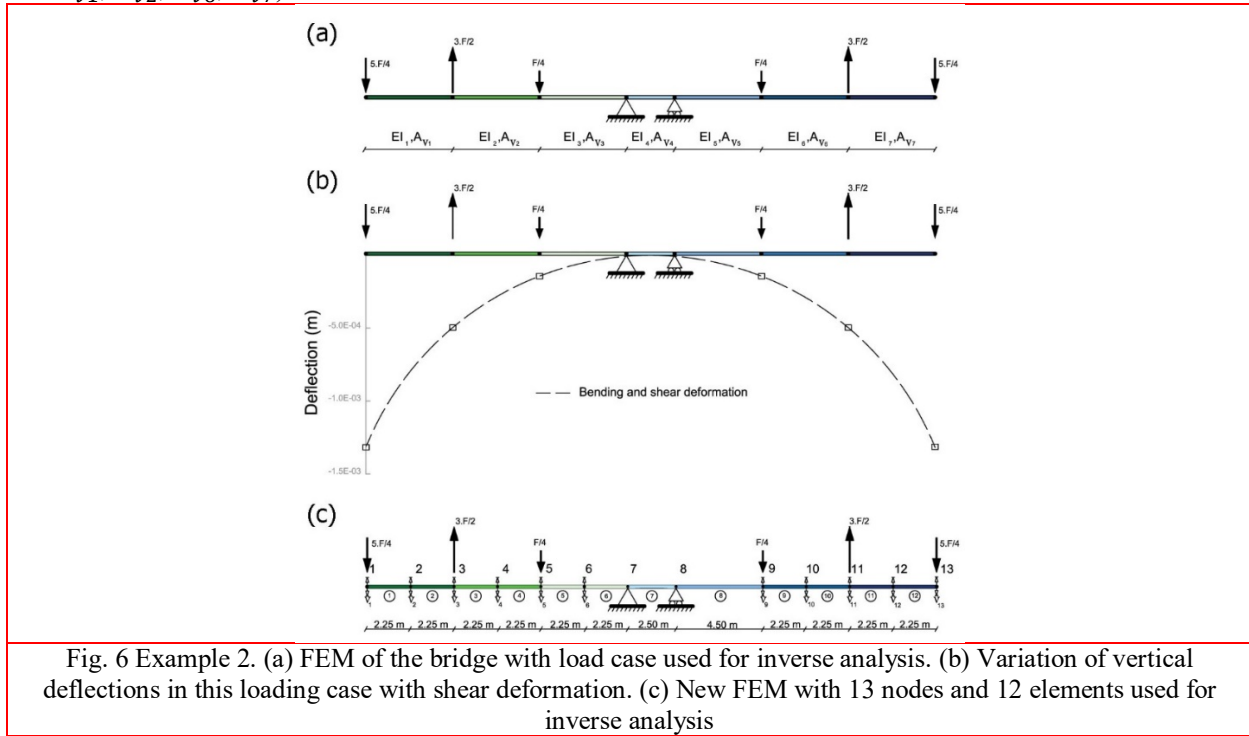

Fig. 6 Example 2. (a) FEM of the bridge with load case used for inverse analysis. (b) Variation of vertical deflections in this loading case with shear deformation. (c) New FEM with 13 nodes and 12 elements used for inverse analysis

Table 2 Properties of the Finite Element Model of the Bridge

Area [m^2]	12.52
Shear Area [m^2]	9.83
Inertia [m^4]	35.62
Steel Young's Modulus [GPa]	210
Concrete Young's Modulus [GPa]	35
Poisson's Ratio γ	0.3

In order to identify the 11 unknown mechanical properties at least, 11 measurements are required. As it was showed before, OM is not able to identify mechanical properties only with vertical deflections. However, it is examined and it is confirmed that no results were obtained with the measurement set of all possible vertical deflections (it is to say v1, v2, v3, v4, v5, v6, v9, v10, v11, v12, v13, v14, v15, v16) proposed for FEM presented in figure 6.c when traditional OM is applied. To observe parameters with OM, the variation of deflection and rotation should be taken into account. In order to observe parameters just by vertical deflection in bridge example, COM is applied. Table 3 presents the initial value coefficient of different unknown inertia and shear area which is randomly chosen between 0.5 and 1.5 for the optimization process.

Table 3 Initial value coefficient of the Bridge Unknown Properties

I_1	0.791
I_2	0.688
I_3	1.078
I_4	1.486
I_5	0.963
I_6	0.941
I_7	1.230
Q_1	1.312
Q_2	1.255
Q_6	0.944
Q_7	0.618

COM managed to observe unknown shear area and inertia in 14 iterations, the evolution of shear area and inertia ratio throughout the iterative process are presented in Fig.7 a and b, respectively.
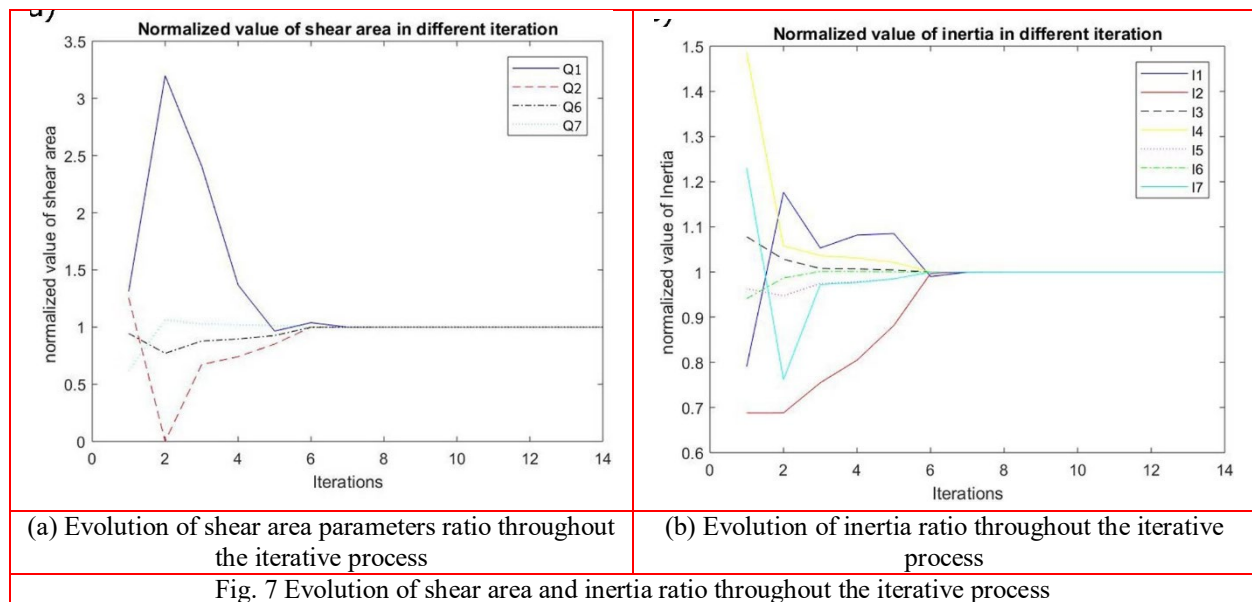
(a) Evolution of shear area parameters ratio throughout the iterative process	(b) Evolution of inertia ratio throughout the iterative process
Fig. 7 Evolution of shear area and inertia ratio throughout the iterative process	

To prove the consistency of the new method, 200 analyses with random initial value coefficients between 0.5 and 1.5 are conducted for the bridge. From 200 analyses, in 62 analyses the optimization process was not convergent to the solution and no result was acquired, 37 results of optimization process were removed, due to the fact that the result did not have any physical sense (nonsense values e.g. negative values). The normalized average, standard deviation and coefficient of variation of the remaining results as well as the mode is presented in Table 4.

Table. 4 obtained results from random initial values

	Average	CoV	Standard deviation
I_1	1.000	0.001	0.000
I_2	1.000	0.002	0.001
I_3	0.975	2.279	0.791
I_4	0.993	12.229	4.324
I_5	0.969	2.888	0.996
I_6	0.999	0.004	0.002
I_7	1.000	0.001	0.001

Tomas et al. (2018) compared differences between the estimated flexural stiffnesses (EI) and the actual values (EI) in the seven elements of the bridge example without including the shear effects into the stiffness matrix of OM. According to this work when shear deformations are included into the measurements (error free measurements), significant errors (e.g. -65,5 % in segments 1 and 7 or +26,7% in segments 2 and 6) appear in the observed flexural stiffnesses in OM. As it can be seen for table 4, these differences are greatly reduced with COM.

However, the shear area of some elements is not activated due to the loading case, making impossible the observation of shear areas of elements 5, 6, 7 and 8. This example proves the efficiency of the proposed COM to estimate inertia when shear effects are taken into account.

4. Conclusions

Most Structural System Identification (SSI) methods neglect shear deformation as this phenomenon is usually negligible in comparison with flexural deformation. However, it can play a significant role in some structures. According to the literature, the only detailed study which addressed the particular effects of this deformation in static SSI tests is the observability method (OM). But due to the complexity and linearity of equations, observability method fails to observe parameters just by vertical deflection. To fill this gap, this paper introduces the effects of shear deflections on the constrained observability method (COM). This method adds some nonlinear constrains to OM. Hence, the complex system of equations is solved numerically after including the nonlinear constrains.

A simply supported beam is studied, in order to show the inability of OM included shear effects to observe any parameter just by vertical deflections. To solve this problem, the formulation of constrained observability method (COM) is updated to include shear deformation. The COM performance in a simply supported beam shows the power of new method to observe value of parameters just by vertical deflection. Applicability of the COM on an actual thin web structure is studied an intermediate construction stage of a cantilever composite bridge in China. The results of this study shows that how the value of material properties can be observed by COM when the effects of shear are included in equations. Eventually, the results of COM are compared with the result of traditional OM when the effects of shear deformation are included into measurement sets, in order to illustrate the potential power of updated COM process.

Acknowledgements

References

1. Altunisik, A. C., Gunaydin, M., Sevim, B., & Adanur, S. (2017). System identification of arch dam model strengthened with CFRP composite materials. *Steel and Composite Structures*, 25(2), 231-244.

2. Araki, Y., Miyagi, Y (2005), "Mixed integer nonlinear least-squares problem for damage detection in truss structures", *Journal of Engineering Mechanics*, **131**(7) (2005), 659–667.

3. American society of Civil engineers, Structural Identification of Constructed Systems, American Society of Civil Engineers, Reston, VA 2013.

4. AASTHO (2017), LRFD Bridge Design Specifications, (8th Edition), American Association of State Highway and Transportation Officials; Washington, DC, USA.

5. Breuer, P., Chmielewski, T., Górski, P., Konopka, E., Tarczyński, L (2015), "Monitoring horizontal displacements in a vertical profile of a tall industrial chimney using Global Positioning System technology for detecting dynamic characteristics", *Structural Control and Health Monitoring*, **22** (7), 1002-1023.

6. Castillo, E., Conejo,A. J., Pruneda, R. E., Solares, C (2007), "Observability in linear systems of equations and inequalities: applications", *Computers and Operations Research*, **34** (6) 1708–20.

7. Castillo, E., Nogal, M., Lozano-Galant, J.A., Turmo, J (2016), "Solving Some Special Cases of Monomial-Ratio Equations Appearing Frequently in Physical and Engineering Problems", *Mathematical Problems in Engineering*.

8. Castillo, E., Cobo, A., Jubete, F., Pruneda, R.E. and Castillo, C (2000), "An orthogonally based pivoting transformation of matrices and some applications", *SIAM Journal on Matrix Analysis and Applications*, **22**(3),666-681.

9. Castillo, E., Jubete, F., Pruneda, R.E. and Solares, C (2002), "Obtaining simultaneous solutions of linear subsystems of equations and inequlities", *Linear Algebra and its Applications*, **364** (1-3),131-154.

10. Chen, Y.S. and Yen, B. T. (1980), Analysis of Composite Box Girders, Report N0 380.12, Fritz Engineering Laboratory Library.

11. Dowling, J., Obrien, E. J., González, A (2012), "Adaptation of Cross Entropy optimization to a dynamic Bridge WIM calibration problem", *Engineering Structures*, **44** ,13-22.

12. Deretić-Stojanović, B., Kostic, S.M (2017), "A simplified matrix stiffness method for analysis of composite and prestressed beams", *Steel and Composite Structures*, **24** (1), 53-63.

13. Dong, X. Zhao, L. Xu, Z. Du, S. Wang, S. Wang, X. and Jin, W(2017), "Construction of the Yunbao Bridge over the yellow river", EASEC-15. 2017, Xi'an, China.

14. Eurocode (2005), Design of Concrete Structures—Concrete Bridges—Design and Detailing Rules, European Committee for Standardization: Brussels, Belgium.

15. Gevers, M. (2006). A personal view of the development of system identification: A 30-year journey through an exciting field. IEEE Control Systems, **26**(6), 93-105.

16. Górski, P., Stankiewicz, B., Tatara, M (2018), "Structural evaluation of all-GFRP cable-stayed footbridge after 20 years of service life", *Steel and Composite Structures*, **29** (4),527-543.

17. Gracia-Palencia, A.J., Santini-Bell, E., Sipple, J.D. Sanayi, M (2015), "Structural model updating of an in-service bridge using dynamic data", *Structural Control and Health Monitoring*, **22** (10), 1265-1281.

18. Hou, Z., Xia, H., Y, W., Zhang, Y., Zhang, T (2015), "Dynamic analysis and model test on steel-concrete composite beams under moving loads", *Steel and Composite Structures*, **18** (3) ,565-582.

19. Huo, R., Liu, W., Wu, P., Zhou, D (2017), "Analytical solutions for sandwich plates considering permeation effect by 3-D elasticity theory", *Steel and Composite Structures*, **25** (2), 127-139.

20. Kahya, V., Turan, M (2018), "Vibration and buckling of laminated beams by a multi-layer finite element model", Steel and Composite Structures", **28** (4), 415-426.

21. Khayat, M., Poorveis, D., Moradi, S (2017), "Buckling analysis of functionally graded truncated conical shells under external displacement-dependent pressure", *Steel and Composite Structures*, **23** (1), 1-16.

22. Kumar, P., Srinivas, J (2018), "Transient vibration analysis of FG-MWCNT reinforced composite plate resting on foundation", *Steel and Composite Structures*, **29** (5), 569-578.

23. Karabelivo, K., Cue'llar, P., Baebler, M., Rucker, W (2015), "System identification of inverse, multimodal and nonlinear problem using evolutionary computing-application to a pile structure supported in nonlinear springs", *Engineering Structure*, 101, 609-620.

24. Liao, J., Tang, G., Meng, L., Liu, H., Zhang, Y (2012), "Finite element model updating based on field quasi-static generalized influence line and its bridge engineering application", *Procedia Engineering* ,**31**, 348–353.

25. Lozano-Galant J.A, Nogal M, Castillo E, Turmo J (2013), "Application of observability techniques to structural system identification", *Computer-Aided Civil and Infrastructure Engineering*, **28** (6), 434–450.

26. Li, Z., Park, H. S., Adeli, H (2017), "New method for modal identification of super high-rise building structures using discretized synchrosqueezed wavelet and Hilbert transforms", *The Structural Design of Tall and Special Building*, **26** (3), e1312.

27. Li, J., Jiang, L., Li, X (2017), "Free vibration of a steel-concrete composite beam with coupled longitudinal and bending motions", *Steel and Composite Structures*, **24** (1), 79-91.

28. Li, J., Huo, Q., Li, X., Kong, X., Wu, W (2014), "Dynamic stiffness analysis of steel-concrete composite beams", *Steel and Composite Structures*, **16** (6), 577-593.

29. Lee, J.W., Coi, K.H and Huh, Y.C (2010), "Damage detection method for large structures using static and dynamic strain data from distributed fiber optic sensor", *International Journal of Steel Structure* ,**10** (1) , 91-97.

30. Lozano-Galant, J.A., Nogal, M., Paya-Zaforteza, I., and Turmo, J (2014), "Structural system identification of cable-stayed bridges with observability techniques", *Structure and Infrastructure Engineering*, **10** (11), 1331-1344.

31. Lozano-Galant, J.A., Nogal, M., Turmo, J., Castillo, E (2015), "Selection of measurement sets in static structural identification of bridges using observability trees", *Computers and Concrete*, **15** (5), 771–794.

32. Lei, J., Lozano-Galant, J.A., Nogal, M., Xu, D., Turmo, J (2016), "Analysis of measurement and simulation errors in structural system identification by observability techniques", *Structural Control and Health Monitoring* , **24**(6), e1923.

33. Lei, J., Xu, D., Turmo, J (2017), "Static structural system identification for beam-like structures using compatibility conditions", *Structural Control and Health Monitoring*, **25**(1), e2062.

34. Lei, j., Nogal, M., Lozano-Galant, J.A., Xu, D. and Turmo, j (2017), "Constrained observability method in static structural system identification", *Structural Control and Health Monitoring*, **25** (1), e2040.

35. Mei, L., Mita, A. and Zhou, J. (2016), "An improved substructural damage detection approach of shear structure based on ARMAX model residual", *Structural Control and Health Monitoring*, **23** (2), 218-236.

36. MATLAB and Optimization Toolbox Release 2017b, The MathWorks, Inc., Natick, Massachusetts, United States.

37. Nogal, M., Lozano-Galant, J.A., Turmo, J. and Castillo, E (2015), "Numerical damage identification of structures by observability techniques based on static loading tests", *Structure and Infrastructure Engineering*, **12** (9), 1216-1227.

38. Nguyen, D.K. & Tran, T.T (2018), "Free vibration of tapered BFGM beams using an efficient shear deformable finite element model", *Steel and Composite Structures*, **29** (3) ,363-377.

39. Pisano, A.A (1999), "Structural System Identification: Advanced Approaches and Applications". PhD. Ph.D. Dissertation, Università di Pavia, Italy.

40. Pajonk, O (2009), "Overview of System Identification with Focus on Inverse Modeling", *Technische Universität Braunschweig*, **63**.

41. Przemieniecki, J.S. (1968),*Theory of Matrix Structural Analysis* . Library of Congress Catalog Card Number

42. Sirca Jr, G.F., & Adeli, H. (2012). System identification in structural engineering. *Scientia Iranica*, **19**(6), 1355-1364.

43. Singh, S.K. & Chakrabarti, A (2017), "Hygrothermal analysis of laminated composites using C0 FE model based on higher order zigzag theory", *Steel and Composite Structures*, **23**, 41-51.

44. Soto, I.L., Rojas, A.L (2017), "Modeling for fixed-end moments of I-sections with straight haunches under concentrated load", *Steel and Composite Structures*, **23** (5), 597-610.

45. Sayyad, A.S (2011), "Comparison of various refined beam theories for the bending and free vibration analysis of thick beams", *Applied and Computational Mechanics*, **5**, 217–230.

46. Thirumalaiselvi, A., Anandavalli, N., Rajasankar, J., Iyer, N.R (2016), "Numerical evaluation of deformation capacity of laced steel-concrete composite beams under monotonic loading", *Steel and Composite Structures*, **20** (1), 167-184.

47. Timoshenko, S. P (1921), "On the correction for shear of the differential equation for transverse vibrations of prismatic bars", *Philosophical Magazine*, **41** (6) , 742–746.

48. Tomas, D., Lozano-Galant, J.A., Ramos, G., Turmo, J (2018), "Structural system identification of thin web bridges by observability techniques considering shear deformation", *Thin-Walled Structures*, **123**, 282-293.

49. Vicente, M.A., Gonzalez, D.C., Minguez, J., Schumacher, T (2018), "A Novel Laser and Video-Based Displacement Transducer to Monitor Bridge Deflections", *Sensors*, **18**(4), 970-985.

50. Walsh, B. J., González, A (2009), "Assessment of the Condition of a Beam Using a Static Loading Test", *Key Engineering Materials*, 413–414, 269-276.

51. Wang, J., Li, T., Luo, L (2018), "Theoretical and experimental study on deflection of steel-concrete composite truss beams", *Steel and Composite Structures*, **29** (1), 91-106.

52. Yan, A., Golinval, J (2005), "Structural damage localization by combining flexibility and stiffness methods", *Engineering Structures*, **27** (12) ,1752–1761.

53. Yang, Y., Chen, Y., Zhang, J., Xue, Y., Liu, R., Yu, Y (2018), "Experimental investigation on shear capacity of partially prefabricated steel reinforced concrete columns", *Steel and Composite Structures*, **28** (1), 73-82.

Appendix 2

Shear rotation analysis in stiffness matrix methods: A state of the art and application in the direct and inverse analyses.

Seyyedbehrad. Emadi[4a], Jose A. Lozano-Galant[2b], Ye Xia[*3], Jose Turmo[1c]

[1]Department of Civil and Environmental Engineering, Universitat Politècnica de Catalunya (UPC) BarcelonaTECH, Barcelona, Spain.

[2] Department of Civil Engineering, University of Castilla-La Mancha, Ciudad Real, Spain.

[3]Department of Bridge Engineering, Tongji University, Shanghai, China

Abstract: According to Timoshenko's beam theory, nodal rotations are produced by bending and shear effects. Bending rotations can be easily calculated by Euler-Bernoulli stiffness matrix method. On the other hand, shear rotations are traditionally neglected as their effects are practically negligible in most structures. In addition, calculating the effects of shear rotation in structures by stiffness matrix method have some limitations. Nevertheless, neglecting the shear effects might lead to significant errors in the simulation of some structural cases both in the direct and the inverse analysis. Although some inverse analysis methods including shear deformations have been recently presented in the literature. Nevertheless, all they failed to add shear rotations as they only focus on the analysis of the vertical deflections produced by shear. Therefore, when actual rotations on site are used to estimate the mechanical properties of the built elements by an inverse simulation, neglecting shear rotation effects might result in significant errors in the properties observed. To fill these gaps, after a thorough literature review, a set of parametric analyses is carried out to evaluate the role that shear rotation plays in the structural behavior of structures with different slenderness ratios. In addition, this paper studies, for the first time in the literature, the effect of shear rotations in the inverse analysis in order to show the importance of shear rotation in different structures. With this aim, the

[a] Ph.D., seyyed.behrad.emadi@upc.edu

[b]Associate Professor, joseantonio.lozano@uclm.es

[c] Professor, gonzalo.ramos@upc.edu

[*] Corresponding Author, Associate Professor, P.E., yxia@tongji.edu.cn

analysis of the slenderness ratios enables to define in which structural systems shear rotation effects can be neglected in both direct and inverse analysis.

Keywords: Structural system identification; Observability method; Shear rotation; Stiffness matrix method state of the art.

1. Introduction

Structural modeling is related to the simulation of the behavior of structures. It is achieved based on processes in which physical problems based on a set of simplifying assumptions are explicated into mathematical ones. There are many studies related to modeling the structural behavior of beams (e.g. [1-3]). Most of these studies are based on either the Euler-Bernoulli [4] or the Timoshenko's beam theory [5]. According to many scholars (see e.g. [6,7]) shear deformations are traditionally neglected in Euler-Bernoulli's beam theory approach as this theory assumes the plain section deformation. This assumption states that plane sections remain plane and perpendicular to the neutral axis during bending deformation [8] and accordingly, no shear strains appear.

This theory fails for most loading cases, as the only loading case resulting in zero shear force is a constant bending moment alongside the beam. Hence, Euler-Bernoulli's beam theory only holds for this particular case. This assumption traditionally used in slender beams, where shear deformations are usually smaller than the flexural ones, and therefore, their effect can be neglected. In these cases, the absence of shear strains and deformations can be considered as a modeling error [9]. Nevertheless, in structures lacking a unidimensional geometry (such as deep beams) shear deformation might play an important role and its effects should be introduced into the formulation [10]. Eurocode EN 1992-1-1 [11] characterizes deep beams as those which span is three times smaller than the overall section depth. ACI committee 318 [12] describes these beams as beams whose spans are equal to or less than four times the depth of the beam. Shear deformation effects can also play an important role in the other two dimensional structures, such as sandwich beams [13].

Timoshenko [14,15] was the first one dealing with the shear effects in beams. In fact, he included the effects of both shear vertical deflections and shear rotations into this theory. In this approach (known as Timoshenko's beam theory or first-order shear deformation theory) two different rotations are considered: rotation due to the bending, w_b, and rotation due to the shear, w_r. The difference between the two methods in a simply supported beam is presented in Figure 1. Also, this figure includes Euler-Bernoulli's beam theory Figure 1.b and Timoshenko's beam theory Figure 1.c. Shear rotation can be described as a difference between the derivative of deflection and the final cross-section rotation.
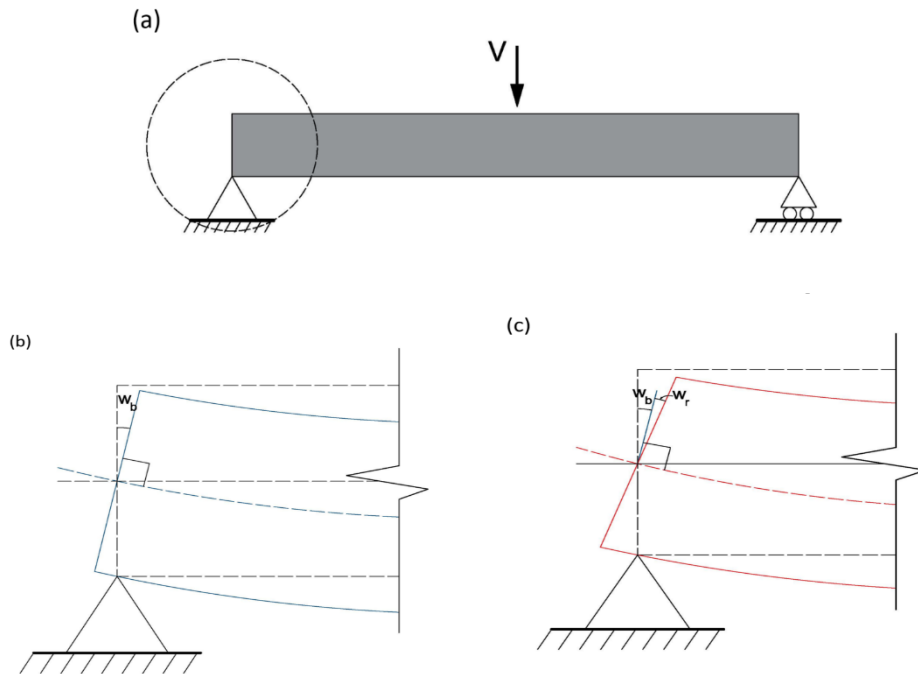
Fig.1 Beam theory on the beam support. (a) A simply supported beam with a zoomed support.   (b) Euler-Bernoulli's beam theory on the beam support. (c) Timoshenko's beam theory on the beam support.

Timoshenko's theory was improved by Mindlin [16], who simplified the transverse shear strain distribution as a constant distribution through the beam thickness. In this approach, a shear coefficient was used to appropriately represent the strain deformation energy in real structures. This shear coefficient can be used to include the effects of the non-constant shear stresses and strains in the members' cross-section. To capture the variation of shear stress avoiding the use of shear coefficients, higher orders of shear deformation theories can be also considered (see e.g. [17,18]). This is the case of the Finite Element Method (FEM), which is a numerical problem-solving method [19-21]. To do so, large equations are divided into smaller and simpler ones. The concept of the FEM was first developed by Clough [22] for solving problems in solid-state mechanics (plate-bending problems to be more specific). Turner et al. [23] described the application of finite elements for the analysis of aircraft structures and is pointed to as one of the main contributions to the growth of the FEM. The FEM approach allows the continuum to be discreted into a finite number of elements and ensures that the characteristics of the continuous domain can be determined by combining the similar properties of discrete elements per node. Hutton [24] refers to FEM as the most powerful and common technique for computer-based analysis in engineering. In addition, this procedure

can be used for both simple and complex structures [25-27]. Consequently, the FEM has been thoroughly implemented to solve a broad range of problems in different fields of science and engineering and it has grown rapidly over the years [28,21] which makes FEM a numerically universal tool for solving differential equations. Indeed, the fast-growing recognition of Finite Elements methodology is associated with the computer's growth. This led to the rapid development of the process, which now offers the key for rational structural design and the analysis of aeronautical fluid dynamics and electric magnetism required for physics through various commercial and research codes [29]. All of the information concerning these finite elements methods were presented, along with numerous correspondents at a meeting held in Swansea in January 1964 and 1965 formally published [30] and several other seminars such as Fraeijs de Veubeke (1965). The most common FEM model in the analysis of the structures is the stiffness matrix method, where the solution that is currently used for complex structures is the method described as stiffness method, in which the displacements given to the ends (nodes) of an element are correlated with the forces at acting at these ends [31]. This method was initially proposed by Louis Navier [32] then, Alfred Clebsch [33] developed the method and studied more details of the Stiffness method. Clebsch, A. presented a succinct technique for the linear analysis to evaluate a moment-free 3D truss. In 1883 Barr´e de Saint Venant [34] studied the same problem (a French translation of [33] with more detailed discussions).

Before the advent of computers, only a small number of unknown variables could be calculated by the stiffness method. Therefore, to deal with this problem Southwell [35], developed his relaxation methods. Although it is not practical for hand calculation to solve a complex problem with this method, the iterative process of elimination in his further studies (Southwell [36,37]), enables solving very complex problems. In addition, Turner 1962 [38], contributed to developing the stiffness method and formulated it in more detail. The main inconvenience for the more complex structures is that hand methods of analysis become excessively inapplicable. In the 1930s, a matrix form procedure was initiated to illustrate the whole process of linear equations in the stiffness method systematically. Now, this procedure is known as stiffness matrices method (SMM) [39–47]. SMM is one of the major common methods of the FEM approach for analyzing the structural behavior of beam-like structures [48-51], especially this method is suited for computer-analysis of complex structures [52] due to a large number of linear modules could well be constructed by matrices. In 1938 Fraser, et al. [53] published the first paper with the expression and terminology of the matrix system. This condition led to the development of matrix methods of analysis in the late 1940s and early 1950s (such as [54, 55]).

Standard engineering methods can be employed in other areas of engineering. For example, electrical components can be assembled to form a circuit the same as the structure assembling bars. This concept was

already proven in [56]. In the analysis of designing aircraft which is described by Levy in 1937 [57], it is believed that all normal stresses are taken up by the spars and ribs and all shear stresses by the panels. the analogous approach was employed by Falkenheiner [58], Lang and Bisplinghoff [59], as well. Hrenikoff proposed a system for solving problems of linear elasticity [60]. a rectangular arrangement of the trusses model is presented by [61]. Related equations of SMM arised in electrical networks, and these follow similar formulations to structural engineering problems [62]. Similar to Kirchhoff and Maxwell, Gabriel Kron [63] explained a close comparison between electrical and mechanical networks for the solution of 3D frames in a complete matrix algorithm. He was the first one who considered these stiffness matrices along the diagonal of a large-scale matrix. Argyris made considerable progress in the use of matrices in structural engineering [64] applying the methods proposed by Kron. Clearly, the particular computational advantage of the SMM is about using a local definition of the shape function (known as stiffness matrix). It is a local assembly of the structure of matrix equations firstly presented by [65]. The purpose of their approach relies on the formation of a relationship between forces imposed at nodes of an element of a structure, and the displacement related to the force. Nowadays, There is a wide range of software packages available that address static and dynamic problems.

Traditionally, the stiffness matrices method, also known as the direct stiffness method, is particularly suitable as one of the structural analysis methods for the computer-automated analysis of complex structures including the statically indeterminate type [42]. The SMM is mostly based on Euler–Bernoulli's beam theory and the shear effects are neglected [66]. But in some structures (such as deep beams), shear deformations might play an important role and these effects cannot be ignored (see e.g. [9]). Some authors proposed innovative stiffness matrices to include the shear effects into the SMM formulations [6, 67-70]. In beams, shear deformation can be analyzed by the sum of two components: (1) vertical and axial deflections, and (2) rotations. In order to include the effects of the shear rotation in SMM, some authors developed their mathematical models [71-77]. In these models, SMM formulations were too simple to consider shear rotation effects. In fact, specific boundary conditions were considered to remove unnecessary equations from the beam equilibrium system. But these methods have limited applicability as they can only be used in simple cases and their equations are different for each case. The first FEM for Timoshenko beam theory was proposed by McCalley [78], who developed a two-node, four-degree of freedom element (transverse displacement and cross-section rotation at every node).

This FEM was extended to a tapered beam by Archer [72]. The values of the shear coefficient for different cross-sections were proposed by Cowper [79]. At the time Kapur [73] found that in a clamped-end element (such as the fixed end of a cantilever beam), Archer's formulation could not represent the exact boundary

conditions (as the rotation due to shear is constrained to be zero). To deal with this problem, Kapur developed a new element based on a cubic displacement function for both the bending and the shear displacements. In this formulation both effects (shear rotation and bending rotation) were analyzed separately, resulting in an eight degree of freedom beam element. The FEM presented by Kapur works properly when there are four unknowns per node (such as in simply-supported beams and cantilevers). However, in complex structures, where adjacent elements are not collinear, Kapur's element does not work properly. Different authors used slightly different approaches for their FEM's and achieved almost the same results as Kapur. Various types of FEMs for Timoshenko's beam elements are proposed in the literature. These methods are based on similar assumptions with small differences [80-82]. Thomas et al. [83] described many of the early models presented in the literature to deal with shear. He categorized the elements of these models into two classes: simple and complex. On the one hand, a simple element is considered with only two degrees of freedom at each of its two nodes. On the other hand, a complex element has more than four degrees of freedom (having nodes with more than two degrees of freedom or more than two nodes per element).

According to the literature, a number of different SMM approaches can be found to include shear rotations into the simulation of simple and complex elements. But complex structural cases which have discontinuities in cross-sections or non-collinear elements can only be analyzed by the FEM's whose nodal variables are bending rotation and transverse displacement [83]. It is important to notice that the effect of shear rotation is neglected in this SMM formulation. A detailed formulation of this type of common Timoshenko's beam theory SMM can be found in many works, such as, for example, in Przemieniecki [84]. On the other hand, where, there are continuous cross-section or beam-column, several SMM based on Timoshenko's beam theory are proposed by different authors [85-88].

System Identification (SI) is a process to calibrate unknown parameters of a system that is employed in a number of different engineering fields [89]. One of the pioneers in this approach was Friedrich Gauss who developed the Gauss-Newton method of finding parameter values in a trajectory model for measuring the trajectories of the dwarf planet. SI has emerged in the area of electronic engineering and, after a while, has been applied to other engineering fields [90, 91]. Among its applications, it is to highlight the structural system identification (SSI). This approach uses the structural response to nondestructive tests to identify unknown structural parameters (such as axial or flexural stiffnesses) [92]. This approach is also known as the inverse analysis. A number of methods are presented for SSI in the literature (e.g. [93, 94]). Since SMM is a suitable technique for computer-based analysis in engineering, it is one of the major ways of doing this modeling [95-97]. The details of the main SSI methods presented in the literature can be found in ASCE

[98]. Among these procedures, it is to highlight the observability method (OM). This technique is based on the SMM and it has proved its efficiency in different structural cases such as frame structures, beams, trusses and cable-stayed bridges [99-106]. One of the main features of the OM is the linearization of the unknown variables. This assumption implies that a significant loss of information is possible. Constrained observability method (COM) proposed by Lei et al. [107] solved the linearization problem of OM by summing up some nonlinear constraints to the system of equations. Unlike OM, which is a mathematical approach, the COM approach solves the system numerically by minimizing numerical errors. The effects of shear deformations were included into the SSI Observability Method (OM) by Tomas et al. [9]. The main difficulty of this work is that it is based on the common Timoshenko SMM, and therefore, the method is not able to consider the effects of the shear rotations. There are more SSI methods based on SMM considering the effect of shear on their formulation (e.g. [80-82]), but effects of shear rotation are neglected in all of them since these effects are neglected in the formulation of the common Timoshenko SMM models. Therefore, it can be concluded that all SSI methods based on SMM are not able to consider the effects of shear rotation. As a result of this flaw, a new SMM method is required to consider the shear rotation in both simulation and SSI approach.

The aim of this paper is to illustrate the importance of shear rotations, which are traditionally neglected in structural simulations due to the complexity of the equations and the reduced effects in most structures. These effects, however, might play an important role in some structures (such as deep beams) and neglecting them may lead to important errors in both the direct and the inverse analysis. In addition, a new method is presented to calculate shear rotations based on the SMM. In this method, the shear rotation is calculated separately and added to the bending rotation computed from SMM. In order to illustrate the cases where shear rotations cannot be neglected, a set of guidelines is proposed for different structures.

This article is organized as follows: In Section 2, the SMM including shear vertical deformations is briefly presented. An example is analyzed to illustrate the inability of both the commercial software (based on SMM) and the common SMM to calculate the value of shear rotation. This inability to simulate shear rotations leads to wrong simulations of some structures (e.g. deep beams). In Section 3 a new method for analyzing the shear rotation in structures is presented. In addition, a parametric analysis of different structures is presented to illustrate the important role that shear rotations might play in some geometries. Moreover, the effects of neglecting shear rotation in the formulation of the SSI method for some structural cases with different slenderness ratios are analyzed. Also, in section 4, a more complicated structure is analyzed to show the ability of the new method to simulate a more complicated structure and effects of the neglecting shear rotation in the inverse analysis. Finally, the conclusions obtained are drawn in Section 5.

2.Shear deformation analysis on the stiffness matrix method

This nodal equilibrium equation commonly used in Timoshenko's SMM [108-110] can be presented as:

$$[K] \cdot \{\delta\} = \{f\}, \tag{1}$$

where [K] is the stiffness matrix; $\{\delta\}$ is the displacements vector, which includes the horizontal, vertical and rotational displacements; and $\{f\}$ is the external force vector, which includes the horizontal forces, vertical forces, and moments. Some methods are developed in the literature to include the shear effects into the SMM [80-82]. However, the complexity in the system of equations might produce the following problems: (1) failing to include the effect of the shear rotations. Those methods are considered as common Timoshenko's beam theory SMM which are not able to consider shear rotation in their formulations (e.g. [84]), (2) methods based on assumptions that make impossible their application in general complex structures [83].

In the 2D analysis, for a six degrees of freedom beam element (one horizontal deflection, u, a vertical deflection, v and a rotation w at the initial and final nodes) of length L and constant cross-section, the common Timoshenko's stiffness matrix is showed in Equation 2:

$$[K] = \begin{bmatrix} \dfrac{EA}{L} & 0 & 0 & -\dfrac{EA}{L} & 0 & 0 \\[2mm] 0 & \dfrac{12EI}{L^3(1+\emptyset)} & \dfrac{6EI}{L^2(1+\emptyset)} & 0 & -\dfrac{12EI}{L^3(1+\emptyset)} & \dfrac{6EI}{L^2(1+\emptyset)} \\[2mm] 0 & \dfrac{6EI}{L^2(1+\emptyset)} & \dfrac{EI(4+\emptyset)}{L(1+\emptyset)} & 0 & -\dfrac{6EI}{L^2(1+\emptyset)} & \dfrac{EI(2-\emptyset)}{L(1+\emptyset)} \\[2mm] -\dfrac{EA}{L} & 0 & 0 & \dfrac{EA}{L} & 0 & 0 \\[2mm] 0 & -\dfrac{12EI}{L^3(1+\emptyset)} & -\dfrac{6EI}{L^2(1+\emptyset)} & 0 & \dfrac{12EI}{L^3(1+\emptyset)} & -\dfrac{6EI}{L^2(1+\emptyset)} \\[2mm] 0 & \dfrac{6EI}{L^2(1+\emptyset)} & \dfrac{EI(2-\emptyset)}{L(1+\emptyset)} & 0 & -\dfrac{6EI}{L^2(1+\emptyset)} & \dfrac{EI(4+\emptyset)}{L(1+\emptyset)} \end{bmatrix} \tag{2}$$

The stiffness matrix [K] includes the information of axial stiffness EA, flexural stiffness EI and the length of the element L, where E, I and A are Young modulus, inertia and area, respectively. A coefficient Ø (shear parameter) is present in some elements of Equation (2). This parameter is as follows:

$$\emptyset = \frac{12EI}{GA_v L^2} \tag{3}$$

where G is the shear modulus and A_v is the shear area, shear modulus might be written as:

$$G = \frac{E}{2(1 + v)} \qquad (4)$$

zhere the coefficient v is Poisson's ratio. The effect of shear rotation is neglected in this stiffness matrix. As it explained in the literature, many authors tried to develop methods to add shear rotations to their stiffness matrices, but none of these methods can be applied in complex structural cases. In fact, even commercial simulation programs based on the stiffness matrix (such as SAP 2000 [26] and Midas [111] neglect shear rotations, too). In these software total rotations are equal to the bending rotations and shear effects are only considered in vertical deflections. To show the inability of these methods to calculate the total value of the rotations, an illustrative example is presented in the following section.

2.1 Example 1: Simply supported beam

Consider the 10 m long and 0.2 m wide simply supported beam modeled with 3 nodes and 2 beam elements depicted in Figure 2.a. This structure can be considered as a deep beam, where shear effects are not negligible. This beam has a constant cross-section and the value of its young modulus, shear area, cross-sectional area and inertia along the beam are 30 GPa, 0.833 m2, 1 m2 and 2.083 m4, respectively. Dimensions of the beam cross-section are presented in Figure 2.b and its mechanical properties are listed in Table 1. The boundary conditions of the structure are horizontal and vertical displacements restricted in node 1 and vertical displacement restricted in node 3 (this is to say, $u_1=v_1=v_3= 0$). The beam is subjected to a concentrated vertical force in node 2 of 100kN ($V_2= -100$kN).
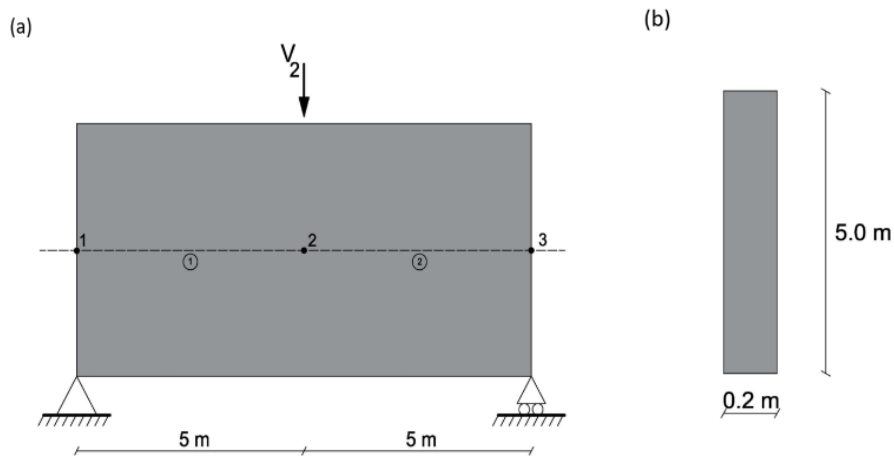

Figure 2. Example 1: (a) FEM for a simply supported beam. (b)Dimensions of beam cross-section.

Table 1. Properties of the FEM of the simply supported beam.

Properties (unit)	Values
Area [m2]	1.000
Shear Area [m2]	0.833
Inertia [m4]	2.083
Concrete Young's Modulus [GPa]	30.000
Poisson's Ratio γ	0.250

To calculate the bending and shear response of the structure in this simple example, formulations based on Timoshenko beam theory can be used. The value of bending vertical deflections for the loading case presented in Figure 2.a, v_b at mid-span be written in Eq. (5). From Timoshenko [15], the value of vertical deflection due to shear, v_s at mid-span of this structure is calculated as in Eq. (6). Also, the value of bending rotation w_b at node 1 is presented in Eq. (7). Where V1 is the shear force at note number 1. Shear rotation w_s at the node number 1 can be calculated from Timoshenko's [15] assumptions as it is presented in Eq. (8).

$$v_b = \frac{V_2 * L^3}{3 * E * I} \tag{5}$$

$$v_s = \frac{V_2}{2 * A_v * G} * L \tag{6}$$

$$w_b = \frac{V_1 * L^2}{4 * E * I} \tag{7}$$

$$w_s = \frac{V_1}{A_v * G} \tag{8}$$

To show the inability of different structural analysis methods to calculate shear rotations, the vertical deflections and total rotations (sum of rotation due to shear and bending) of Example 1 obtained from Sap2000 [26], common Timoshenko SMM [84] and formulations based on Timoshenko beam theory are compared in Table 2.

Table 2. Properties of the FEM of the simply supported beam.

Methods	Total rotation in node 1 (rad)	Bending rotation in node 1(rad)	Total vertical deflection in node 2 (m)
SAP 2000	0.01	0.01	-0.058
Common Timoshenko SMM	0.01	0.01	-0.058
formulations based on Timoshenko beam	0.015	0.01	-0.058

As it can be seen in Table 2, the value of total rotation and bending rotation obtained by SAP2000 [26] are equal to each other which means the effects of shear rotations are neglected in this software. Also, the effects of shear rotations are disregarded in common Timoshenko SMM. In this particular case, the results of hand calculation for total rotations (0.015 rad) is 50 % higher than those obtained by the other analyzed methods. These results illustrate the important role that shear rotations might play and the fact that they are systematically neglected in most structural analysis methods (independently of the beam geometry). In the case of the vertical deflections, table 2 shows that all methods include properly the shear effects as the same results are obtained by all the analyzed procedures. Obviously, the magnitude of the shear rotations depends greatly on the beam geometry. To show in which cases shear rotation can be considered negligible and when it should be introduced into the simulation, a new simulation method is proposed in the following section and a parametric analysis performed.

3.A simulation method for the shear rotations in beams

To introduce the effects of shear rotation into the common Timoshenko's SMM, a new procedure is developed in this section, as shown in figure 3. Firstly, the bending rotation of each node can be computed by the SMM. Then the shear rotation of each element is calculated by the formulations based on Timoshenko beam method presented in Eq. (8). According to this equation, the shear rotation for each element can be calculated only by shear forces, shear area and shear modulus. Shear area and shear modulus can be directly obtained from the mechanical properties of the structure, while the shear forces are obtained from the results of the SMM analysis. By summing up the value of shear and bending rotation the total rotation of each node can be obtained. The new method is summarized in the following three steps:

- **Step 1:** Compute the bending rotation of each node by SMM.
- **Step 2:** Calculate the shear rotation of each element with the shear forces obtained in Step 1.
- **Step 3:** Obtain the total rotation at the end of each beam by summing up the value of the shear and the bending rotations obtained in Steps 1 and 2. It is to highlight that shear rotations are proportional to the shear diagram. Hence, discontinuities in the shear effort diagram introduced by point loads or reactions imply discontinuities in the shear rotations. Elements converging to the same node can have different rotations at this node.

A summary of the procedure is shown in the flow chart in Figure 3. In the following sections, a set of parametric analyses using the new method is performed on beams with different geometry, to evaluate when

the effect of the shear rotation is significant. Also, an inverse analysis for a simply supported beam is performed to evaluate the sensitivity of the OM to the errors of the shear rotation measurements.
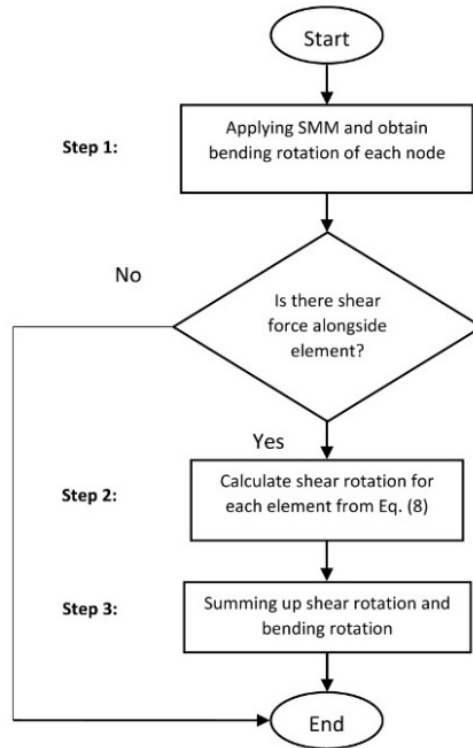

Figure 3. Flow chart of the procedure of adding shear rotation to common SMM

3.1 Example 1: Simply supported beam with a concentrated load

Consider the cross-section of the simply supported beam presented in Figure 2.b. Material properties of the simply supported beam can be found in table 1. The boundary conditions of the structure are horizontal and vertical displacements due to bending restricted in node 1 and vertical displacement restricted in node 3 (this is to say, $u_1=v_1=v_3= 0$) and the only external force applied in this numerical loading test is a concentrated vertical force of 100kN (V= 100kN). To evaluate the effect of the shear rotations at node number 1, a parametric analysis is carried out. In this analysis, the length of the beam (L) varies from 1 to 15 meters while the height (h) remains constant. As expected, Fig. 4 illustrates how the slenderer beam, the lower the effect of the shear deformation is. As presented in Fig 4.a, the shape of the shear rotation variation is linear which means the shear rotation variation is independent of the length of the beam and the value of shear rotation in different L/h is equal to 0.005 radians. But the values of bending rotations vary from 0.0025

to 0.5625 radians where the length to height ratios are between 1 to 15. The percentage of error when shear rotation is neglected for different L/h ratio is shown in Figure 4.b. For illustrative purposes, the limits of 2 % and 5% are also indicated in this figure. The ratio limits for deep beams proposed by the Eurocode EN [11] and by the ACI Committee 318 [12] are highlighted.
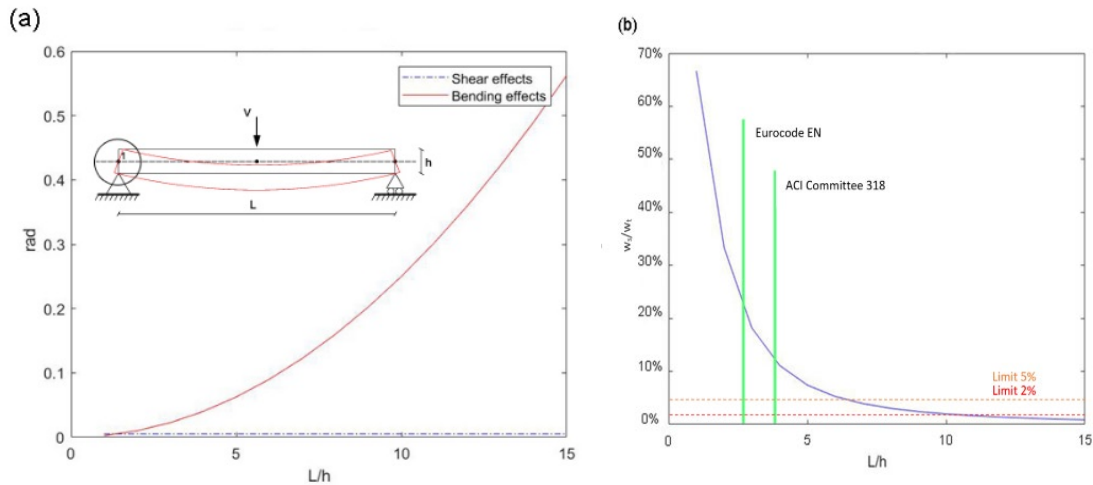

Figure 4. Example 1: (a) Rotation due to bending and shear at the node number 1. (b) Percentage of error in measurement in node number 1, when bending rotation is just considered.

In Fig. 4.b, 5 % error is gained when L/h ratio is equal to 6.197. In the same way, a 2 % error corresponds to a beam length-to-height ratio of 9.914. Also, the measurement error in node 1 is 18.185 percent where the ratio of L/h is 3 (deep beam limitation by Eurocode EN) and it is 11.113 percent when the L/h ratio is 4 (ACI Committee 318 proposed limitation).

3.2 Example 2: Simply supported beam with a distributed load

Consider a beam with the same material properties and boundary conditions of the simply supported beam presented in Example 1. The external force in this numerical loading test is a distributed vertical force of 100/L kN applied alongside the beam, in such a way that the total load in the beam equals 100 kN. A parametric analysis is carried out to illustrate the role of the shear rotations. The length of this beam is varied from 1 to 15 meters and the height of the beam is considered constant. As presented in Fig 5.a, the value of shear rotation in terms of the L/h ratio is equal to 0.005 radians and it is linear. The values of bending rotations are varied from 0.001 to 0.409 radians where the length to height ratios are between 1 to 15. The percentage of error when shear rotation is neglected for different L/h ratio is shown in Figure 5.b.

The ratio limits for deep beams proposed by the Eurocode EN [11] and by the ACI Committee 318 [12] are highlighted. Moreover, the limits of 2 % and 5% error are also indicated in Figure 5.
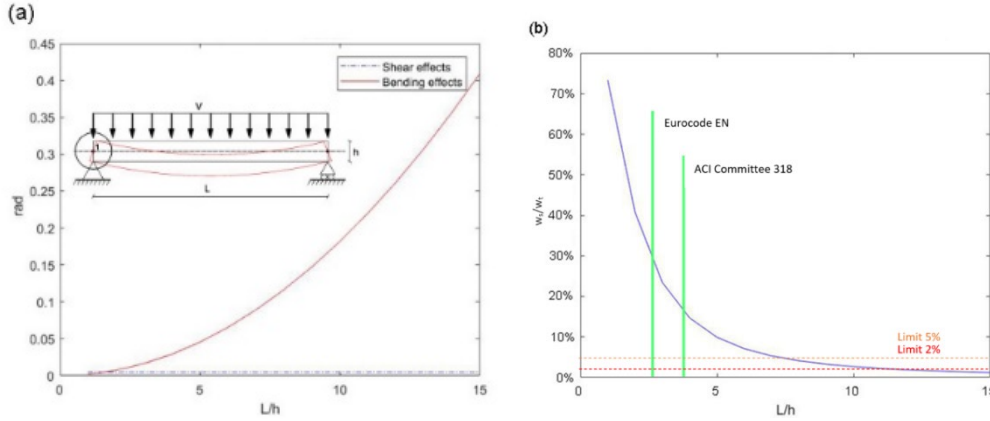

Figure 5. Illustration of example 1: (a) Rotation due to bending and shear at the node number 1. (b) Percentage of error in measurement in node number 1, when bending rotation is just considered.

As it is expected, Fig. 5.a shows in deep beam effects of shear rotations are more than slender ones. In Fig. 5.b, errors in rotations in different lengths of elements for node number 1 are presented, 5 % error is gained when L/h ratio is equal to 7.265. In the same way, a 2 % error corresponds to a beam length-to-height ratio is 11.639. Also, the measurement error in node number 1 is 23.409 percent where the ratio of L/h is 3 (deep beam limitation by Eurocode EN [11]) and 14.670 percent when the L/h ratio is 4 (ACI Committee 318 [12] proposed limitation).

3.3 Example 3: Cantilever Beam

Consider a cantilever beam with the same cross-section and same properties as in Example 1 modeled with a single beam element and two nodes. The boundary conditions of the structure are total horizontal and vertical displacements and rotation due to bending restricted in node 1 (this is to say, $u_1=v_1=w_{b1}=0$). The only external force applied in this numerical loading test is a concentrated vertical force in node 2 of 100kN ($V_2=100$kN). A parametric analysis is carried out to evaluate the role of the shear rotations on node number 2. In this analysis, the length of the beam is varied from 1 to 15 meters and the height of the beam is considered constant. As presented in Fig. 6.a, the shape of the shear rotation variation is linear and the value of shear rotation in different L/h is equal to 0.010 radians. But the values of bending rotations are varied from 0.020 to 4.501 radians where the length to height ratios are between 1 to 15. As it is expected, Fig. 6.a shows how in deep cantilever beams the effects of shear rotations are greater than those obtained in slender

ones. The percentage of error when shear rotation is neglected for different L/h ratio is shown in Figure 6.b. The ratio limits for deep beams proposed by the Eurocode EN [11] and by the ACI Committee 318 [12] are highlighted. Moreover, the limits of 2% and 5% are also indicated in Figure 6.
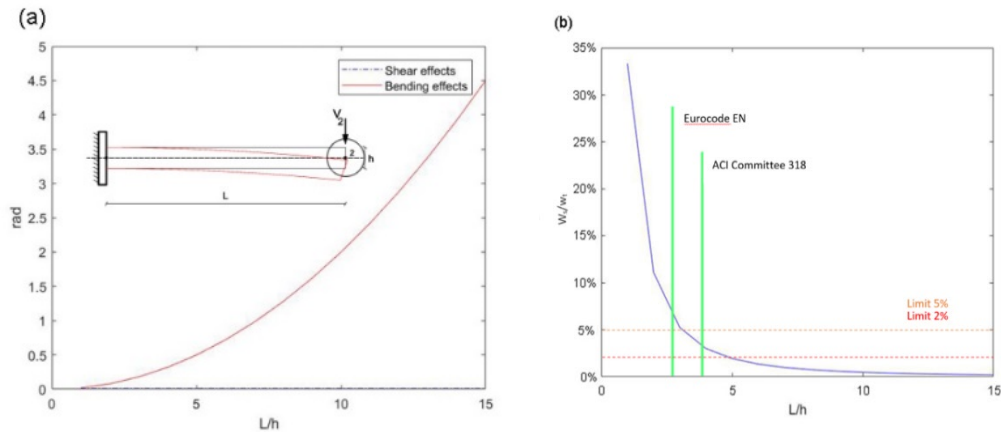

Figure 6. Illustration of example 2: (a) Rotation deflection due to bending and shear at node number. (b) Percentage of error in measurement in node number 2, when bending rotation is just considered.

In Fig. 6.b, 5 % error is expected when L/h ratio is equal to 3.118. In the same way, a 2 % error corresponds to a beam length-to-height ratio of 4.964. Also, the measurement error in node 2 is 5.264 percent where the ratio of L/h is 3 (deep beam limitation by Eurocode EN [11]) and 3.031 percent when the L/h ratio is 4 (ACI Committee 318 [12] proposed limitation).

3.4 Inverse analysis

A major concern in SSI methods in actual structures is related to the errors in measurements. As SSI methods based on SMM are not able to consider the effects of shear rotation in complex structures, this phenomenon can lead to modeling errors. This is due to the fact that the rotation measured on-site will not correspond with the one considered by the model (shear rotations are neglected in the equations). Depending on the structure, these modeling errors can surpass measurement errors. These errors will appear even in noise-free measurements and they will affect the estimation of structural properties in SSI methods. To establish a guideline for different structural cases, a sensitivity analysis is developed in this section for the three previous structures (Example 1,2 and 3). In this analysis, the total rotation (sum of shear rotation and bending rotation) in different length to height ratio (1 to 15) is tested. Effects of these errors in estimating the inertia in different structural cases (simply supported beam with a concentrated load of

example 1, simply supported beam with a distributed load of example 2 and cantilever beam of example 3) can be seen in Fig. 7. The ratio limits for deep beams proposed by the Eurocode EN [11] and by the ACI Committee 318 [12] are also indicated. The results of these analyses illustrate the cases where the calculation of shear rotation in SSI methods is important.
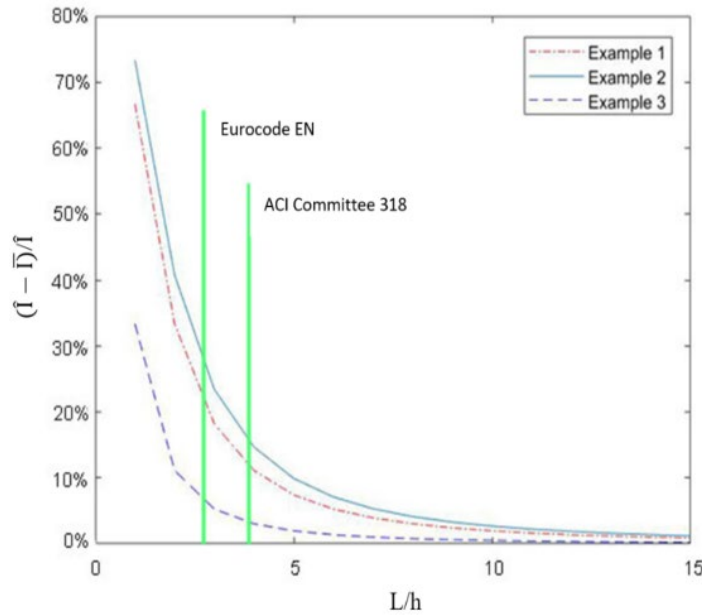

Figure 7. Percentage of error in inertia estimation based on the length to depth ratio when shear rotation is not formulated in SMM.

Where the ratio of L/h is 3 (deep beam limitation by Eurocode EN), the error in inertia estimation for a simply supported beam with a concentrated load, a simply supported beam with a distributed load and the cantilever beams are 18.179 %, 23.401 % and 5.262 %, respectively. in addition, when the L/h ratio is 4 (ACI Committee 318 proposed limitation) the error in the estimation of inertia for a simply supported beam with a concentrated load, a simply supported beam with a distributed load and the cantilever beams are 11.101 %, 14.665 % and 3.030 %, respectively. The results from Fig. 7 shows the fact that the effects of shear rotation on inverse analysis are even more important than in the direct one and the effects of shear rotations in the inverse analysis should not be neglected.

4.Example of application

To show the applicability of the new method in complex structures, the problem of bridge construction by the balanced cantilever method is presented here. In this kind of construction method, the deflections of different segments have to be forecast, to build the new segments with the proper precamber. Precamber is updated for each step of construction after a thorough topographical survey. This data can be used by inverse analysis for model updating to increase the accuracy of the precamber calculations. Although shear deflections may not be very important for a fully developed cantilever, the modeling error due to the neglecting of shear effects for the first segments may lead to inaccurate estimations of bending stiffnesses [112]. The structure chosen for this example is a simplified model of an intermediate construction stage of the Yunbao Bridge over the Yellow River in China (see Fig. 8.a). The bridge includes a span of 48m+9×90m+48m. It is a rigid frame-continuous composite bridge of 906 meters long. The height of the box girder beam ranges 5.5m to 2.7m from the supported end to the mid-span with a parabola curve of 1.8 power [113]. The bridge is built on cantilever. The analyzed construction stage is 29.5 m long and contains 3 segments of each side of the per segment (2.5 m) and a formwork traveler at the end of each span as it is presented in Fig 8.b.


(a)

(b)
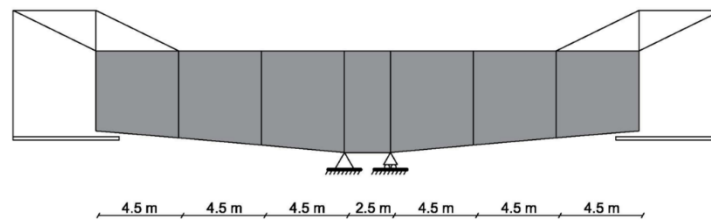
Figure 8. Example of application: (a) Yunbao Bridge under construction in China. [113] (b) Sketch of the analyzed construction stage.

The simplified geometry of the real bridge is analyzed. The connection between the concrete and the steel is assumed as rigid (total connection), and the relative slip between both materials is neglected. A typical cross-section of the composite deck is presented in Fig. 9.a. The FEM of the structure considered in this paper has 8 nodes and 7 elements and it is presented in Fig 9.b. The mechanical and material properties are listed in Table 3.
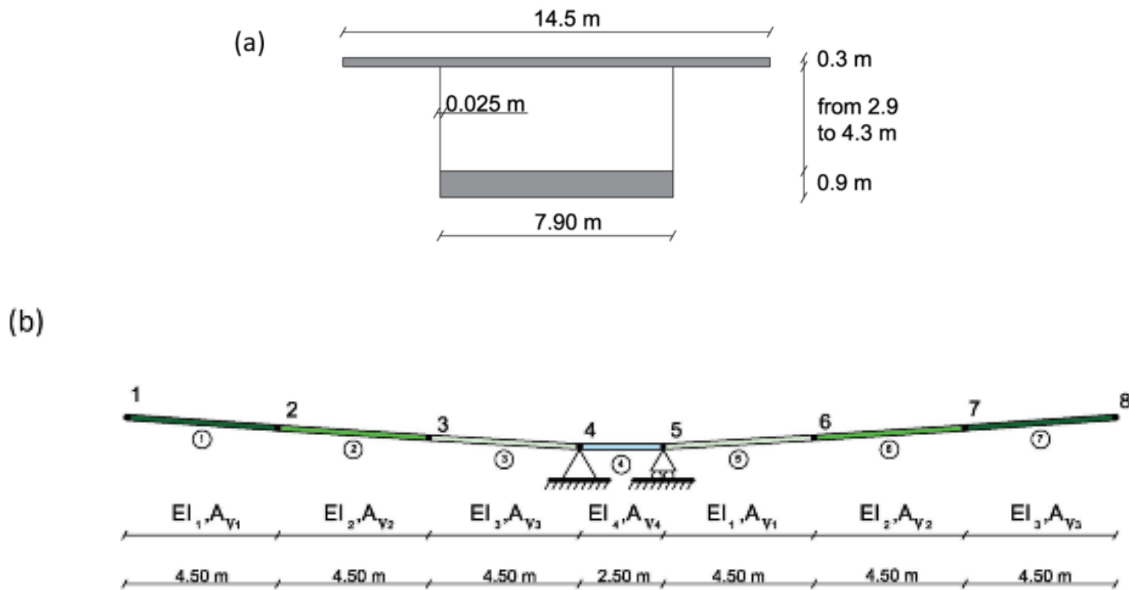
Figure 9. Numerical analysis: (a) Cross-section of Yunbao Bridge in China. (b) FEM of the bridge

Table 3. Properties of the Finite Element Model of the Bridge.

Parameters	Elements number 1 and 5	Elements number 2 and 6	Elements number 3 and 7
EA [m2]	4.33E+11	4.38E+11	4.43E+11
GAv [m2]	1.10E+10	1.25E+10	1.43E+10
EI [m4]	1.34E+12	1.69E+12	2.13E+12

The load case used is derived from Fig. 10, where the weight F (1041 kN) of the formwork traveler (Fig. 8.b) is assumed as 60 % of the maximum weight of the bridge segment. The effect of each form traveler in the deck is assumed as a pair of vertical forces of values 0.25F and 1.25F (226 kN, upwards and 1267 kN, downwards) as presented in Fig 10.a. the analyzed load case results from the combination of the loads applied by form traveler and the weight of the bridge segments. The segments loads are considered

distributed loads alongside segments. The resultant load case introduced in the simulation is shown in Fig 10.b.
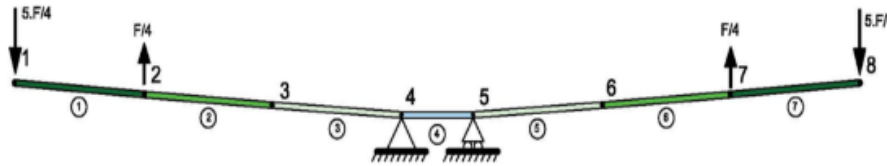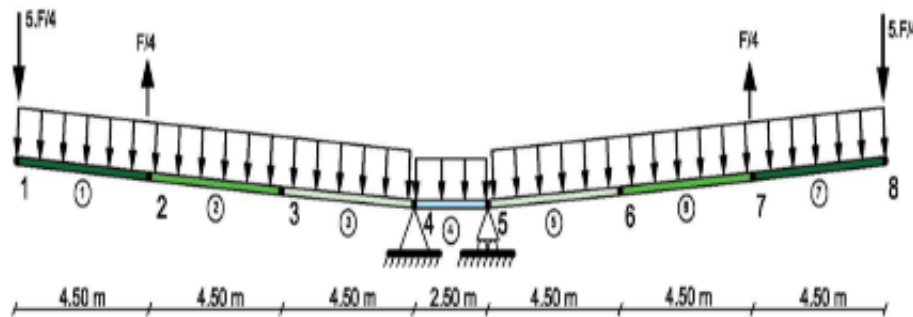

Figure 10. Definition of the load case: (a) load case applied by formwork traveler. (b) Load case used for the analysis.

The rotations in these 3 points are calculated by the proposed method. The results obtained from the new method and the ratio between the shear rotation and bending rotation can be seen in Table 4.

Table 4. Rotation in nodes calculated by the new method.

Node number	Shear rotation w_s (m)	Bending rotation W_b (m)	Percentage of error in the model (w_s/w_t)
Node number 1	-1.23E-04	-1.29E-04	48.93%
Node number 2	-1.68E-04	-1.16E-04	59.08%
Node number 3	-2.17E-04	-7.90E-05	73.28%

In this example, the maximum error in the calculations of shear rotations will be on node number 3. This will lead to an error in the calculation of the bending stiffness of element 3 of 73.420%. In comparison with

results from other Timoshenko's beam methods, obtained results prove the potential power of the proposed method. Also, they show the applicability of the new method where cross-sections are discontinued, elements are non-collinear and there are external loads applied in the different elements. It is important to highlight that no other Timoshenko beam theory FEM in literature is able to calculate total rotation (including both shear and bending effects) in structural schemes with such features.

5.Conclusions

Matrix form procedure of stiffness method was initiated to illustrate the whole process of linear equations in the method systematically. Especially this method is suited for computer-analysis of complex structures due to a large number of linear modules that could well be constructed by matrices. Stiffness matrix methods are used normally to analyze complex structures neglecting shear rotations. The literature review also shows a lack of stiffness matrix methods able to calculate shear rotations in models no collinear, discontinued and with external loads. Also, all Structural System Identification (SSI) methods reviewed in literature neglect rotation due to shear in their formulation as this phenomenon is usually less significant than the bending rotation. Despite the important role that this rotation might play especially in members with a low span-to-depth ratio, no detailed study addressing the particular effects of this rotation in inverse analysis can be found in the literature. To fill this gap, this paper presents the first study focused on shear rotation effects. To show how important the role of shear rotation might be, several different structures (a simply supported beam with a concentrated load, a simply supported beam with a distributed load and a cantilever with a concentrated load) with different length to height ratios are studied. In fact, these examples illustrate that the difference between Timoshenko's theory and Euler-Bernoulli's theory in terms of rotation is higher for members with low length-to-height ratio. In fact, for deep beams ratio between the shear rotation and bending rotation can be significant. Also, a model of a bridge built in cantilever is analyzed to show the applicability of the method. It should be mentioned that no other Timoshenko beam theory FEM in literature is able to calculate total rotation (including both shear and bending effects) in a structural model including the same features.

For the first time in literature, the sensitivity of the SSI methods to this modeling error is performed. The study of this sensitivity analysis might provide some insight into which structures rotation due to shear should be taken into account and in which cases these effects can be neglected.

Acknowledgments

References

1- Zarga, D., Tounsi, A., Bousahla, A. A., Bourada, F., & Mahmoud, S. R. Thermomechanical bending study for functionally graded sandwich plates using a simple quasi-3D shear deformation theory. Steel and Composite Structures, 32(3). (2019) 389-410. doi:10.12989/scs.2019.32.3.389

2- López-Colina, C., Serrano, M. A., Lozano, M., Gayarre, F. L., Suárez, J. M., & Wilkinson, T. (2019) Characterization of the main component of equal width welded I-beam-to-RHS-column connections. Steel and Composite Structures, 32(3). 337-346. doi:10.12989/scs.2019.32.3.337

Chao, S., Wu, H., Zhou, T., Guo, T., & Wang, C. (2019) Application of self-centering wall panel with replaceable energy dissipation devices in steel frames. Steel and Composite Structures, 32(2) 265-279. doi:10.12989/scs.2019.32.2.265

3- Kawano, A., Zine, A. (2019) Reliability evaluation of continuous beam structures using data concerning the displacement of points in a small region. Engineering Structures. 180 379-387. 10.1016/j.engstruct.2018.11.051.

4. Arefi, M., Pourjamshidian, M., & Ghorbanpour Arani, A. (2019) Dynamic instability region analysis of sandwich piezoelectric nano-beam with FG-CNTRCs face-sheets based on various high-order shear deformation and nonlocal strain gradient theory. Steel and Composite Structures, 32(2) 157-171. doi:10.12989/scs.2019.32.2.151

5. Lu, Y., Panagiotou, M. (2014) Three-Dimensional Cyclic Beam-Truss Model for Nonplanar Reinforced Concrete Walls. Journal of Structural Engineering. 140. 04013071. DOI: 10.1061/(ASCE)ST.1943-541X.0000852.

6. Ozdagli, A. I., Liu, B., Moreu, F. (2018) Measuring Total Transverse Reference-Free Displacements for Condition Assessment of Timber Railroad Bridges: Experimental Validation. Journal of Structural Engineering. 144 040180471.

7. Dahake, A., Ghugal, Y., Uttam, B., Kalwane, U.B. (2014) Displacements in Thick Beams using Refined Shear Deformation Theory. Proceedings of 3 rd International Conference on Recent Trends in Engineering & Technology.

8. Tomas, D., Lozano-Galant, J.A., Ramos, G., Turmo, J. (2018) Structural system identification of thin web bridges by observability techniques considering shear deformation. Thin-Walled Structures, 123 282-293.

9. Dym, C.L., Williams, H.E. (2007) Estimating Fundamental Frequencies of Tall Buildings. Journal of Structural Engineering. 133 1479-1483.

10. EN 1992-1-1: Eurocode 2: Design of concrete structures - Part 1-1: General rules and rules for buildings. CEN, Brussels, 2002, Belgium.

11. ACI committee 318 Building code requirements for structural concrete and commentary. American Concrete Institute, Detroit, 2000, USA

12. Chen, D. Kitipornchai, S.; Yang, J. Nonlinear free vibration of shear deformable sandwich beam with a functionally graded porous core, Thin-walled structures, 107 (2016) 39-48.

13. Timoshenko, S. P. (1921) On the correction for shear of the differential equation for transverse vibrations of prismatic bars. Philosophical Magazine 41 (6) 742–746.

14. Timoshenko, S. P. (1922) On the transverse vibrations of bars of uniform cross-section. Philosophical Magazine. 43 125-131.

15. Mindlin, R. D. (1951) Influence of rotatory inertia and shear on flexural motions of isotropic elastic plates. ASME Journal of Applied Mechanics. 18 31–38.

16. Reddy, J. N. (1984) Energy and Variational Methods in Applied Mechanics, New York: John Wiley. ISBN: 978-0-471-89673-9.

17. Reddy, J. N. (2006) An introduction to the finite element method, McGraw-Hill Education, ISBN: 9780072466850

18. Meier, C., Popp, A. & Wall, W.A. Geometrically Exact Finite Element Formulations for Slender Beams: Kirchhoff–Love Theory Versus Simo–Reissner Theory. Arch Computat Methods Eng 26, 163–243 (2019). https://doi.org/10.1007/s11831-017-9232-5.

19. Zeng, W., Liu, G.R. Smoothed Finite Element Methods (S-FEM): An Overview and Recent Developments. Arch Computat Methods Eng 25, 397–435 (2018). https://doi.org/10.1007/s11831-016-9202-3

20. Dixit, P., Liu, G.R. A Review on Recent Development of Finite Element Models for Head Injury Simulations. Arch Computat Methods Eng 24, 979–1031 (2017). https://doi.org/10.1007/s11831-016-9196-x.

21. Clough, R.W.: The Finite Element Method in Plane Stress Analysis. Second ASCE Conference on Electronic Computation, Pittsburgh, PA, p. 345-378 (1960).

22. Turner, M. J., Clough, R. W., Martin, H. C. and Topp, L. J. (1956). Stiffness and Deflection Analysis of Complex Structures. J. Aeron. Sci., 23, 805-824

23. Hutton, D. Fundamentals of finite element analysis Boston: McGraw-Hill, [2004].

24. Bathe, K.J. Finite Element Procedures. K.J. Bathe Watertown MA,2016 ISBN 978-0-9790049-5-7.

25. CSI, CSI Analysis Reference Manual for SAP2000, ETABS, SAFE and CSiBridge, Berkeley, California, USA, 2016.

26. Rapp E., "Microfluidics: Modelling, Mechanics and Mathematics", Elsevier (2017) ISBN 9781455731411, https://doi.org/10.1016/B978-1-4557-3141-1.50048-4

27. Rao, S. "The Finite Element Method in Engineering (Sixth Edition")", Butterworth-Heinemann (2018) ISBN 9780128117682, https://doi.org/10.1016/B978-0-12-811768-2.03001-7
Zienkiewicz, O. C. (1996). Origins, milestones and directions of the finite element method-A personal view doi:10.1016/S1570-8659(96)80002-0.

28. Zienkiewicz OC. Displacement and equilibrium models in the finite element method by B. Fraeijs de Veubeke, Chapter 9, pages 145–197 of Stress Analysis, Edited by O. C. Zienkiewicz and G. S. Holister, Published by John Wiley & Sons, 1965. Int J Numer Methods Eng.

29. Zienkiewicz, O. (2004). The birth of the finite element method and of computational mechanics. International Journal for Numerical Methods in Engineering. 60. 3 - 10. 10.1002/nme.951.

30. Navier L. Resumé des lecons sur l'application de la Mécanique. Ecole de Ponts et Chaussées, Paris, 1826.

31. Clebsch A. Theorie der Elasticität fester Körper, Berlin, 1862.

32. Saint-Venant Barré de. Course lectures Ecole Polytechnique, Paris, 1838.

33. Southwell RV. Stress calculation in frameworks by the method of systematic relaxation of constraints. Proceedings of the Royal Society 1935; 15:36–95.

34. Southwell RV. Relaxation Methods in Theoretical Physics, vol. I. Clarendon Press: Oxford, 1946.

35. Southwell RV. Relaxation Methods in Theoretical Physics, vol. II. Clarendon Press: Oxford, 1956.

36. Turner MJ, Martin HC, Weikel RC. Further development and applications of the stiffness method. AGARD Structures and Materials Panel, Paris, France in AGARDograph 72, 1962.

37. Duncan WJ, Collar AR. A method for the solution of oscillation problems by matrices. Philosophical Magazine 1934; 17(Series 7):865

38. Duncan WJ, Collar AR. Matrices applied to the motions of damped systems. Philosophical Magazine 1934; 19(Series 7):197

39. Frazer RR, Duncan WJ, Collar AR. Elementary Matrices. Cambridge University Press: Cambridge, MA, 1960. 24. Kron G. Tensorial analysis of elastic structures. Journal of the Franklin Institute 1944; 238:399–442

40. Rocas, M., García-González, A., Larráyoz, X. Nonintrusive Stochastic Finite Elements for Crashworthiness with VPS/Pamcrash. Arch Computat Methods Eng (2020). https://doi.org/10.1007/s11831-019-09397-x.

41. Garoni, C., Speleers, H., Ekström, S. et al. Symbol-Based Analysis of Finite Element and Isogeometric B-Spline Discretizations of Eigenvalue Problems: Exposition and Review. Arch Computat Methods Eng 26, 1639–1690 (2019). https://doi.org/10.1007/s11831-018-9295-y

42. Zohdi, T.I. Rapid Voxel-Based Digital-Computation for Complex Microstructured Media. Arch Computat Methods Eng 26, 1379–1394 (2019). https://doi.org/10.1007/s11831-018-9284-1

43. Greiner, D., Periaux, J., Emperador, J.M. et al. Game Theory Based Evolutionary Algorithms: A Review with Nash Applications in Structural Engineering Optimization Problems. Arch Computat Methods Eng 24, 703–750 (2017). https://doi.org/10.1007/s11831-016-9187-y

44. Vigliotti, A., Auricchio, F. Automatic Differentiation for Solid Mechanics. Arch Computat Methods Eng (2020). https://doi.org/10.1007/s11831-019-09396-y

45. Nodargi, N.A. An Overview of Mixed Finite Elements for the Analysis of Inelastic Bidimensional Structures. Arch Computat Methods Eng 26, 1117–1151 (2019). https://doi.org/10.1007/s11831-018-9293-0

46. Kumar, D., & Srivastava, A. Elastic properties of CNT-and graphene-reinforced nanocomposites using RVE. Steel and Composite Structures, 21(5) (2016). 1085-1103. doi:10.12989/scs.2016.21.5.1085

47. Singh, S. K., & Chakrabarti, A. (2017) Hygrothermal analysis of laminated composites using C0 FE model based on higher order zigzag theory. Steel and Composite Structures, 23(1) 41-51. doi:10.12989/scs.2017.23.1.04.

48. Fang, G., Wang, J., Li, S., & Zhang, S. (2016) Dynamic characteristics analysis of partial-interaction composite continuous beams. Steel and Composite Structures, 21(1) 195-216. doi:10.12989/scs.2016.21.1.195.

49. Chaudhary, S., Pendharkar, U., & Nagpal, A. K. (2007) An analytical-numerical procedure for cracking and time-dependent effects in continuous composite beams under service load. Steel and Composite Structures, 7(3) 219-240. doi:10.12989/scs.2007.7.3.21.

50. Weaver W., Gere J.M. (1990) Computer-Oriented Direct Stiffness Method. In: Matrix Analysis of Framed Structures. Springer, Boston, MA DOI https://doi.org/10.1007/978-1-4684-7487-9_4.

51. Fraser RA, Duncan WJ, Collar AR. Elementary Matrices and some Applications to Dynamics and Differential Equations. Cambridge University Press: Cambridge, 1938.

52. Turner. M.J. (1959) The Direct Stiffness Method of Structural Analysis. Structural and Materials Panel Paper, AGARD Meeting, Aachen

53. Argyris, J., Dunne, P.C. (1952), "Structural Analysis, Structural Principles and Data, Part 2", Handbook of Aeronautics No. 1, The New Eva Publ. Co. Ltd, London.

54. Kirchhoff GR. Annalen der Physic und Chemie 1847; 72.

55. Levy S. Computation of influence coefficients for aircraft structures with discontinuities and sweepback. Journal of the Aeronautical Sciences 1937; 14:547.

56. Falkenheiner H. Calcul systématique des caracteristiques elastic des systémes hyperstatiques. La Recherche Aéronatique 1950; 17:17.

57. Lang AL, Bisplinghoff RL. Some results of sweptback wing structural studies. Journal of the Aeronautical Sciences 1951; 18:751.

58. Hrenikoff A. Solution of problems of elasticity by the framework method. Journal of Applied Mechanics 1941; A8(1):169–175.

59. McHenry D. A lattice analogy for the solution of stress problems. Journal of the Institute of Civil Engineer 1943; 21:59–82.

60. Megson, T.H.G. (2019) "Structural and Stress Analysis (Fourth Edition)" Butterworth-Heinemann, ISBN 9780081025864, https://doi.org/10.1016/B978-0-08-102586-4.09993-5.

61. Kron G. Tensorial analysis of elastic structures. Journal of the Franklin Institute 1944; 238:399–442.

62. Argyris JH. Energy theorems and structural analysis. Aircraft Engineering 1954; 26:347–356, 383–394; 1955; 27:42–58, 80–94, 125–134, 145–158.

63. Walter Ritz. 1909. Theorie der transversalschwingungen einer quadratischen platte mit freien Rändern. Ann. Der Physik 333, 4 (1909), 737–786. OI:https://doi.org/10.1002/andp.19093330403.

64. Sayyad, A.S. (2011) Comparison of various refined beam theories for the bending and free vibration analysis of thick beams; Applied and Computational Mechanics, 5 217–230

65. Heyliger, P.R., Reddy, J.N. (1988) A higher-order beam finite element for bending and vibration problems, J. Sound Vib. 126(2), 309-326

66. Nickel, R.E., Secor, G.A. (1972) Convergence of consistently derived Timoshenko beam finite elements, Int. J. Numer. Meth. Engng. 5 243-253.

67. Prathap, G. Bhashyam, G.R. (1982) Reduced integration and the shear flexible beam element, Int. J. Numer. Methods Engrg. 18 195-210.

68. Tessler, A., Dong, S. B. (1981) On a hierarchy of conforming Timoshenko beam elements, Comput. Struct. l4(3-4) 335-344

69. Davis, R., Henshell, R.D., Warburton, G. B. (1972) A Timoshenko beam element, Journal of Sound and Vibration. 22 (4) 475-48

70. Archer, J.S. (1965) Consistent matrix formulations for structural analysis using finite-element techniques. American Institute of Aeronautics and Astronautics Journal. 3 1910-1918.

71. Kapur, K. K. (1966) Vibrations of a Timoshenko beam, using finite element approach. Journal of the Acoustical Society of America, 40 1058-1063

72. Severn, R. T. (1970) Inclusion of shear deformation in the stiffness matrix for a beam element. Journal of Strain Analysis 5 239-241

73. Carnegie, W., Thomas, J., Dokumaci, E. (1969) An improved method of matrix displacement analysis in vibration problems. The Aeronautical Quarterly 20 321-332.

74. Ali, R., Hedges, J.L., Mills, B. (1971) The Application of Finite Element Techniques to the Analysis of an Automobile Structure: First Paper: Static Analysis of an Automobile Chassis Frame. Automobile Division 185 665-674.

75. Ali, R., Hedges, J.L., Mills, B. (1971) Dynamic analysis of an automobile chassis frame, Automobile Division. 185 683-690

76. McCalley, R. B. (1963) Rotary inertia ccrrectior: for mass matrices. General Electric Knolls Atomic Power Laboratory, Schenectady, New York, Report DIG/SA. 68-73.

77. Cowper, G.R. (1966) The shear coefficient in Timoshenko's beam theory. Journal of Applied Mechanics 33 335-340. doi:10.1115/1.3625046

78. Augarde, C.E. (1997). Numerical modelling of tunneling processes for assessment of damage to buildings. DPhil thesis, University of Oxford.

79. Astley, R.J. (1992). Finite elements in solids and structures: an introduction. Chapman and Hall, London.

80. Pickhaver, J.A. (2006) Numerical modelling of building response to tunneling. Ph.D. thesis, University of Oxford

81. Thomas, D.L., Wilson, J.M., Wilson, R.R. (1973) Timoshenko beam finite element. Journal of sound and vibration. 31(3) 315-330.

82. Przemieniecki, J.S. (1968) Theory of Matrix Structural Analysis. Library of Congress Catalog Card Number 67, 19151.

83. Sapountzakis, E. J. and Kampitsis, A. E., (2010) Nonlinear dynamic analysis of Timoshenko beam-columns partially supported on tensionless Winkler foundation, Computers and Structures, 88, 1206-1219.

84. Sapountzakis, E. (2011). Nonlinear Analysis of Shear Deformable Beam-Columns Partially Supported on Tensionless Three-Parameter Foundation. Archive of Applied Mechanics. 81. 1833-1851. 10.1007/s00419-011-0521-4.

85. Sapountzakis, E. J. & Kampitsis, A.E., (2011). Nonlinear response of shear deformable beams on tensionless nonlinear viscoelastic foundation under moving loads. Journal of Sound and Vibration. 330. 5410–5426. 10.1016/j.jsv.2011.06.009

86. Dikaros, I. & Sapountzakis, E. (2014). Generalized Warping Analysis of Composite Beams of an Arbitrary Cross Section by BEM. I: Theoretical Considerations and Numerical Implementation. Journal of Engineering Mechanics. 10.1061/(ASCE)EM.1943-7889.0000775.

87. Sirca, G.F., Adeli, H. (2012) System identification in structural engineering. Scientia Iranica, 19 1355–1364.

88. Pisano, A.A (1999), "Structural System Identification: Advanced Approaches and Applications". PhD. Ph.D. Dissertation, Università di Pavia, Italy.

89. Gevers, M. (2006). A personal view of the development of system identification: A 30-year journey through an exciting field. IEEE Control Systems, 26(6), 93-105.

90. Pajonk, O. (2009) Overview of System Identification with Focus on Inverse Modeling. Technische Universität Braunschweig 63.

91. Liao, J., Tang, G., Meng, L., Liu, H., Zhang, Y. (2012) Finite element model updating based on field quasi-static generalized influence line and its bridge engineering application. Procedia Engineering 31 348–353.

92. .Lozano-Galant JA, Nogal M, Castillo E, Turmo J. (2013) Application of observability techniques to structural system identification. Computer-Aided Civil and Infrastructure Engineering 28 434–450

93. Deretic-Stojanovic, B., & Kostic, S. M. (2017) A simplified matrix stiffness method for analysis of composite and prestressed beams. Steel and Composite Structures, 24(1) 53-63. doi:10.12989/scs.2017.24.1.053

94. Li, J., Jiang, L., & Li, X. (2017) Free vibration of a steel-concrete composite beam with coupled longitudinal and bending motions. Steel and Composite Structures, 24(1). 79-91. doi:10.12989/scs.2017 24.1.07

95. Khayat, M., Poorveis, D., & Moradi, S. (2017) Buckling analysis of functionally graded truncated conical shells under external displacement-dependent pressure. Steel and Composite Structures, 23(1) 1-16. doi:10.12989/scs.2017.23.1.001

96. ASCE, Structural Identification of Constructed Systems, American Society of Civil Engineers, Reston, VA 2013

97. Lei, J., Lozano-Galant, J.A., Nogal, M., Xu, D., Turmo, J. (2016) Analysis of measurement and simulation errors in structural system identification by observability techniques. Structural Control and Health Monitoring, doi: 10.1002/stc.1923.

98. Lei, J., Xu, D., Turmo, J. (2017) Static structural system identification for beam-like structures using compatibility conditions. Structural Control and Health Monitoring, 25(1) e2062.

99. Castillo, E., Nogal, M., Lozano-Galant, J.A., Turmo, J. (2016) Solving Some Special Cases of Monomial-Ratio Equations Appearing Frequently in Physical and Engineering Problems. Mathematical Problems in Engineering.

100. Lozano-Galant, J.A., Nogal, M., Paya-Zaforteza, I., and Turmo, J. (2014) Structural system identification of cable-stayed bridges with observability techniques. Structure and Infrastructure Engineering, 10 1331-1344

101. Lozano-Galant, J.A., Nogal, M., Turmo, J., Castillo, E. (2015) Selection of measurement sets in static structural identification of bridges using observability trees. Computers and Concrete, 15 771–794.

102. Nogal, M., Lozano-Galant, J.A., Turmo, J. and Castillo, E. Numerical damage identification of structures by observability techniques based on static loading tests. Structure and Infrastructure Engineering, 12 (2015) 1216-1227.

103. Lozano-Galant, J. A., Emadi, S. B., Ramos, G., & Turmo, J. (2018). Structural system identification of shear stiffnesses in beams by observability techniques. Paper presented at the IABSE Symposium, Nantes 2018: Tomorrow's Megastructures, S24-111-S24-118.

104. Emadi, S., Lozano-Galant, J. A., Xia, Y., Ramos, G., & Turmo, J. (2019). Structural system identification including shear deformation of composite bridges from vertical deflections. Steel and Composite Structures, 32(6), 731-741. doi:10.12989/scs.2019.32.6.73.

105. Lei, j., Nogal, M., Lozano-Galant, J.A., Xu, D. and Turmo, j. (2017b) Constrained observability method in static structural system identification. Structural Control and Health Monitoring, 25 e2040.

106. Aquino, W., & Erdem, I. (2007) Implementation of the modified compression field theory in a tangent stiffness-based finite element formulation. Steel and Composite Structures, 7(4) 263-278. doi:10.12989/scs.2007.7.4.263

107. Çavdar, Ö., Bayraktar, A., Çavdar, A., & Adanur, S. (2008) Perturbation based stochastic finite element analysis of the structural systems with composite sections under earthquake forces. Steel and Composite Structures, 8(2) 129-144. doi:10.12989/scs.2008.8.2.129.

108. Kim, N. (2009) Dynamic stiffness matrix of composite box beams. Steel and Composite Structures 9(5) 473-497. doi:10.12989/scs.2009.9.5.473.

109. Midas Civil [Computer software] Midas Information Technology Co.2015, Ltd. http://en.midasuser.com/product/civil_overview.asp.

110. Valerio, P., Ibell, T. J., & Darby, A. P. (2011) Shear assessment of prestressed concrete bridges. Proceedings of the Institution of Civil Engineers: Bridge Engineering, 164(4) 195-210. doi:10.1680/bren.2011.164.4.195

111. Dong, X. Zhao, L. Xu, Z. Du, S. Wang, S. Wang, X. and Jin, W. (2017) Construction of the Yunbao Bridge over the yellow river, EASEC-15. October 11-13, Xi'an, China Dong, X. Zhao, L. Xu, Z. Du, S. Wang, S. Wang, X. and Jin, W. (2017) Construction of the Yunbao Bridge over the yellow river, EASEC-15. October 11-13, Xi'an, China

Appendix 3

Observing material properties in beams from actual rotations

S. Emadi[a], J.A. Lozano-Galant[b], Y. Xia[c], J. Turmo[a]

[a] Department of Civil and Environmental Engineering, Universitat Politècnica de Catalunya (UPC) BarcelonaTECH, Barcelona, Spain.

[b] Department of Civil Engineering, University of Castilla-La Mancha, Ciudad Real, Spain.
[c] Department of Bridge Engineering, Tongji University, Shanghai, China

ABSTRACT:

Shear deflection effects are Traditionally neglected in most structural system identification methods. Unfortunately, in some structures, like deep beams, this assumption might lead to significant errors. Although some inverse analysis methods based on the stiffness matrix method including shear deformation effects have been presented in the literature, none of these methods is able to deal with actual rotations on their formulations. Recently, the observability techniques, one of the first methods for the inverse analysis of structures included the shear effects. In this approach, Timoshenko's beam theory was Introduced into the stiffness matrix method. The effects of shear rotation are neglected in the common Timoshenko's beam theory stiffness matrix methods. When actual rotations on site are used to estimate the mechanical properties in the inverse analysis, it can result in serious errors in the observed properties. This characteristic might be especially problematic in structures such as deep beams where only rotations can be measured. To solve this problem and to increase the applicability of the observability techniques this paper proposes a new approach to include shear rotations into the inverse analysis by observability techniques. This modification is based on the introduction of a new iterative process. To illustrate the applicability and potential of the proposed method, the inverse analysis of several examples of growing complexity is presented.

Keywords: Structural system identification; Observability method; Shear rotation; Stiffness matrix method.

1.Introduction:

Structural modeling is associated with the simulation of structural response. This goal is traditionally achieved by transforming physical problems into mathematical ones based on a number of assumptions and

hypotheses. Many studies are performed to the model of the beam structural response [e.g. 1 2 [3]4] and most of them are based on either Euler-Bernoulli's beam theory [5] or Timoshenko's beam theory (known as first-order shear deformation theory) [6]. Due to the plain section deformation assumption, shear deformations are neglected by Euler-Bernoulli's beam theory (see e.g. [7,8]). This theory states that plane sections remain perpendicular to the neutral axis during and after bending deformation [9], and accordingly that shear forces and stresses are zero. Euler-Bernoulli's beam theory only holds for cases wherein constant bending moments are applied alongside the structures. Therefore, Euler-Bernoulli's beam theory is usually applying for slender beams With negligible shear deformations and in this approach, shear effects are considered modeling errors [10]. Nevertheless, in some structures (such as deep beams), the shear deformation cannot be neglected and it must be included into the formulation [11]. The definition of these deep beams might differ slightly from one code to the other. For example, on the one hand, Eurocode EN 1992-1-1:2004 [12] characterizes deep beams as beams with slenderness wherein the beam span is three times less than the overall section depth. On the other hand, ACI committee 318 [13] describes these beams as beams wherein beams spans equal to or less than four times of the depth of the beam.

Timoshenko [14,15] was the first one who introduced the shear effects into beams with the so-called first-order shear deformation theory. In fact, the shear effects are included in his theory in both the vertical deflections and the rotations. In Timoshenko's beam theory rotation due to the bending, w_b, and rotation due to the shear, w_r are considered separately and analyzed independently. In this theory rotation between the cross section and the bending line is allowed. The differences between methods in a simply supported beam with concentrated load, V at mid span are presented in Figure 1. Where Euler-Bernoulli's beam theory (Fig. 1.b) and Timoshenko's beam theory (Fig. 1.c) at the zoomed support of Fig 1.a can be seen.

(a)
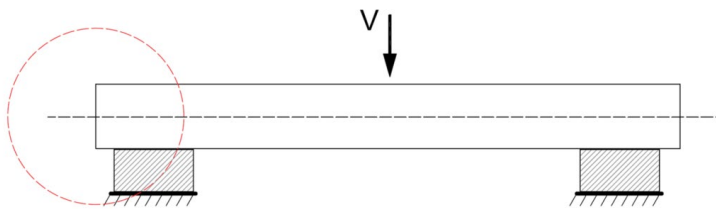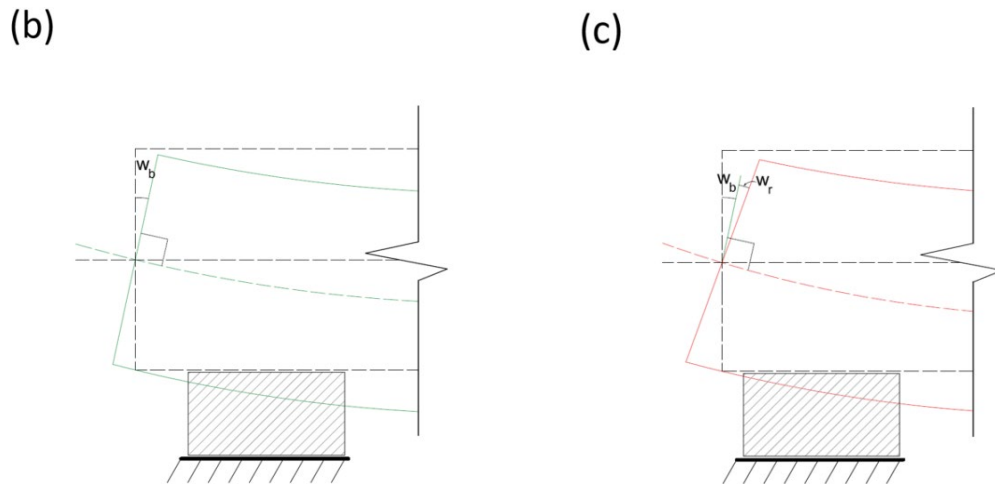
Figure 1. (a) A simply supported beam with a zoomed support. (b) Euler-Bernoulli's beam theory on the beam support. (c) Timoshenko's beam theory on the beam support.

Finite Element Method (FEM) is a numerical problem-solving method based on a concept in which large equations are divided into smaller and simpler equations. FEM is a common technique for computer-based analysis in engineering [16]. The Stiffness Matrix Method (SMM) is one of the major methods of FEM approach for analyzing the structural Response of beam-like structures [20-24], especially suited for computer-analysis of complex structures [17]. Recently, Emadi et al. (2020) reviewed the different models which are based on Timoshenko's beam theory. According to this work, a number of SMM approaches included shear rotation into their SMM's formulations. However, most of these methods fail to simulate structural cases with discontinuities in the cross sections, meeting non-collinear elements or imposed loads in the different elements. The only SMM can analyze these cases are the FEM's that nodal variables are bending rotation and transverse displacement (the effects of shear rotation are neglected in this SMM formulation). It should be mentioned that none of these methods take into account the shear rotation effects. Many works, for instance, in Przemieniecki [18], contain a detailed formulation of the common Timoshenko beam theory SMM. This stiffness matrix overlooks the effect of shear rotation. Indeed the effects of shear rotation are neglected even in commercial simulation software based on the stiffness matrix (such as SAP 2000 [19]). In these programs simulated rotations are equal to the bending rotations, the shear effects only are considered in the vertical deflections.

System Identification (SI) represents a modeling process for unknown variables in a certain system of equations used in various engineering fields [20 21]. The SI goal is to be able to characterize adequately the parameters of a certain system. since its introduction, it has been extended to most engineering fields [22 23]. Structural system identification (SSI) can be framed in the context of the SI that deals with the design of mathematical models. These mathematical models are used for the structural response for identifying the structural parameters (like flexural stiffnesses or axial stiffnesses) [5].
In the literature, several methods for SSI are proposed (e.g. [24 25 26]). Most of them are based on the SMM (see e.g. [27 28 29 30]). The details of the main SSI methods are shown in the literature are addressed in [31]. Most of SSI methods are not able to quantify correctly the parameters of structures when shear

effects are not negligible. This can be explained by the fact that most SSI methods based on SMM normally use Euler-Bernoulli's beam theory (see e.g. [32 33]), this assumption underestimates deflections and overestimating the natural frequencies since the shear effects are disregarded [34]. The effects of shear deformations in their SMM models are studied by some authors [35 36]. As Emadi et al. (2020) showed, the effects of shear rotations are neglected in the SMM; therefore, these effects are neglected in SSI methods based on SMM. Although the neglecting of shear rotation can produce error in the result of SSI methods, normally these errors can be overlooked. Nevertheless, in some structures (such as deep beams) shear effects might play an important role. In these cases, shear effects should be introduced into the formulation in order to reduce the errors of SSI methods.

Obviously, shear rotations are practically negligible in beam like structures. Nevertheless, in some cases these effects are considerable and the inability of considering these effects should be considered modeling error (error in modeling the structure). The observability method (OM) is an SSI method based on the system of equations of the SMM. In this procedure, the mechanical properties (e.g. Flexural stiffness EI) can be quantified from the deformations measured in static tests. OM has proved its efficiency in different structural typologies (such as trusses, beams, frame structures, and cable-stayed bridges) [37 38 39 40 41 42 43]. The analysis of these structures is based on a polynomial systems of equations, and it is not as simple as it may look due to the coupled equations. To solve this problem, a numerical optimization approach (constrained observability method (COM)) [44] can be used to decouple the coupled linearized variables. Recently, Emadi et al. (2020) included the effects of shear deformations into the Constrained Observability Method (COM). Unfortunately, this application (like other SSI methods based on SMM in the literature) is not able to take into account the actual rotations as shear rotation effects are not included into the formulation.

The aim of this paper is to fill this gap by presenting a new method based on OM to observe the material properties from actual rotations measured on-site for any kind of structure (even in those where the shear rotations are not negligible). To do so, an iterative process is proposed. In this process, estimated shear rotations are subsequently subtracted from the actual rotations on site. Then the normal COM can be performed in terms of bending rotations and bending and shear vertical deflections. Also, in iterative steps, the properties of the assumed material are successively updated from the inverse observations.

This article is organized as follows: In Section 2, a brief explanation of both the OM and the COM are presented and the importance of shear rotation is discussed. In Section 3 a new method for analyzing the effects of the shear rotation in COM is presented. In Section 4, different structures are analyzed to show the important role that shear rotations might play in some geometries. Moreover, the applicability and accuracy of the new method in different structures are presented. Finally, the conclusions obtained are drawn in Section 5.

2. Explanation of the observability method and assumptions

For the SMM, the equations of nodal equilibrium might be written as:

$$[K] \cdot \{\delta\} = \{f\}, \tag{1}$$

where the horizontal, u, vertical, v and rotational displacements, w are parts of $\{\delta\}$, the stiffness matrix $[K]$ covers information about axial stiffness EA, flexural stiffness EI and the length of the element L. The horizontal forces, vertical forces, and moments are included in the external force vector $\{f\}$.

The main disadvantages of this method are the complexity in the system of equations might lead to the following problems: (1) they are not able to include the effect of shear rotation into the SMM methods, these methods are considered as common Timoshenko's beam theory SMM (e.g. Przemieniecki [15]), (2) methods which consider the effects of shear rotation due to some assumptions, they are not applicable in general complex structures Emadi et al. (2020). In the OM, as in any inverse tool, some parameters of the nodal displacements $\{\delta\}$ are measured on-site to identify the unknown mechanical properties in the SMM when the geometry, the boundary conditions, and the load case in a certain static load test are determined. To do so, equation 1 can be rewritten as presented in Eq. (2), where all the known quantities are collected into the coefficient matrix $[B]$ and the vector $\{D\}$. Therefore, $[B]$ and $\{D\}$ are known, while all the unknowns are placed into the vector $\{Z\}$. Eq. (2) can be solved to observe unknown equations with the help of algebraic operations. for more information, readers are recommended to review [45 35].

$$[B] \cdot \{z\} = \{D\}, \tag{2}$$

In the OM the linearity of the system is assumed and coupled product of variables (and products of variables such as Young Modulus E and Inertia I are considered as a unique variable EI). Where N_A is the unknown axial stiffnesses and N_F is the unknown flexural stiffnesses. Theoretically, the number of measurements should be at least equal to the number of unknowns; therefore, $N_A + N_F$ measurements are expected to be enough to observe all unknown parameters. Lei et al. [47] found that due to lack of nonlinear constraints among product variables in OM, in most cases, it is not able to observe material properties with minimum required measurements. Lei et al. [47] proposed COM which solves the system of equations numerically after including the nonlinear constraints. This is to say that COM does not provide any symbolic solution. As they are only based on the numerical solution of the system. For this reason, in order to produce results with COM, initial numerical values should be assigned to the unknown parameters. The procedure of COM can be initiated with any number as the initial value, but in order to speed up the convergence in the optimization process, a random ratio between 0.5 to 1.5 of the theoretical values is normally proposed. In order to apply the optimization process, the objective function of COM can be defined as follow:

$$\{\in\} = [B \quad] \cdot \{Z \quad\} - \{D\}, \tag{3}$$

Where $\{\in\}$ is the residuals of the equations which is a vector with the same number of rows as the original vector $\{Z\}$. The objective function of the optimization process is to minimize the square sum of the residuals, $\in$ in Eq. (3). The optimization toolbox of Matlab [46] has been used to obtain the optimal solution of the objective function. Before starting the optimization process the objective function should be normalized. The algorithm for SSI by COM is summarized as follows:

- **Step 1**: Apply SSI by OM to check whether any variable is observed. If all unknown parameters are observed, there is no need to go to the COM process, otherwise, go to step 2.
- **Step 2**: Obtain the equation (2) from the OM and generate the objective function.
- **Step 3**: Obtain the normalized unknown parameters.
- **Step 4**: Guess the unknowns parameters' initial values, apply bounds for the solution and solve the optimization process, in order to find the least acceptable value for vector $\{\in\}$.

For more information about the COM, the reader is addressed to [47].
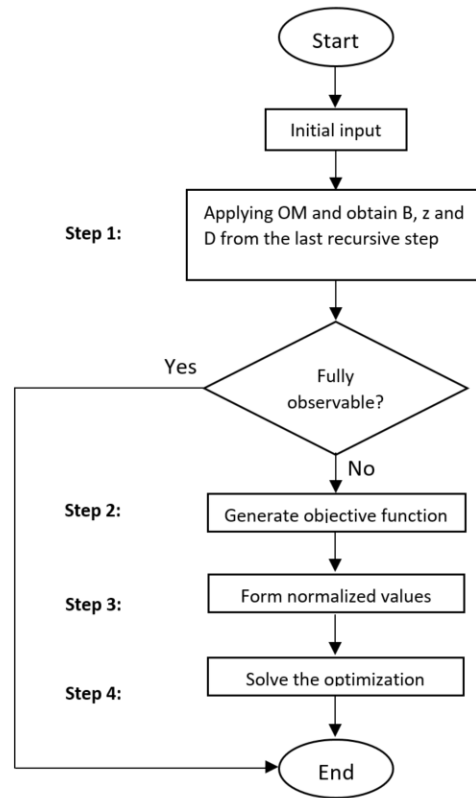
Figure 2. *Flow chart of structural system identification by COM.*

Since the COM method was based on Euler-Bernoulli's SMM, it was not able to consider the effects of shear deflections. This problem was solved by Emadi et al. (2019) who introduced the effects of shear deformation into the COM process. Due to lack of considering shear rotation in SMM, COM is not able to observe the value of material properties, correctly when rotations are included into the measurement sets. This method is not suitable for measuring rotations as wrong results are obtained even in noise-free measurements when this type of deformations is considered. Emadi et al. (2020) studied the effects of this impotence in considering shear rotations in SSI methods based on SMM. In this work, the theoretical rotations (sum of shear rotation and bending rotation) were tested in beams with different geometries (1 to 15 length to height ratio). Effects of these errors in estimating the inertia in different structural cases of a simply supported beam with a concentrated vertical force; simply supported beam with a distributed vertical force and a cantilever with a concentrated vertical force were tested. As Emadi et al. (2020) showed, the effects of neglecting shear rotation in inverse analysis were not negligible, even in the cases that beams cannot be considered a deep beam(based on Eurocode EN [12] and by the ACI Committee 318 [13]).

3. Proposed methodology

A new procedure is developed in this section in order to introduce the effects of shear rotation into the SSI. In this procedure, firstly, material properties are assumed randomly (between 0.5 to 1.5 of theoretical values). Then the shear rotation of each element is calculated based on assumed material properties. The Eq. (4) can be used for calculation of shear rotation, v_s in each element based on Timoshenko's beam theory [13,14].

$$v_s = \frac{V}{2 * A_v * G} * L \tag{4}$$

where A_v is the shear area, V is the shear force and shear modulus G might be written as:

$$G = \frac{E}{2(1+v)}, \tag{5}$$

where the coefficient v is Poisson's ratio. According to Eq. (4), the shear rotation for each element only depends on shear forces, shear area and shear modulus. On the other hand, shear area and shear modulus are directly obtained from the assumed mechanical properties of the structure, while the shear forces can be obtained from the results of the direct SMM analysis. By subtracting the value of shear rotation from the theoretical rotation of each node bending rotation can be obtained (theoretical rotation is the sum-up of shear and bending rotation). Therefore, The COM process is able to be used due to the fact that the SMM is defined on the assumption of neglecting the effects of shear rotation. In order to reach a certain level of efficiency in this procedure, the observed value of COM process can be used for calculating new shear rotations and iterative process can be performed several times. In order to limit the computational cost and the optimization time, the stopping criterion was defined with the following stopping criteria: 1) when the iterative process is performed more than 200 times and 2) when the difference between normalized values of observed material properties in 2 subsequent iterative processes are less than $1e^{-3}$. The new method is summarized in the following 4 steps:

- **Step 1:** Assume material properties, randomly (real value multiply by a coefficient between 0.5 to 1.5)
- **Step 2:** Calculate the shear rotation of each element from the assumed material properties. It is to highlight that the material properties can be obtained through either estimated values (for the first time) or observed material properties in COM procedure (in the iterative process).
- **Step 3:** Obtain the bending rotation from the calculated shear rotation in step 2 and perform COM procedure.
- **Step 4:** Check the stopping criteria if one of them is satisfied, the process stops, otherwise go to step 2.

A summary of the procedure is shown in the flow chart in Figure 3. In the following sections, a set of examples with growing complexity are analyzed in order to show the applicability and potential of the proposed method.
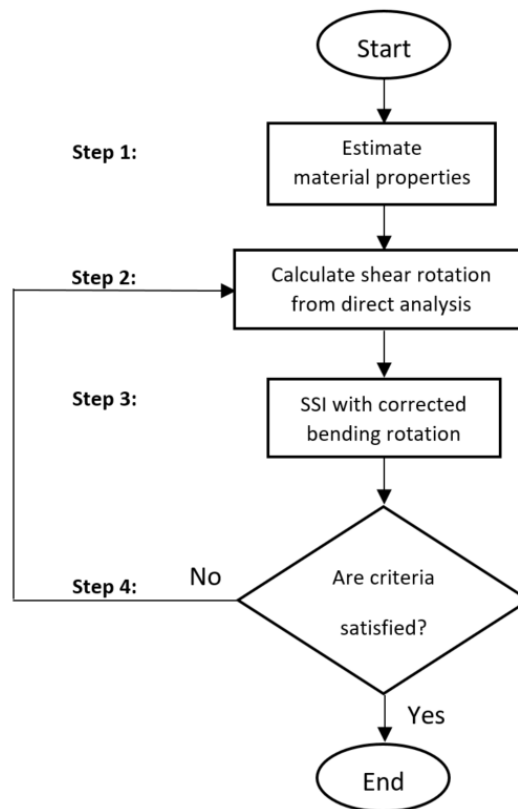
Figure 3. *Flow chart of COM by 2 iteration process.*

4. Applications

In order to show the applicability of the new method, several examples with different levels of complexity are analyzed in this section. It is to say that due to the fact that there is no horizontal force in these examples, the axial resistant mechanisms are neglected in this example. Also, measurement errors in this paper are neglected. The effects of these unavoidable errors will be considered in the next study by the authors.

4.1 Example 1: simply supported beam with 2 iteration process

Consider the 4 m long and 0.2 m wide simply supported beam modeled with 3 nodes and 2 beam elements depicted in Figure 4. This beam has a constant cross-section and the value of its Young modulus, shear area, cross-sectional area and inertia along the beam are 30 GPa, 0.800 m^2, 1 m^2 and 2.083 m^4, respectively. Its mechanical properties are listed in Table 1. The boundary conditions of the structure are horizontal and vertical displacements restricted in node 1 and vertical displacement restricted in node 3 (this is to say, $u_1=v_1=v_3= 0$). The beam is subjected to a concentrated vertical force in node 2 of 100kN ($V_2= 100$kN).
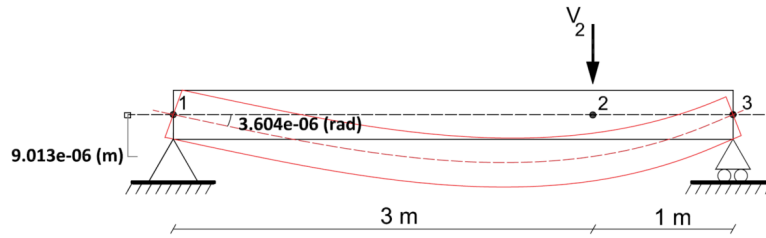
Figure 4. Example 1. FEM for a simply supported beam with the value of rotation on Node 1 and vertical deformation at Node 2.

Table 1. Properties of the FEM of the simply supported beam.

Area [m²]	1.000
Shear Area [m²]	0.800
Inertia [m⁴]	2.083
Concrete Young's Modulus [GPa]	30.000
Poisson's Ratio γ	0.250

For the inverse analysis of the structure, V_2, the length of the elements, Poisson's ratio and Young modulus are assumed as known, while the inertia, I and the shear area A_v are assumed as unknown. To define the two unknown parameters assumed in example 1 are A_v and I, a measurement set of at least two rotations is required to identify the values of unknowns. Nevertheless, no set of two rotations in COM enables the proper identification of the unknown parameters. Therefore, a set of a vertical deflection and a rotation should be measured together (it is to say w_1 and v_2). The values of measurement set are obtained from Timoshenko's beam theory simulation can be seen in Fig 4. Table 2 presents 10 different sets of the initial value coefficients for inertia and shear area which is randomly chosen between 0.5 and 1.5 for the optimization process.

Table 2 Initial value coefficient of the Bridge Unknown Properties

I	Q
1.25	0.94
0.66	0.95
1.29	0.58
0.81	0.73
1.03	1.41
0.67	0.65
1.10	1.33
0.76	1.04
1.15	1.50
1.19	0.58

In the following comparison, the evolution of the normalized values of the shear area and inertia ratio throughout the iterative steps for different initial values are presented in figures 5.a. and 5.b, respectively.

(a)

(b)
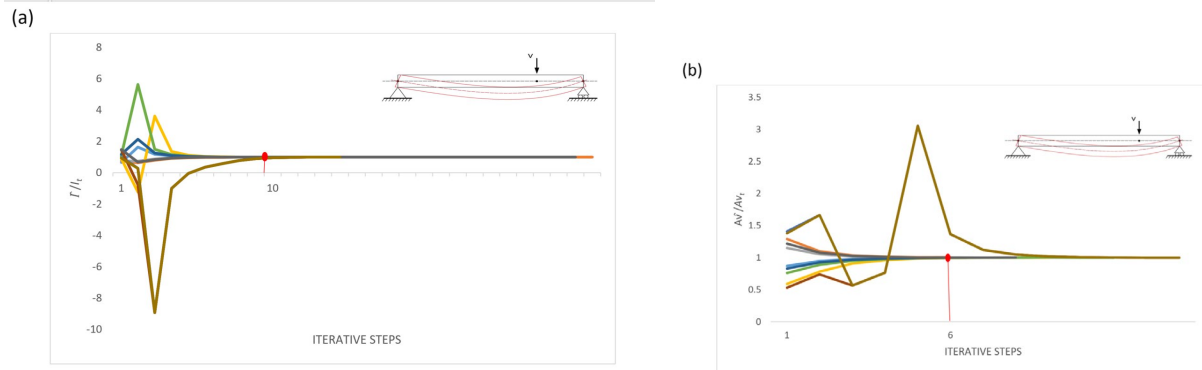
Figure 5. (a) Normalized values of inertia in different iterative steps. Where $\hat{I}$ is the estimated value of inertia area and I_t is the exact value of inertia. (b) Normalized values of shear area in different recursive steps. Where $\widehat{Av}$ is the estimated value of shear area and Av_t is the exact value of shear area.

In Fig. 5.a, the criterion is satisfied after 10 iterative steps for the initial value of 1.024 and the normalized value of inertia is gained equal to 1.003. In the same way, after 6 iterative steps, the criterion is satisfied for the shear area when the initial value is 0.58. Also, the final normalized value of observed shear area is 0.999. It is to say that if traditional COM (with lack of ability to consider shear rotation) is applied in this example, the observed normalized value of inertia and shear area will be 0.277 and 1.600, respectively. This example illustrates the inability of traditional COM to identify the correct value of parameters when theoretical rotations are considered in the measurement set.

3.2 Example 2: Cantilever beam with 2 iteration process

Consider a cantilever beam with the same cross section and same properties as in Example 1 modeled with one beam element and 2 nodes as it is presented in Fig 6. The boundary conditions of the structure are total horizontal and vertical displacements and rotation due to bending restricted in node 1 (this is to say, $u_1=v_1=w_{b1}=0$). The only external force applied is a concentrated vertical force in Node 2 of 100kN ($V_2=100$kN). V_2, the length of the elements, Poisson's ratio and Young modulus are assumed as known in the inverse analysis, while the inertia I and the shear area A_v are assumed as unknown. Since the only two unknown parameters assumed in example 2 are A_v and I, a measurement set of at least two rotations is required to identify their values of unknowns. Nevertheless, no set of two rotations in COM enables the proper identification of the unknown parameters. Therefore, a set of vertical deflection and rotation should be measured together in this example. To perform the COM, a measurement set that consists of one rotation and one vertical deflection (w_2 and v_2) is employed. The theoretical rotation and vertical deformation are presented in Fig. 6. it is to say that the measured values are obtained from Timoshenko's beam theory.
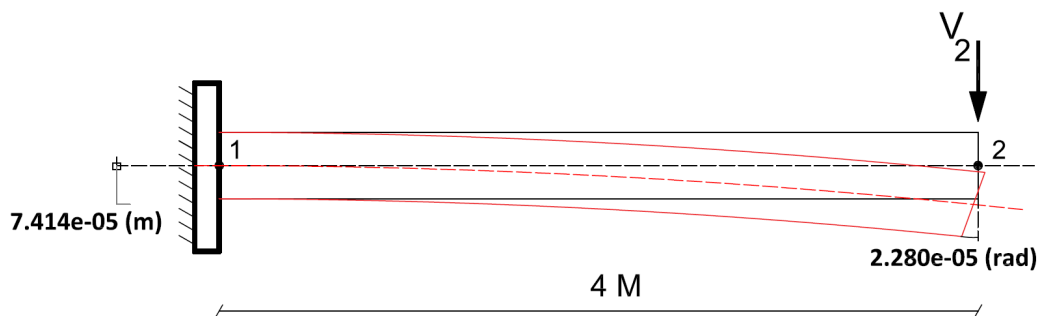
Figure 6. *Example 2. FEM for a cantilever beam with the value of vertical deformation and rotation at Node 2.*

In the following comparison, the evolution of the normalized values of the shear area and inertia ratio throughout the iterative process with 10 different initial values which are randomly selected between 0.5 and 1.5 are presented in figures 7.a. and 7.b, respectively. The initial value coefficients are presented in Table 3.

Table 3 Initial value coefficient of the Bridge Unknown Properties

| I	Q
0.61	0.93
1.46	1.41
0.50	0.68
1.27	0.76
1.32	0.65
1.37	0.64
0.58	1.37
0.90	1.08
0.76	1.05
1.30	0.65
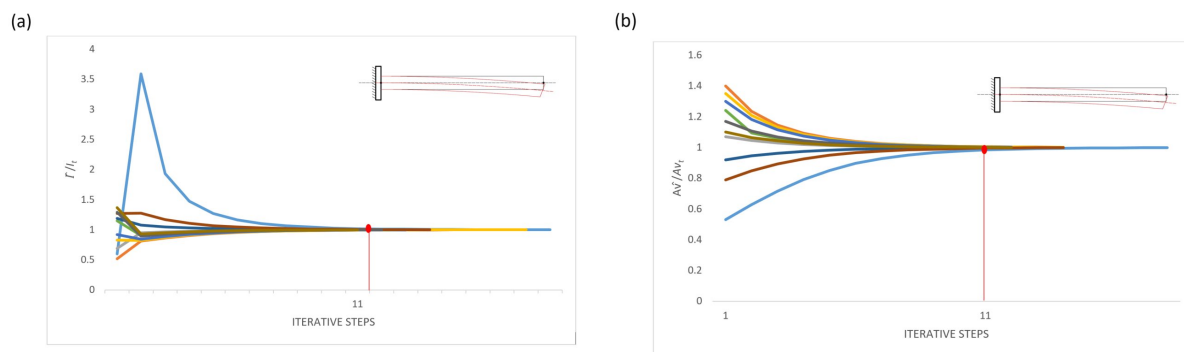
Figure 7. (a) Normalized values of inertia in different iterative steps. (b) The normalized values of shear area in different iterative steps.

In Fig. 7.a, the iterative steps for observing inertia stops after 11 steps for the initial value equal to 0.85 and the normalized value of Inertia is equal to 0.999. In the same way, the final result of shear area which is obtained after 11 iterative steps is 1.006 with the initial value of 1.13. Also, the observed normalized values of the traditional COM process for this example are 0.562 and 3.000 for Inertia and shear area, respectively.

3.3 Example 3: Application to a composite bridge

To show the possible application of the two iteration process, the problem of the construction of a bridge by the balanced cantilever method is presented here. In these structures, deflections should be anticipated in advance in order to calculate how to build the precamber structures in the different segments. to update this precamber structure for every step during construction, complete topographic surveying is usually performed. Therefore, an inverse analysis can be employed for providing information for this model updating process. However, shear effects might not play a very important role for a full developed

cantilever, neglecting the effects of shear rotation in the first segment will lead to the unreliable estimation of the bending stiffness. A simplified model of the Yunbao Bridge over the Yellow River in China (see Fig. 8) is studied in this section to show the Applicability of the new method to solve this problem. The structure span is 90m long, but only an intermediate construction stage is considered in this example. The studied construction stage includes the construction of two symmetric cantilevers. The length of each deck segment is 4.5m and the length of the segment over the pile is 2.5m. The total length of the model is 29.5 m. The mechanical and material properties are defined by the method of the transformed section [47] are listed in Table 4.

Table 4. Properties of the Finite Element Model of the Bridge.

Area [m^2]	12.52
Shear Area [m^2]	9.83
Inertia [m^4]	35.62
Steel Young's Modulus [GPa]	210
Concrete Young's Modulus [GPa]	35
Poisson's Ratio γ	0.3

Fig. 8 Composite bridge on-site (China) [48]

Actual site data is not considered in this structure and the structural response is simulated numerically. Effects of creep and shrinkage in concrete are neglected. The load test used simulates the movement of the formwork traveler (Fig. 9). The weight F of the formwork traveler (weight of formwork included) is considered as the 60 % of the weight of the segment (1041 kN). The effect of each form traveler in the deck is considered as two vertical forces. The values of these two forces are 0.25F and 1.25F (226 kN, upwards and 1267 kN, downwards). Load case of the bridge model is calculated by reducing the effects of stage i (Fig. 9.a), from stage i+1 (Fig. 9.c), wherein the formwork traveler is moved forward to the next segment. Load cases of the stages i and i+1 are expressed in Figures 9.b and 9.d, respectively. The consequent load case introduced in the simulation is shown in Fig. 9.e. It is to highlight that the vertical resultant of such forces in each side of the cantilever is zero.

Fig. 9 Definition of the load case: (a, b) Stage i. (c, d) Stage i+1. (e) Load case used for the inverse analysis
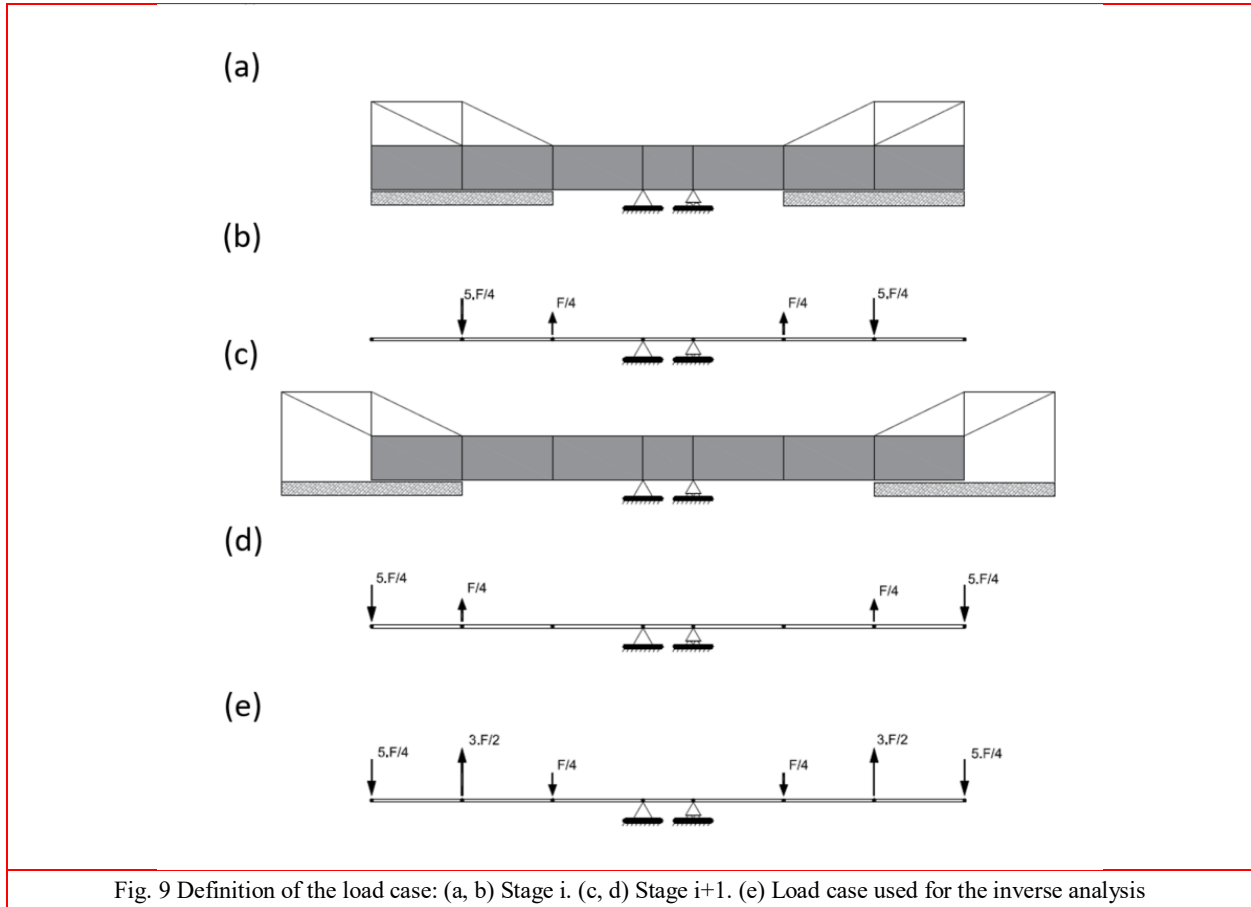
The simplified FEM of this structure is presented in Fig. 10. This FEM includes 7 elements and 6 point loads. In the inverse analysis, Young modulus and area of all elements are considered known parameters. Since there is no axial load, the axial stiffness is not activated in this example; therefore, only flexural behavior is analyzed. In this example, the construction of the first and last elements are considered. So, shear area and Inertia in elements numbers 2, 3, 4, 5 and 6 are considered known properties. The shear area and inertia of all other beam elements (that is to say I_1, I_7 and A_{v1}, A_{v7}) are assumed as unknowns.


Fig. 10. Example 3. FEM of the bridge with load case used for inverse analysis.
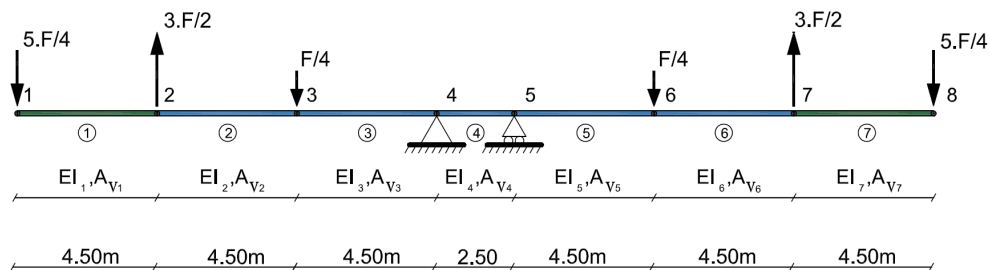
In this example, there are 4 unknowns, but since the model is symmetric, 2 unknowns can be considered instead of 4 unknown (I_1 and A_{v1} instead of I_1, I_7 and A_{v1}, A_{v7}). In order to identify the 2 unknown

mechanical properties at least, 2 measurements are required. COM is not able to observe any properties only with rotations in this example. To observe parameters with the method, the variation of deflection and rotation should be taken into account (it is to say, w1 and v1). The value of theoretical rotation and vertical deflection of node 1 are 2.280e-05 (rad) and 7.414e-05 (m), respectively. Timoshenko's beam theory is used to calculate the values of measured variables in the node number 1 in example 3. The initial value coefficients of unknown inertia and shear area (I_1 and A_{v1}) randomly chosen between 0.5 and 1.05 are showed in Table 5. In the following comparison, the evolution of the normalized values of the shear area and inertia ratio throughout the iterative process with 10 different initial values which are randomly selected between 0.5 and 1.5 are presented in figures 11.a. and 11.b, respectively.

Table 5: Initial value coefficient of the Bridge Unknown Properties

| I	Q
0.85	0.58
1.33	0.55
1.086	1.03
1.05	1.28
1.42	1.43
0.79	0.63
1.26	1.07
1.25	0.97
0.88	0.51
1.07	0.84
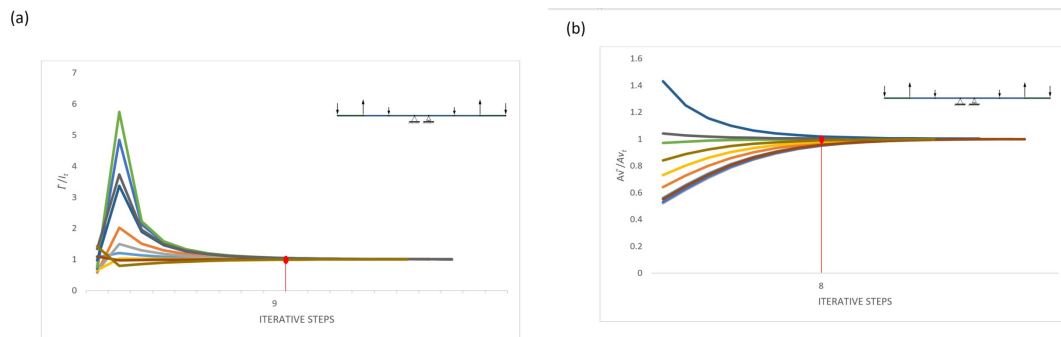
Figure 11. (a) Normalized values of inertia in different iterative steps with random initial value coefficients. (b) Normalized values of shear area in different iterative steps with random initial value coefficients.

The new method manages to observe the unknown shear area in 14 recursive steps and Inertia in 14 recursive steps, the evolution of shear area and inertia ratio throughout the iterative process, are presented in Fig.11.a and b, respectively. It is important to highlight that traditional COM is not able to identify the accurate value of mechanical properties when theoretical rotations are measured. However, it is examined and the normalized values of observed material properties are 0.528 and 3.000 for inertia and shear area. This example proves the efficiency of the proposed COM to estimate inertia and shear area when shear rotations are taken into account. Also, it is important to highlight that no other SSI method based on SMM in literature is able to include the value of shear rotation into account.

5.Conclusions

Most Structural System Identification (SSI) methods neglect shear effects as this phenomenon is usually negligible in comparison with flexural deformation. In fact, stiffness matrix methods are used normally to analyze complex structures neglecting shear rotations. However, it can play a significant role in some structures, as deep beams. According to the literature, even those studies which address the particular effects of this deformation in static SSI tests, neglect the effects of shear rotation. However, this failed to consider the effects of shear rotation can lead to significant errors in observing material properties in the inverse analysis.

To fill this gap, the formulation of Constrained observability method (COM) is updated to include shear rotation. The COM performance in several examples is tested to show the power of the new method to observe the value of the structural parameters when the actual rotations are included into the measurement sets. To show the applicability of the COM on complex structures, a simplified model of an intermediate construction stage of a cantilever composite bridge in China is studied. The results of this study show how the value of material properties can be observed by COM when the actual rotations are included into the measurement set. It is to say that the result of COM method without considering shear rotation when actual rotations are included into the measurement set is studied, in order to show the sensitivity of the SSI methods to this modeling error. The study of this sensitivity analysis might provide some insight into which structures rotation due to shear should be taken into account and in which cases these effects can be neglected.

This research presents the application of the method for error-free measurement sets. Possible modeling errors have been also neglected. The effect of the measurement errors will be studied in the future. The application of the method to the actual measuring sets from real structures will also be envisaged.

Acknowledgments

References

1. *Albero, V., Espinós, A., Serra, E., Romero, M.L., Hospitaler, A. Numerical study on the flexural behaviour of slim-floor beams with hollow core slabs at elevated temperature. Engineering Structures. 180. (2019) 561-573 10.1016/j.engstruct.2018.11.061.*

2. *Faccio, C., Pegoraro Cardozo, A.C., Monteiro Junior, V., Neto, A. Modeling wind turbine blades by geometrically-exact beam and shell elements: A comparative approach. Engineering Structures. 180 (2019) 357-378. 10.1016/j.engstruct.2018.09.032.*

3. *Weaver W., Were J.M. (1990) Computer-Oriented Direct Stiffness Method. In: Matrix Analysis of Framed Structures. Springer, Boston, MA,DOI https://doi.org/10.1007/978-1-4684-7487-9_4.*

4. *Wang, S., Liu, Y., He, J., Xin, H., Yao, H. Experimental study on cyclic behavior of composite beam with corrugated steel web considering different shear-span ratio. Engineering Structures. 180 (2019) 669-684. 10.1016/j.engstruct.2018.11.044.*

5. *Kawano, A., Zine, A. Reliability evaluation of continuous beam structures using data concerning the displacement of points in a small region. Engineering Structures. 180 (2019) 379-387. 10.1016/j.engstruct.2018.11.051.*

6. *Hoang, T., Foret, G., Duhamel, D. Dynamical response of a Timoshenko beams on periodical nonlinear supports subjected to moving forces. Engineering Structures. 176 (2018) 673-680. 10.1016/j.engstruct.2018.09.028.*

7. *Lu, Y., Panagiotou, M. Three-Dimensional Cyclic Beam-Truss Model for Nonplanar Reinforced Concrete Walls. Journal of Structural Engineering. 140 (2014) 04013071. DOI: 10.1061/(ASCE)ST.1943-541X.0000852.*

8. *Ozdagli, A. I., Liu, B., Moreu, F. Measuring Total Transverse Reference-Free Displacements for Condition Assessment of Timber Railroad Bridges: Experimental Validation. Journal of Structural Engineering. 144 (2018) 040180471.*

9. *Dahake, A., Ghugal, Y., Uttam, B., Kalwane, Dr. Displacements in Thick Beams using Refined Shear Deformation Theory. Proceedings of 3 rd International Conference on Recent Trends in Engineering & Technology. 2014.*

10. *Tomas, D., Lozano-Galant, J.A., Ramos, G., Turmo, J. Structural system identification of thin web bridges by observability techniques considering shear deformation. Thin-Walled Structures, 123 (2018) 282-293.*

11. *Dym, C.L., Williams, H.E. Estimating Fundamental Frequencies of Tall Buildings. Journal of Structural Engineering. 133 (2007) 1479-1483.*

12. *EN 1992-1-1:Eurocode 2: Design of concrete structures - Part 1-1: General rules and rules for buildings. CEN, Brussels, 2002, Belgium.*

13. *ACI committee 318 Building code requirements for structural concrete and commentary. American Concrete Institute, Detroit, 2000, USA*

14. *Timoshenko, S. P. On the correction for shear of the differential equation for transverse vibrations of prismatic bars. Philosophical Magazine 41 (6) (1921) 742–746.*

15. *Timoshenko, S. P. On the transverse vibrations of bars of uniform cross-section. Philosophical Magazine. 43 (1922) 125-131.*

16. *[16] CSI, CSI Analysis Reference Manual for SAP2000, ETABS, SAFE and CSiBridge, Berkeley, California, USA, 2016.*

17. *Weaver W., Gere J.M. (1990) Computer-Oriented Direct Stiffness Method. In: Matrix Analysis of Framed Structures. Springer, Boston, MA, DOI https://doi.org/10.1007/978-1-4684-7487-9_4.*

18. *Przemieniecki, J.S.Theory of Matrix Structural Analysis. Library of Congress Catalog Card Number 67(1968), 19151.*

19. *Midas Civil [Computer software] Midas Information Technology Co.2015, Ltd. http://en.midasuser.com/product/civil_overview.asp.*

20. *Sirca Jr, G.F., & Adeli, H. (2012). System identification in structural engineering. Scientia Iranica, 19(6), 1355-1364.*

21. *Altunisik, A. C., Gunaydin, M., Sevim, B., & Adanur, S. (2017). System identification of arch dam model strengthened with CFRP composite materials. Steel and Composite Structures, 25(2), 231-244*

22. *Gevers, M. (2006). A personal view of the development of system identification: A 30-year journey through an exciting field. IEEE Control Systems, 26(6), 93-105.*

23. *Pisano, A.A (1999), "Structural System Identification: Advanced Approaches and Applications". PhD. Ph.D. Dissertation, Università di Pavia, Italy.*

24. *Enokida, R. (2019). Stability of nonlinear signal-based control for nonlinear structural systems with a pure time delay. Structural Control and Health Monitoring, 26(8) doi:10.1002/stc.2365*

25. *Zhang, F. -., Yang, Y. -., Xiong, H. -., Yang, J. -., & Yu, Z. (2019). Structural health monitoring of a 250-m super-tall building and operational modal analysis using the fast bayesian FFT method. Structural Control and Health Monitoring, 26(8) doi:10.1002/stc.2383*

26. *Fu, Y., Peng, C., Gomez, F., Narazaki, Y., & Spencer, B. F., Jr. (2019). Sensor fault management techniques for wireless smart sensor networks in structural health monitoring. Structural Control and Health Monitoring, 26(7) doi:10.1002/stc.2362*

27. *Boumechra, N. (2017). Damage detection in beam and truss structures by the inverse analysis of the static response due to moving loads. Structural Control and Health Monitoring, 24(10) doi:10.1002/stc.1972*

28. *Casciati, S., & Elia, L. (2017). Damage localization in a cable-stayed bridge via bio-inspired metaheuristic tools. Structural Control and Health Monitoring, 24(5) doi:10.1002/stc.1922*

29. *Chatzieleftheriou, S., & Lagaros, N. D. (2017). A trajectory method for vibration based damage identification of underdetermined problems. Structural Control and Health Monitoring, 24(3) doi:10.1002/stc.1883*

30. *Shafieezadeh, A., & Ryan, K. L. (2011). Demonstration of robust stability and performance of filter-enhanced H 2/LQG controllers for a nonlinear structure. Structural Control and Health Monitoring, 18(6), 710-720. doi:10.1002/stc.387*

31. *Catbas, Necati & kijewski-correa, tracy & Aktan, A. (2013). Structural Identification of Constructed Systems: Approaches, Methods, and Technologies for Effective Practice of St-Id. 10.13140/2.1.1218.1761.*

32. *Dincal, S., & Stubbs, N. (2014). Nondestructive damage detection in euler-bernoulli beams using nodal curvatures - part I: Theory and numerical verification. Structural Control and Health Monitoring, 21(3), 303-316. doi:10.1002/stc.1562*

33. *Caddemi, S., Caliò, I., Cannizzaro, F., & Morassi, A. (2018). A procedure for the identification of multiple cracks on beams and frames by static measurements. Structural Control and Health Monitoring, 25(8) doi:10.1002/stc.2194*

34. *Sayyad, A.S. Comparison of various refined beam theories for the bending and free vibration analysis of thick beams; Applied and Computational Mechanics, 5 (2011) 217–230.*

35. *Leblouda, M., Junaid, M.T., Barakat, S., Maalej, M. Shear buckling and stress distribution in trapezoidal web corrugated steel beams; Thin-walled structures, 113 (2017) 13-26.*

36. *Liu, S., D Ziemian, R., Chen, L., Chan, S-L. Bifurcation and large-deflection analyses of thin-walled beam-columns withnon-symmetric open-sections; Thin-walled structures, 132 (2018) 287-301*

37. *Lei, j., Nogal, M., Lozano-Galant, J.A., Xu, D. and Turmo, j. Constrained observability method in static structural system identification, Structural Control and Health Monitoring, 25 (2017) e2040.*

38. *Lozano-Galant JA, Nogal M, Castillo E, Turmo J. Application of observability techniques to structural system identification; Computer-Aided Civil and Infrastructure Engineering 28 (2013) 434–450.*

39. *MATLAB and Optimization Toolbox Release 2017b, The MathWorks, Inc., Natick, Massachusetts, United States.*

40. *Chen, Y.S. and Yen, B. T. (1980) Analysis of Composite Box Girders, Fritz Engineering Laboratory Library, Report N0 380.12.*

41. *Dong, X. Zhao, L. Xu, Z. Du, S. Wang, S. Wang, X. and Jin, W. Construction of the Yunbao Bridge over the yellow river, EASEC-15. 2017, October 11-13, Xi'an, China.*

42. Emadi, S., Lozano-Galant, J. A., Xia, Y., Ramos, G., & Turmo, J. (2019). Structural system identification including shear deformation of composite bridges from vertical deflections. Steel and Composite Structures, 32(6), 731-741. doi:10.12989/scs.2019.32.6.73.

43. Emadi, S., Lozano-Galant, J. A., Xia, Y., Ramos, G., & Turmo, J. (2020). Shear rotation analysis in stiffness matrix methods: A state of the art and application in the direct and inverse analyses. Computers and Composite Structures, (under review)